Title
Expanding the bioluminescent toolkit for in vivo imaging

Permalink
https://escholarship.org/uc/item/5dt6g5pz

Author
Paley, Miranda Amelia

Publication Date
2014

Peer reviewed|Thesis/dissertation

UNIVERSITY OF CALIFORNIA,
IRVINE

Expanding the bioluminescent toolbox for *in vivo* imaging

DISSERTATION

submitted in partial satisfaction of the requirements
for the degree of

DOCTOR OF PHILOSOPHY

in Chemistry

by

Miranda Amelia Paley

Dissertation Committee:
Assistant Professor Jennifer A Prescher, Chair
Associate Professor Andrej Luptak
Professor Sheryl Tsai

2014

DEDICATION

To:

Elaine Calzolari

Beneath the leaves of a plant, that's named for milk
that bleeds milk, we search for chrysalides,
things that I've never seen, but whose name I like.
And I think as I look of all the things

you've taught me to name-larkspur, loose-
strife, sea lavender, plants called hens
and chickens, butter and eggs, your eyes
bright with such knowledge and solid as nouns.

Just so, you tell me now of creatures
who choose the underbelly of these leaves to make
wombs of, studded with gold, from which emerge
Monarchs that range the length of the Atlantic

in hordes-one more fact I must have missed
by skipping the fourth grade. And when, today,
we find no trace of anything resembling this
miracle you mention, and I'm about to say

you made it up, you bend down, break a pod,
and blow unlikely butterflies in the sky's face-
not black and orange like Monarchs, but cloud-
thought white, or like the way I mark my place

when I read your eyes, which witnessing claim:
This is the world. Try to learn its name.

-Gary Miranda

ii

TABLE OF CONTENTS

Page

LIST OF FIGURES

LIST OF TABLES

ACKNOWLEDGMENTS

I would like to express the deepest appreciation to my committee chair, Dr. Jennifer Prescher for supporting my ideas, experiments and aspirations. Many professors would have balked at the idea of their first student abandoning the bench, you only asked, "So how do we do this?" Thank you.

I would like to thank my committee members, Dr. Andrej Luptak and Dr. Sheryl Tsai. No one has challenged and helped me refine my scientific ideas in the way that Dr. Luptak has. I will always appreciate the way that Dr. Tsai guided me through the process of preparing my independent proposal idea during my advancement to candidacy.

The rest of the UCI faculty and staff have been equally supportive and inspiring. In particular, I would like to thank Dr. Greg Weiss for stepping in as my temporary advisor until Jenn started, Dr. Andy Borovik for keeping me grounded, Drs. Suzanne Blum and Liz Jarvo for sitting on my qualification exams and Dr. Donald Blake for generously spirited conversations at the pub. Thanks as well to all the wonderful professors I had in classes. A special thank you to the ladies in the chemistry department office for always being so kind and accommodating.

The Prescher lab has been a crazy but wonderful place to be for the last 5 years. I will always feel a special affinity for the other four of "the first five": Dave McCutcheon, Lidia Nazarova, Dave Patterson and Rachel Steinhardt. We went through the worst of it together, and came out for the better. Thanks to Joanna Laird and Krysten Jones for always being available for bio-related questions. I have really enjoyed and appreciated Dr. Hui-Wen's experience and humor in lab the last two years. To Will Porterfield, Colin Rathbun and Brendan Zhang: I'm happy that the luciferase-luciferin project is being left in such adept hands.

I would like to acknowledge all my teachers from elementary school all the way up to my graduate experience, inside science and out, because without a thorough education in both the arts and sciences, I wouldn't be where I am today. Betsy Lewis, Jana Clark, Leni Arnett, Andre Shaw, Sable Collins, Andrea Wiseman, Greg Painter, Mark Hughes Dr. Mark Levandoski, Dr. Andy Mobley, Dr. Stephen Sieck, Dr. John Fennell, Dr. Rafael Cabeza and Dr. Jon Tunge each taught me something different and equally valuable.

To my family, Dad and Tobi; I really would have quit without your love, support, and gentle prodding. Dad: are you so proud it's creepy? To my aunties, Laura Calzolari, Judy Paley, Marsha Engel, Linda Levinsky and Dr. Nancy Gary I am happy to have so many of you in my life and in my corner. The casual reader might note that with that many surnames, not all those listed above are related to me. You know what they say though: friends are the family you get to choose. I am lucky to have both kinds.

I am forever grateful to my friends without whom I never could have completed my PhD. Specifically, I want to thank Dr. Jess Arter-Williams, Tess Cohen, Will Hartwig Anna Gilbert, Lindsay King Miller, Kritika Mohan, Dr. Tivoli Olsen, Gidget Tay, Dr. Greg Williams, Carl Vogel and Dr. Iva Yonova for their love and support.

Thanks to the poet Gary Miranda for permission to reprint my mother's favorite poem as part of her dedication.

Last, but definitely not least, Trevor Cornell has been my partner and chief hand-holder for most of this journey. I love you. I love us. I seem to have clammed up on the page but I hope I tell you in person often enough how much you mean to me. I am excited for our futures and taking on the world together.

The text of Chapter 1 is a reprint of the material as it appears MedChemComm. The co-author listed in this publication directed and supervised research which forms the basis for that chapter.

CURRICULUM VITAE
Miranda Amelia Paley

EDUCATION AND TRAINING
University of California, Irvine, Irvine, CA
Doctor of Philosophy in Chemistry
December, 2014

Grinnell College, Grinnell, IA
B.A. Biological Chemistry, with Honors,
May, 2009

RESEARCH EXPERIENCE
University of California-Irvine, Irvine, CA
Graduate Student
Department of Chemistry
Advisor: Dr. Jennifer Prescher
Thesis Topic: Expanding the bioluminescent toolbox for *in vivo* imaging

University of Colorado-Boulder, Boulder, CO
Research Assistant
The Institute for Behavioral Genetics
Advisors: Drs. Michael Marks and Sharon Grady
Research Topic: Mapping nicotinic receptor ligand affinity in the murine brain

The University of Kansas, Lawrence, KS
NSF REU fellowship
Advisor: Dr. Jon Tunge
Research Topic: Formation of *N*-alkylpyrroles via intermolecular redox amination

WORK EXPERIENCE
Managing Editor
ACS Central Science,
American Chemical Society, Washington DC
January, 2015 - present

Graduate Teaching Assistant,
Department of Chemistry,
University of California-Irvine
Chemical Biology (graduate course), Winter 2011, Winter 2014
General Chemistry Discussions Fall 2010, Winter 2011, Fall 2012, Winter 2013
General Chemistry Lab, Spring 2010, Spring 2011 (Honors course)

Undergraduate Teaching Assistant,
Department of Chemistry, Grinnell College, Grinnell Biological Chemistry
Mentor, Spring 2009 Organic Chemistry Lab, Fall 2008 Inorganic/ Analytical
Chemistry Lab, Fall 2007

HONORS AND AWARDS
Semi finalist AAAS Mass Media Science and Engineering Fellowship
Teaching Award, Lower Division (UCI)
Smith Prize for Outstanding Biological Chemistry Senior (Grinnell)
Kappie Spencer Scholarship (Grinnell)
Samuel H. Elbert '28 Scholarship (Grinnell)
Best Poster Presentation, Mid-summer NSF research update symposium (KU)
Florence Smith-Sifferd Women in Science Scholarship (Grinnell)
Trustee Honor Scholarship (Grinnell)

PROFESSIONAL SERVICE
Denver School of the Arts Creative Writing Department Guest Artist
UC Irvine Graduate and Post-Doctoral Student Colloquium Committee Member
Iota Sigma Pi, Calcium Chapter President
Student-Hosted Seminar Committee Member
Iota Sigma Pi, Calcium Chapter Officer, Outreach Activities Co-Chair
Grinnell Women in Science member

PUBLICATIONS
5. Marks, M.J.; Grady, S.; Salminen, O.; Paley, M.; McIntosh, M.; Whiteaker, P. Expression of α6β2*-subtype nicotinic acetylcholine receptors is exceptionally sensitive to down regulation by chronic nicotine administration. *J. Neurochem.* **2014,** 130, 185-98.
4. Evans, M. S.; Chaurette, J. P.; Adams S. T.; Reddy, G. R.; Paley, M. A.; Aronin, N.; Prescher J. A.; Miller, S. C. A synthetic luciferin improves bioluminescence imaging in live mice. *Nat. Methods*. **2014** *4*, 393-5.
3. Paley, M. A.; Prescher, J. A. Bioluminescence: a versatile technique for imaging cellular and molecular features. *MedChemComm* **2014,** *5*, 255-267 2.
2, McCutcheon, D. C.; Paley, M. A.; Steinhardt, R. C.; Prescher, J. A. Expedient synthesis of electronically modified luciferins for biological imaging, *J. Am. Chem. Soc.* **2012**,*134* 7604–7607.
1. Pahadi, N. K.; Paley M. A.; Jana, R.; Waetzig, S. R.; Tunge, J. A. Formation of *N*-Alkylpyrroles via Intermolecular Redox Amination, *J. Am. Chem. Soc.* **2009,** *131* 16626–16627.

INVITED SEMINAR PRESENTATIONS
3. Lighting up Biology: Bioluminescence Imaging to Monitor Cellular Interactions

in Live Animals. OC-ACS High School Awards Dinner Keynote Address, University of California, Irvine, 201

2. Expanding the bioluminescent toolbox *in vivo* imaging. Graduate and Post-doctoral Student Colloquium, University of California, Irvine, Department of Chemistry, 2011.

1. Formation of N-Alkylpyrroles *via* Intermolecular Redox Amination, Grinnell College, 2007.

POSTER PRESENTATIONS

4. Paley, M. A.; McCutcheon, D. C.; Steinhardt, R. C Prasad, S.; Prescher, J.A. Generating luciferase libraries for multi-component bioluminescence imaging, Pfizer Symposium, UC Irvine, 2013.

3. Paley, M. A.; McCutcheon, D. C.; Steinhardt, R. C Prasad, S.; Prescher, J.A. Generating luciferase libraries for multi-component bioluminescence imaging, ACS National Meeting, 2012.

2 McCutcheon, D. C.; Paley, M. A.; Steinhardt, R. C. Efficient Synthesis of luciferin analogs for multi- component imaging. ACS National Meeting, 2012.

1. Effects of Chronic Varenicline in Mice: Comparison to Nicotine. Sharon R. Grady*, Nick C. Ortiz, Miranda Paley, Emily A. Willis, Michael J. Marks. Society for Research on Nicotine and Tobacco National Meeting. 2011.

SKILLS

Laboratory: Molecular Subcloning, Bioluminescence Assays, Tissue Culture, Protein Expression and Purification, Enzyme Assays, Fluorescence Microscopy,

Computer: MS Excel, MS Word, MS PowerPoint, EndNote, Papers, Adobe Photoshop, Adobe NDesign, Chem/BioDraw, DNAStar Suite, MacPymol, XWinNMR,

OTHER RELEVANT EXPERIENCE

Science Communications Intern, June, 2014-present
Johnson & Johnson, New Brunswick NJ
Working in the Corporate Communications division. Responsibilities include, articles for external and internal portals, tweets for the @JNJInnovation handle, updating the Dr. Paul Janssen award website and preparing the NYAS symposium, research for the office of the Chief Medical Officer

Represented UCI at CASE Workshop, March 2014
AAAS, Washington DC
Catalyzing Advocacy in Science and Engineering- workshop. I learned Congressional procedures, the federal budget process, and effective communication. Lobbied US Congressional staff on behalf of UC students.

ABSTRACT OF THE DISSERTATION

Expanding the bioluminescent toolbox for *in vivo* imaging

By

Miranda Amelia Paley

Doctor of Philosophy in Chemistry

University of California, Irvine, 2014

Professor Prescher, Irvine, Chair

Bioluminescence imaging (BLI) is among the most dynamic imaging modalities for visualizing whole cells and gene expression patterns *in vivo*. This technique captures light emission from the luciferase-catalyzed oxidation of small molecule luciferins with highly sensitive CCD cameras. While powerful, current options for multiplexed BLI in mice are limited by the number of luciferase/luciferin pairs found in nature. Our lab aims to expand the bioluminescent toolkit by pairing mutant luciferases with synthetic luciferin analogs, to biochemically resolve multiple targets *via* sequential administration of the substrates. Several generations of luciferase mutant libraries were screened against sterically and electronically modified families of luciferins, in order to find orthogonal pairs. Promising luciferases were expressed recombinantly for biochemical analysis with their respective luciferins. These pairs were evaluated for their potential for multicomponent *in vivo* imaging.

CHAPTER 1: Bioluminescent tools

for the study of biological processes

1.1 Introduction

A complete understanding of living systems requires methods to probe cells and discrete biomolecules within their native environs. Protein trafficking, metabolite production, and even whole cell movements are influenced by diverse spatial and environmental cues that cannot be easily recapitulated outside of a living organism. In recent years, a set of imaging technologies has emerged that enable biological features to be visualized—noninvasively—in whole cells and organisms [1-10]. These methods are providing unprecedented insight into cell and organismal biology, and revealing previously unknown mechanisms of disease formation.

Among the most popular noninvasive imaging tools are the bioluminescent proteins (luciferases) [1-10]. Luciferases, unlike fluorescent probes, do not require incident radiation to produce light. Rather, these enzymes generate photons via the catalytic oxidation of small molecule substrates (luciferins). Luciferases can be expressed in numerous cell and tissue types, and when luciferin is present, light is produced [1,11-13]. There are virtually no endogenous light-emitting processes in mammalian cells and tissues, so the background signal in bioluminescence imaging is negligible. The high signal-to-noise values are attractive for sensitive imaging applications within complex environments. Indeed, bioluminescence has been used to

report on cell movements, gene expression patterns, and even the activities of individual biomolecules in whole tissues and animals [11,14-16]. In living organisms, bioluminescent light can be noninvasively detected at depths of a few centimeters, depending on the relative brightness and intensity of the signal, and the sensitivity of the detector. These distances are compatible with most rodent models and other small research animals. The versatility and user-friendly features of bioluminescence have ensured its application in multiple disciplines and biological discoveries [3,17,18].
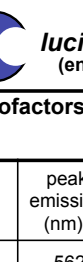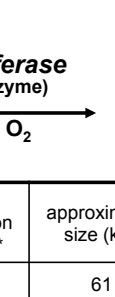
This chapter provides an overview of bioluminescence technology and how it can be used to monitor diverse biological features in complex environments. I first introduce luciferase-luciferin pairs commonly used for imaging and showcase their utility in visualizing cells and gene expression patterns *in vivo*. I then highlight methods to examine discrete biomolecules using engineered bioluminescent probes. These tools can illuminate the functions of proteins and other metabolites in cells and animals, providing a more detailed depiction of biological systems. Last, I describe ongoing work to expand the capabilities of bioluminescence technology using synthetic chemistry and molecular biology. Such advances promise to offer more refined views of cellular and biomolecular functions and potentially reveal new avenues for drug discovery.

1.1a Bioluminescent chemistries and colors

Several luciferase-luciferin pairs have been identified in nature, and a handful have been optimized for use in bioimaging applications (Table 1-1) [19]. The bioluminescent pairs differ in size and structure, but all exploit a common mechanism for light production: the luciferase binds a complementary luciferin and catalyzes the oxidation of the small molecule. The reaction produces an electronically excited

intermediate; relaxation of this molecule to the ground state produces a photon of light. Firefly luciferase (Fluc) and other insect luciferases release ~600 nm photons upon oxidizing a benzothiazole substrate (D-luciferin) with O_2 and ATP [20,21]. The wavelength is primarily dictated by the structure of the small molecule emitter, but also impacted by residues within the enzyme. Thus, while all known insect luciferases utilize D-luciferin, their emission spectra vary owing to subtle differences in enzyme architecture [12,20,22,23]

luciferase	luciferin	peak emission (nm) *	approximate size (kD)	comments	references
firefly luciferase (Fluc)		562	61	Largest percentage of >600 nm light emitted among classes of luciferases. Primarily used intracellularly due to requirement for ATP.	33, 27
click beetle green (CB green)	D-luciferin	537	61		
click beetle red (CB red)		613	61		
Renilla reniformis (Rluc/Rluc8)		482/487	36	All can be used extra-cellularly. Mutant versions (e.g., Rluc8/Rluc8.6/Gluc4) offer brighter and/or more sustained emission.	25, 26, 32, 111, 137, 164
Gaussia princeps (Gluc)	coelenterazine (CTZ)	482	20		
Aequorea victoria (Aequorin)		470	22	Aequorin is "pre-loaded" with CTZ, and light is emitted upon Ca^{2+} binding.	
Lux AB	long chain aldehydes + FMN cofactor	480	A: 42 B: 47	Mostly limited to use in bacteria; lux operon (*luxCDABE*) encodes for all components necessary for light emission.	27, 28, 31
Vargula hilgendorfii (Vluc)	vargulin	462	62	Recently characterized bioluminescent system; can be used in tandem with other luciferase-luciferin pairs.	38

Adapted from 17, 19

Table 1-1 Luciferases and luciferins commonly used in bioluminescence imaging. All luciferases catalyze the oxidation of small molecule substrates (luciferins) to release visible light. Popular luciferase-luciferin pairs, along with their characteristic features, are outlined below. *Emission wavelength given for reaction at 25 °C.

Luciferases from marine organisms, including *Renilla reniformis* (Rluc) and *Gaussia princeps* (Gluc), catalyze the oxidation of an imidazopyrazinone substrate, coelenterazine, and release primarily blue-green light (460-480 nm) [24]. Rluc and Gluc, unlike Fluc, require no exogenous cofactors (other than O_2), making them suitable for use in extracellular environments and other spaces lacking ATP [25,26]. Bioluminescent bacteria also release blue-green light, but employ long-chain aldehydes, heterodimeric luciferases and flavin cofactors in the light-emitting reaction. Interestingly, the luciferase subunits and all enzymes required for bacterial luciferin production are coded within a single operon (*lux*) [27 ,28]. Importing this entire gene sequence into non-luminescent bacteria—or even some eukaryotic cells—is sufficient to make them "glow" continuously [29-31]. By contrast, the luciferin substrates for Fluc, Gluc, and Rluc must be supplied exogenously in a given imaging experiment. The biosynthetic origins of coelenterazine and D-luciferin remain unknown, even though decades have passed since their chemical structures were first identified [12,20,32-34]. The elucidation of these biosynthetic pathways will be aided by efforts to isolate and characterize bioluminescent machinery from other organisms [12,20,21,24,35-38]

Among the bioluminescent pairs, the luciferase and luciferin from the firefly (Fluc and D-luciferin, respectively) are the most widely used for imaging *in vivo* [21]. D-Luciferin is relatively stable and can penetrate most cell and tissue types [39]. Coelenterazine, by contrast, is less bioavailable and requires intravenous administration to reach its targets in vivo. D-Luciferin may be administered *via* an intraperitoneal injection. The benefit of this method is that unlike tail-vein injections, the number of administrations is essentially unlimited and less technically demanding. This luciferin is

also cleared rapidly from animals and prone to air oxidation, resulting in non-specific background signal. Furthermore, coelenterazine luminescence with Rluc and Gluc is blue-green in color; wavelengths of this sort are readily absorbed by hemoglobin and other chromophores *in vivo*, preventing their detection by imaging cameras [16]. Red light (>600 nm) more readily passes through blood and overlying tissues, and these wavelengths are the ones captured by detectors in a typical bioluminescence experiment [11,16]. While Rluc and Gluc emit mostly blue-green light, their emission spectra are sufficiently broad to contain wavelengths >600 nm, and are thus useful for routine bioluminescence imaging. Fluc and click beetle luciferases emit a larger percentage of red light, making them more suitable for *in vivo* applications [40].

1.2 Traditional applications of bioluminescence imaging

Bioluminescence was first harnessed for *in vivo* imaging in 1995, when the *lux* operon was introduced into a non-luminescent strain of *Salmonella typhimurium* [31]. Upon inoculation into mice, the "glowing" bacteria could be readily identified and even localized (noninvasively) to discrete tissues. Moreover, changes in the infection profile were easily visualized in response to antibiotic treatment. This classic study showcased the remarkable sensitivity and broad dynamic range of bioluminescence for imaging in live animals, along with its potential for facilitating therapeutic discovery.

Since then, bioluminescence has evolved into a mainstream technique for visualizing not only bacteria, but also viruses and other pathogens, eukaryotic cells, and even gene expression patterns in live organisms [41,42]. Variants of Fluc, Rluc, and Gluc that offer brighter and more sustained light emission have been described (e.g., Rluc8,

Rluc8.6, Gluc4) [26,43,44], and these can be readily introduced into numerous cell and tissue types using standard gene transfer techniques. For cells and tissues that are refractory to genetic manipulation, luciferase-labeled transgenic mice can serve as convenient sources of bioluminescent material [1]. Finally, the common luciferin substrates can be purchased from commercial vendors, and standard bioluminescence detectors are available at most research settings. The relative simplicity of bioluminescence imaging, combined with these user-friendly features, has enabled rapid discoveries in a broad spectrum of a broad spectrum of fields [3,45,46].

1.2a Cell tracking

Luciferase-expressing cells can be imaged repeatedly and noninvasively in live animals, with the intensity and spatial distribution of the signal correlating with the number of cells and their location, respectively [1]. Thus, bioluminescence imaging is well suited for tracking cells *in vivo*, and many experiments—spanning several disciplines—have capitalized on this feature. For example, Contag and co-workers utilized bioluminescence to monitor hematopoiesis following bone marrow transplantation [47]. Such transplants are routinely used to treat leukemia and other blood cancers. In a typical procedure, a patient's diseased cells are first ablated (via radiation) and then replaced by blood cells from a healthy donor. The donor cells responsible for blood regeneration are hematopoietic stem cells (HSCs) found in bone marrow. HSCs initially engraft in the recipient before dividing and differentiating to reconstitute the hematopoietic system. The success of bone marrow transplantation has been mixed due to host immune clearance and other mechanisms. Thus, methods to visualize HSCs at early time points post-transplantation could offer insights into hematopoiesis and

methods to improve the therapy. Toward this end, the authors harvested bone marrow from luciferase-expressing transgenic mice and delivered it into irradiated recipient mice. The engraftment and proliferation of the cells was visualized upon D-luciferin administration. The images revealed that HSCs take up residence at multiple sites post-transplantation during hematopoiesis, with no single site necessary for full hematopoiesis (Fig 1-1 A). In addition, it was noted that transplantation of a single HSC could result in successful immune cell outgrowth.
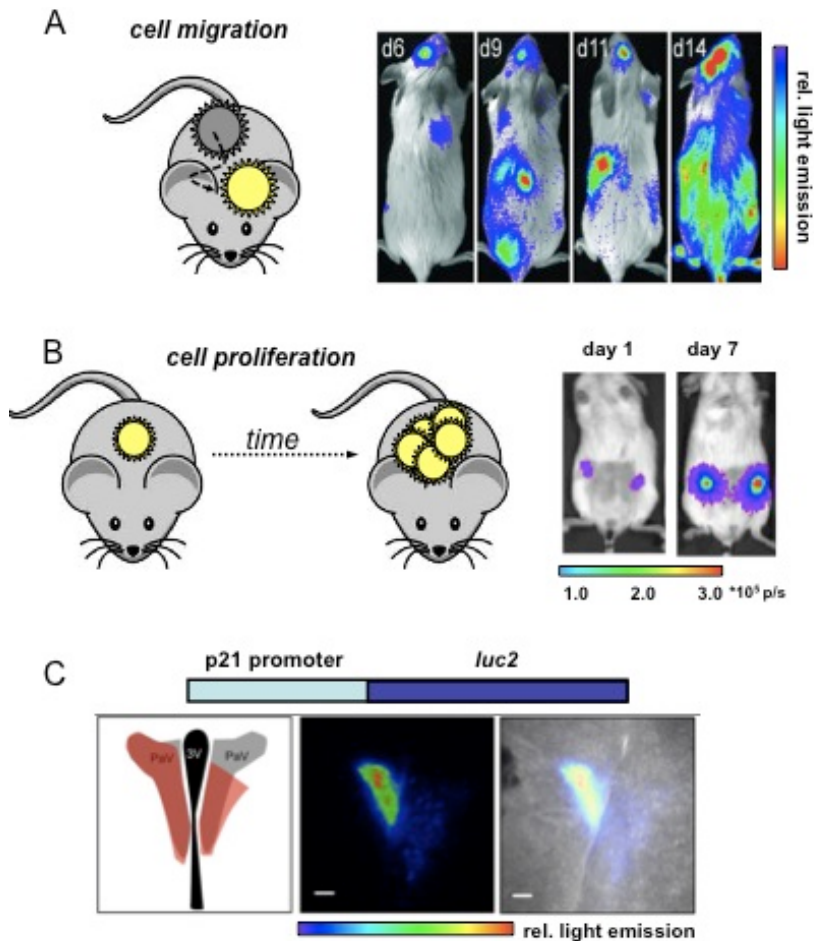
Figure 1-1 Tracking cells and gene expression with bioluminescence imaging. (A) Example of monitoring cell migration. Luciferase-labeled hematopoietic stem cells (HSCs) were transplanted into irradiated mice. Bioluminescence imaging with D-luciferin revealed multiple foci (sites of engraftment) at early time points. HSC differentiation and proliferation resulted in full regeneration of the blood system in these mice (as evident by the increase in spread and intensity of bioluminescent signal). Reprinted with permission from ref. 47. Copyright (2004) National Academy of Sciences, U.S.A. (B) Example of visualizing cell proliferation. Primary human cancer stem cells were transfected with luciferase genes and implanted into mouse mammary fat pads. Bioluminescence imaging revealed cell proliferation several weeks before palpable tumors emerged. Reprinted with permission from ref. 48. Copyright (2010) National Academy of Sciences, U. S. A. (C) To visualize gene expression, a luciferase gene (e.g., luc2) can be fused to the promoter for a gene of interest (e.g., p21). Cellular transcription of the target gene results in luciferase production. Luciferase was inserted downstream of an endogenous p21 promoter in transgenic mice, and regions of the mouse brain were probed for p21 activity using bioluminescence. From left to right: schematic of the mouse brain highlighting the paraventricular nucleus (PVN), the site of expected bioluminescence (red); bioluminescent image of brain tissue; overlay image showing localization of bioluminescent signal in the PVN. This research was originally published in ref. 61. Copyright (2013) the American Society for Biochemistry and Molecular Biology.

In a more recent example, bioluminescence technology was used to rapidly assay the proliferation of cancer stem cells *in vivo* and examine their roles in metastases [48]. The authors isolated cancer stem cells from patient breast tumor biopsies and transduced them with genes encoding Fluc or Rluc. The luciferase-expressing cells were implanted orthotopically in immunocompromised mice and monitored over time. The imaging studies revealed that only certain subsets of cells (i.e., "cancer stem cells") were capable of proliferating *in vivo* and thus perpetuating tumor growth (Figure 1-1 B). These same subsets of cells were also located at secondary tumor sites, establishing one of the first connections between cancer stem cells and metastatic outgrowth. Impressively, as few as 10 Fluc-labeled cells could be visualized *in vivo*, suggesting that bioluminescent tools are amenable to monitoring patient tumor growth and therapeutic responses in surrogate hosts. Similar cell tracking experiments have been performed using immune cells [49,50], stem cells [51-55], and even pathogens [31,45,56,57].

1.2b Visualizing gene expression

In addition to examining whole cell movements and behaviors, bioluminescence technology has been widely employed to monitor gene expression patterns *in vivo* [42]. Such studies can offer more detailed insights into biological mechanisms than cell tracking alone. In a typical experiment, luciferase expression is driven by the promoter sequence for a gene of interest or genetic elements that are responsive to specific transcription factors. The bioluminescent enzyme is thus transcribed only when the relevant genes are "turned on." The magnitude and duration of luciferase expression in these assays mirrors that of the target gene, and expression patterns relevant to inflammation, cancer, and Alzheimer's disease have all been imaged (and often

quantified) in this regard [1,58-60]. In a recent example, Piwnica-Worms and colleagues utilized engineered mice to examine the dynamic expression of p21 *in vivo*. P21 is a cyclin-dependent protein kinase (CDK) inhibitor involved in cell cycle regulation [61]. Mice expressing Fluc under the control of an endogenous p21 promoter were treated with D-luciferin and imaged. Interestingly, fluctuations in bioluminescent light were observed in discrete regions of the brain responsible for nutrient sensing (Figure 1-1 C). These results implicate p21 expression in the regulation of metabolism.

1.2c Monitoring protein abundance and function

A complete mechanistic understanding of living systems requires methods to probe not only cells and gene transcription, but also individual biomolecules. Proteins comprise one of the major classes of cellular biomolecules and fulfill an array of functions. Abnormal protein activities can disrupt major signaling networks, alter biosynthetic pathways, and compromise membrane integrity, all of which can potentiate disease. Given their central roles in cell structure and function, proteins are popular drug targets; new candidates for therapeutic targeting require an increased understanding of protein function in tissues and organisms. Bioluminescence imaging is already having an impact in this area [3]. Over the past decade, engineered luciferases and luciferins have been crafted to report on numerous facets of protein biology, including their localization and stability, interactions with other proteins, and enzymatic functions. Several examples are provided below.

Direct attachment of luciferase to proteins of interest can be used to monitor the location and abundance of the biomolecules. Indeed, luciferase fusions have been used to visualize a variety of proteins, including the signaling biomolecules HIF-1α and β-

catenin [62,63], along with proteins destined for proteasomal degradation [64]. Luciferase fusions alone, though, cannot provide read-outs on discrete protein activities, including their interactions with other proteins. Protein-protein interactions drive major signaling cascades in human cells, and disruption of these contacts often contributes to disease [65]. Luciferase probes can provide noninvasive readouts on protein associations and facilitate screens of therapeutic agents to modulate these networks. In one well-known approach, luciferase and a spectrally matched fluorescent probe are fused to the proteins of interest [66]. When the proteins are far apart, only bioluminescent light emission is observed in the presence of the appropriate luciferin. When the targets are in close proximity, the bioluminescent photons drive the excitation of the fluorescent chromophore, resulting in light emission at a longer wavelength. This phenomenon, termed bioluminescence resonance energy transfer (BRET) has been used to examine kinase-kinase, receptor-peptide, and other protein-protein interactions, in cells and live animals [7,66,67]. BRET studies require spectrally matched probes: the luciferase emission wavelengths must overlap the fluorescent probe's excitation spectrum. Many Rluc-yellow fluorescent protein and Rluc-quantum dot combinations meet this criterion and have been utilized for visualizing protein interactions and other biological processes [64,67,68]. For work *in vivo*, the identification of more red-shifted BRET pairs remains an important goal [69-73]. The Gambhir and Piwnica-Worms labs recently developed BRET systems comprising luciferase-fluorescent protein fusions that emit 550-650 nm light, making them more attractive for deep tissue imaging *in vivo* [44,69,74]. Further improvements in BRET technology are expected with the identification of more

luciferase-fluorescent protein duos in nature [75], along with the development of improved luciferase-nanomaterial conjugates [76,77].

Protein-protein interactions can also be visualized using luciferase complementation [70-73]. In these assays, "split" fragments of a luciferase are attached to proteins of interest. Functional enzyme is produced only when the interacting proteins come into contact and drive the assembly of the complementary pieces [72,73].
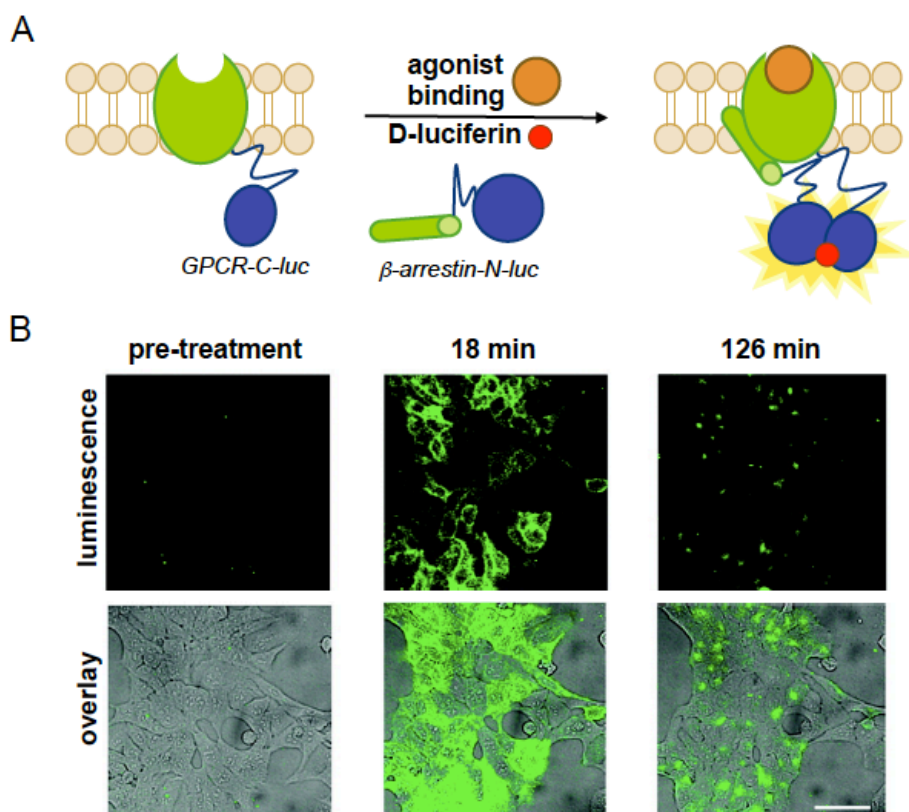
Figure 1-2. Visualizing protein–protein interactions with Fluc complementation. (A) β-Arrestin is an antagonist of GPCRs, de-sensitizing the receptors upon external stimulation. When β-arrestin binds BARK (a known GPCR) in the presence of certain therapeutics, the GPCR is less responsive and, as a result, cells are less sensitive to hormones and other stimuli. BARK–β-arrestin dimerization can be visualized using "split" versions of Fluc. In the presence of GPCR agonists, β-arrestin binds the GPCR, enabling Fluc fragment complementation and bioluminescent signal production. (B) HEK cells expressing GPCR–C- luc and β-arrestin–N-luc were stimulated with a known agonist, isoproterenol and imaged over time. Bioluminescence signal is over- laid on bright field images. Reprinted with permission from ref. 79. Copyright (2012) American Chemical Society.

"Split" versions of Fluc, Rluc, and Gluc have all been described, and used to monitor protein dimerization events, including the rapamycin-induced interaction of FRB and FKBP [70,72,73,78]. In a recent example, Ozawa and co-workers visualized the binding of β-arrestin to β-adrenergic recptor kinase (BARK), a membrane GPCR. When BARK is activated upon agonist binding, β-arrestin subsequently binds the GPCR to turn off the response and reset the system; the rate of β-arrestin association correlates with the potency of the ligand. The authors visualized BARK-β-arrestin binding using split Fluc probes [79]. Upon administration of small molecule agonists, conformational changes in BARK-C-Luc promoted the binding of β-arrestin-N-Luc (Figure 1-2). This dimerization event enabled complementation between the two termini of Fluc, and ultimately light production. Using this split luciferase system, the authors quantified the relative potency of a panel of drugs.

1.3 Measuring enzymatic activities in complex environments

Proteins drive cellular processes not only via their associations with other proteins, but also via enzymatic reactions. Several classes of enzymes have been identified to date, and many—including kinases and proteases—play integral roles in cell signaling. Aberrant enzyme activities are also associated with numerous pathologies and are commonly measured in clinical isolates to diagnose disease [80,81]. Engineered luciferases and luciferins have been developed to report on enzymatic activities in real time. In addition to providing a dynamic readout on protein function in complex environments, these imaging tools can facilitate screens for therapeutics designed to either inhibit or enhance enzymatic activity [82].

Among the most well recognized probes for measuring enzyme function are the "caged" luciferins. These molecules comprise luciferin cores outfitted with steric appendages (i.e., "cages") or other groups that perturb its use in the bioluminescent reaction [83]. Most "cages" are appended to the 6' end of D-luciferin. A small, electron-donating group (e.g., -OH or NH_2) at this position is required for light production [33]; installing electron-withdrawing or bulky groups inhibits bioluminescence [84,85]. If the "cage" is labile to defined enzymatic activity, though, luciferin is released and available for the light emitting reaction. In these cases, light emission provides a direct readout on enzyme function. Phosphatase, sulfatase, and oxidase activity have all been visualized in this regard, and nearly a dozen caged luciferins are now commercially available to measure enzyme function in live cells or lysates (Table 1-2) [83,86-93]. Bertozzi and co-workers recently introduced a novel cage to report on the activity of certain sulfatases (row 3, Table 1-2) [94]. The aryl sulfate-caging group was found to be readily cleaved by sulfatases expressed in *Mycobacterium tuberculosis*, but not those found in human serum. These data suggest that the caged probe may have utility in the clinical diagnosis of pathogens (entry 5, Table 1-2).

Most recently, our group introduced another generalizable luciferin cage based on nitroreductase (NTR) activity. A 6' position nitro group deprives the luciferin core of the electron density required to extrude CO_2 in the oxidation reaction. NTR, a bacterial enzyme not found endogenously in mammalian tissues, reduces aryl nitro groups to highly reactive hydroxyl amines. Porterfield *et. al.,* demonstrated that this hydroxyl aminoluciferin was a robust light emitter, and its instability prevented a large build-up of the uncaged luciferin. This feature prevented large quantities of the probe

from diffusing away and kept it localized near the source, making it well suited for the study of cell-cell interactions. When NTR was expressed in one cell-type of interest, and Fluc is expressed in another, light emission was only observed when the two cell types were in direct contact. Such robust and orthogonal caging schemes will improve our ability to track cell contacts *in vivo* [95].

Table 1-2 Caged luciferins report on enzyme activities. "Caged" versions of D-luciferin have been used to image a variety of enzymatic activities and physiological states.
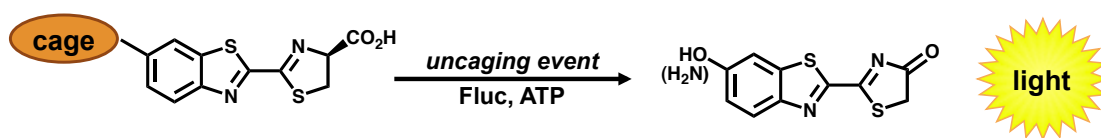
cage	structure	uncaging condition	reference
galactose (Lugal)		β-galactosidase	87
6-amino-acyl peptide	DEVD RVRR/RYKR Nle-P-Nle LRR	caspase 3/7 furin protease proteasome trypsin	88 89 90 91
alkyl amino		monoamine oxidase(s)	92
boronate (PCL-1)		H_2O_2 (non enzymatic)	93
sulfate		sulfatases	94
nitro (Luntr)		nitroreductase (NTR)	95

15
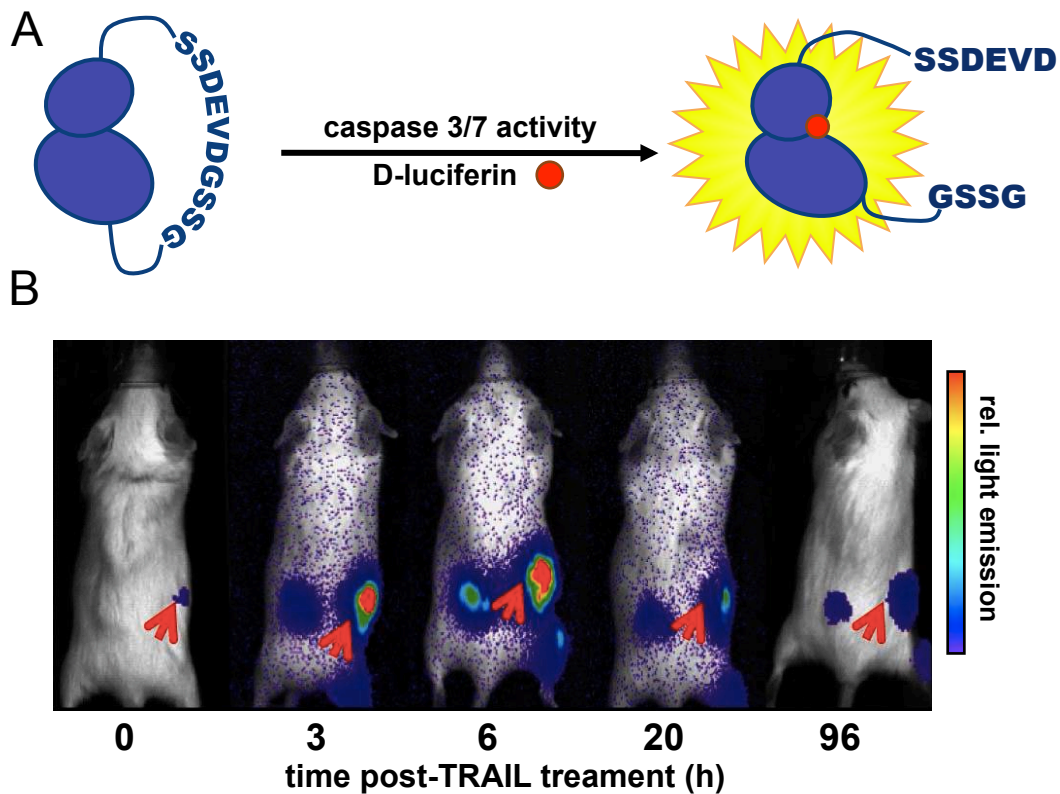
Figure 1-3 Activatable luciferases report on enzymatic activities. (A) A circular Fluc probe (caspase 3/7 GloSensor), comprising a specific caspase recognition sequence (DEVD) was prepared. In the absence of caspase activity, functional Fluc is not formed and bioluminescence is minimal. In the presence of caspase activity, the tether is cleaved, providing functional Fluc. (B) D54-MG glioma cells ($2 * 10^6$) stably expressing the caspase 3/7 bioluminescent reporter were implanted into NOD/SCID mice. When tumors emerged, the animals were treated with TRAIL, an activator of caspase activity. Bioluminescence imaging with D-luciferin revealed an increase in signal over time (red arrows), correlating with caspase induction. Reprinted in accordance with open-access license from ref. 99.

In addition to engineered luciferins, "designer" luciferases can provide direct readouts on enzyme function [96-98]. The majority of these probes comprise cyclic versions of luciferase that are locked into conformations with various linkers, and thus incapable of binding substrate and producing light. Upon cleavage of the tether ("activation" of the probe), the luciferin-binding site is revealed. Wood and colleagues generated a series of such "activatable" luciferases using protease-specific linkers to mask the luciferin-binding pocket. Cleavage of the tethers in the presence of defined protease activity enables luciferin access, light production, and ultimately a readout on protease function. An "activatable" luciferase was recently used to monitor caspase-7 activity in both live cells and *in vivo* tumor models (Figure 1-3) [99].

BRET sensors represent another major class of bioluminescent reporters for enzyme activity. These sensors comprise luciferases that are physically linked to a BRET-matched fluorescent protein [66,100]. If the adjoining link is severed by enzymatic activity, the luciferase and fluorescent protein diffuse apart, and the ensuing reduction in BRET signal correlates with enzyme function. A BRET sensor was recently developed to measure caspase activity in primary macrophages [68]. Caspase-1 is known to activate several inflammatory signaling molecules via proteolytic cleavage. The chemokine IL-1β is one such substrate that plays a pivotal role in cellular apoptosis. Active IL-1β is generated via caspase cleavage of a proprotein (pro-IL-1β). The pro-IL-1β cleavage is rapid and not easily monitored via Western blot or other traditional cell biology assays. To capture this activity, Pelegrin and co-workers designed a BRET sensor comprising Rluc8 and a yellow fluorescent protein (Venus) linked by pro-IL-1β. When expressed in cells and in the absence of high levels of caspase activity, the sensor remains

intact and yellow light is produced upon coelenterazine treatment (Figure 1-4). (The blue photons emitted by Rluc8 are absorbed by Venus and emitted as yellow light.) Upon caspase-1 activation and cleavage of the sensor, Rluc and Venus separate and mostly blue bioluminescent emission is observed (Figure 4 A). The ratio of blue to yellow light in each case can provide a measure of caspase activity and IL1β activation and, more broadly, the inflammatory response (Figure 1-4 B).
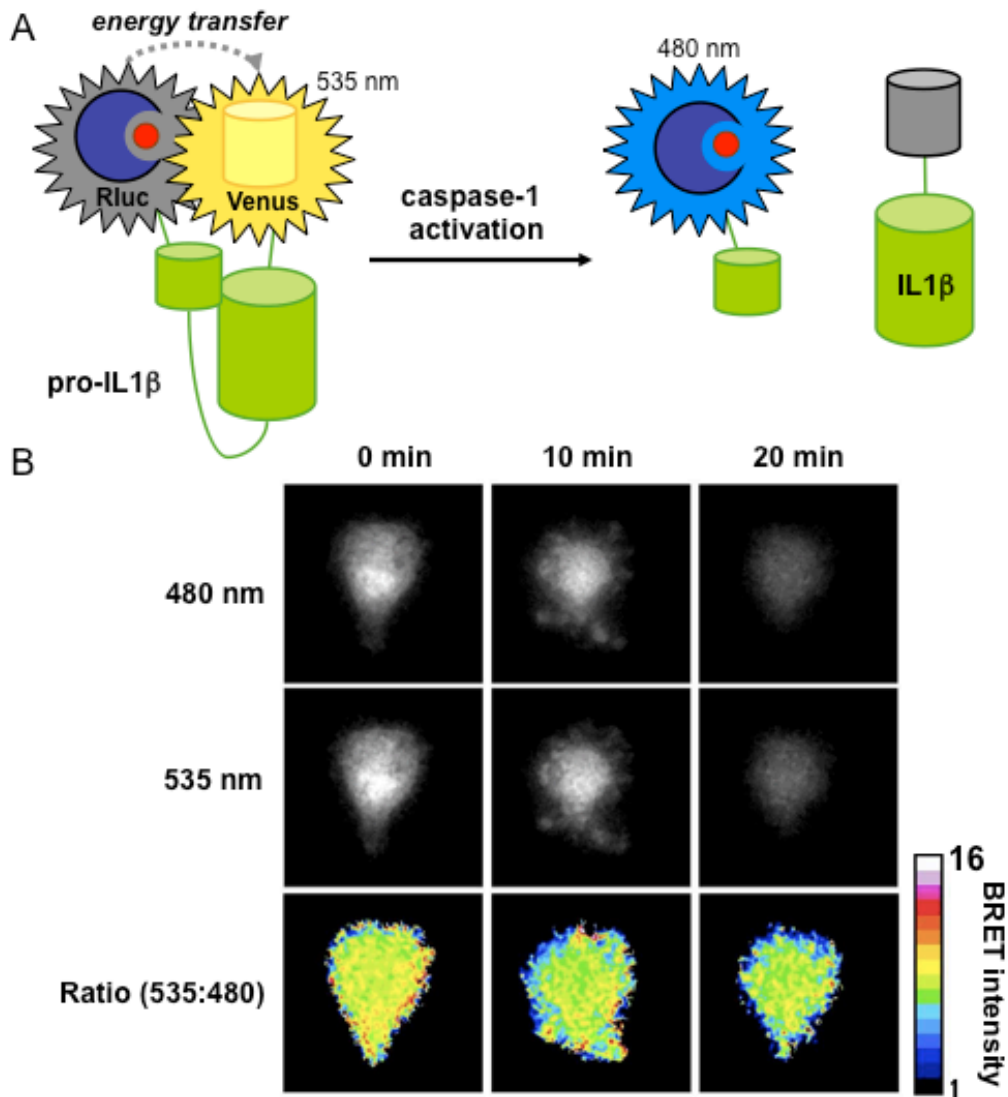
Figure 1-4 Visualizing enzyme function with BRET sensors. (A) IL-1β is produced as a non-active pro-protein in macrophages. When cleaved by the cysteine protease caspase-1, IL-1β stimulates a host of pro- inflammatory responses. The release of active IL-1β can be visualized using a BRET sensor. This probe comprises Rluc, Venus fluorescent protein, and an intervening IL-1β pro-protein sequence. Prior to caspase-1 activation, the sensor remains intact, with the luciferase and fluorescent protein in close proximity (BRET is observed). Upon caspase-mediated cleavage of the pro-protein, Rluc and Venus separate, resulting in reduced BRET signal. In the former case, 535 nm light (Venus emission) is observed in the presence of coelenterazine. In the latter case, mostly bioluminescent light (480 nm) is observed. (B) The Gluc-IL-1β-Venus sensor was transfected into primary macrophages. Upon caspase activation, images were acquired at both 535 nm and 480 nm. Decreased levels of 535:480 nm light were observed over time, correlating with of caspase activity and the presence of active IL-1β. Reprinted with permission from ref. 68. Copyright 2012, The American Association of Immunologists, Inc.

1.4 Probing metabolites with bioluminescent sensors

While proteins comprise the bulk of cellular matter, other biopolymers including glycans and lipids, in addition to metabolites and ions also play pivotal roles in cell biology. Methods to visualize the abundance and activities of these species are thus required for a complete understanding of living systems. Imaging such non-primary gene products has been historically challenging [101]. Such molecules cannot be fused genetically to luciferase or other optical reporters for direct tracking. Rather, indirect methods for visualization must often be employed [102]. Bioluminescent probes can be engineered to report on a diverse array of biomolecules, and examples from the recent literature are highlighted below.

Nucleic acids, like proteins, are often associated with certain physiological states and can report on the presence of pathogens. For example, methods to rapidly detect DNA from "foreign" microorgansisms would simplify and hasten clinical diagnoses, where positive pathogen identification can take days. Toward this end, Kebukuro and colleagues utilized bioluminescence to detect bacterial DNA in biologically relevant sample sizes [103]. Their platform involved zinc finger domains conjugated to Fluc. Zinc fingers recognize specific stretches of nucleic acids and can be readily evolved to bind virtually any target. Bioluminescence imaging of the DNA samples provided a visual readout of the desired sequence with femtomole sensitivity without the need for gel analysis. Eventual automation this type of procedure is promising for clinical

translation. Bioluminescent tools have also been applied to image other major classes of biopolymers, including glycans and lipids [104-106].

Certain small molecule metabolites can also be visualized with bioluminescence technology. For example, all luciferases require molecular oxygen for light production, and bioluminescent emission can be used to approximate O_2 levels in solid tumors [107-109]. Bioluminescence can also report on metabolites that are required for luciferase activities. For instance, Fluc is routinely employed to report on ATP levels in cell extracts and sequencing analyses [110-112]. The photoprotein Aequorin requires exogeneous Ca^{2+} for light production, and can be employed for visualizing calcium flux in nerve cells [113]. For other metabolites and analytes of interest, luciferase reporter genes are often used. Levels of glycolysis intermediates, hormones, and metals have been measured in this regard [110,114-119]. BRET constructs have also proven valuable in sensing small molecules' interaction with other biomolecules within cells [120-122]. Engineered luciferins can also be used to image cellular metabolites [83]. In a recent report, cellular peroxide levels were measured with a phenyl boronate probe (entry 4, Table 2). The boronate group is labile to peroxide, one of many reactive oxygen species (ROS) generated in activated cells [93,123]. More recently, the Chang lab modified this caged probe to report on two analytes relevant to inflammation [124]. This luciferin was ultimately used to image both ROS production and protease activity in various cancer cell lines. We anticipate further multi-analyte imaging studies as new methods for luciferin caging are developed.

1.5 Drug screening and drug development

Since luciferase light emission requires ATP and new protein production, bioluminescence is a simple and direct assay for cell viability and proliferation [40,48,50,55,73]. Indeed, global reductions in light emission have been used as readouts of cell death in many examples introduced in this article[125-129]. Bioluminescence is also an attractive choice for monitoring cell viability and potential therapies in heterogeneous models. The McMillin group recently demonstrated the utility of bioluminescence for drug screening with mixtures of stroma and tumor cells—a more realistic model of human tumors [130,131]. The authors cultured various Fluc-expressing tumor cells with stromal cells in the presence and absence of common chemotherapies. Cytotoxicities were correlated with reductions in light output. While many of the cell lines demonstrated increased resistance to certain drug treatments in the presence of stromal cells, the effect was not common to all cell lines or drugs. These results demonstrate that bioluminescence imaging can provide a facile and high throughput screening method for models that better recapitulate the heterogeneity of human cancers and other diseases. That said, non-specific interactions between pharmacophores and Fluc have historically confounded the discovery of small molecule therapeutics [132-134]. The development of new luciferases and luciferins could potentially circumvent these issues, and work is ongoing in this area [135].

Beyond direct measures of cell death, Bioluminescence has aided drug discovery efforts in additional areas. For example, this imaging technology can be used for the direct tracking of therapeutics *in vivo*. The ability to visualize both protein and small

molecule biologics provides insights into delivery and targeting. In a recent example, Gluc was appended to an anti-CEA antibody and used to detect tumors expressing the CEA antigen *in vivo* [136]. Gluc is among the brightest luciferases characterized to date and is functional in extracellular environments, making it an attractive choice for diagnostic imaging [137,138]. Similarly, small molecule delivery can be probed using luciferins as surrogate drugs. In one example, Wender and co-workers used an octaarginine tailed luciferin to optimize the design of cationic peptide tags for intracellular drug delivery [139]. In these studies, bioluminescent emission correlated with successful drug localization. The authors ultimately utilized the arginine-rich tail to enhance the delivery of Taxol and other chemotherapeutics.

1.6 Building better bioluminescent tools

Despite the broad utility and user-friendly features of existing bioluminescent tools, challenges remain in expanding the scope of the technology. Some of the obstacles arise from the probes themselves. Many luciferase proteins are only quasi-stable in mammalian cells [59]. This instability is useful for visualizing dynamic biological processes, where rapid turnover of the reporter is required. However, it is less desirable for long-term tracking studies or when large photon outputs and sustained emissions are desired. Mutagenesis studies have identified luciferases with improved temperature- and pH-stability in mammalian systems [43,44,140-144]. In a recent example, Tannous and co-workers evolved a variant of Gluc (Gluc4) that is more stable in standard mammalian cell assays and that provides more sustained light emission. Additionally, it has been

noted that reactive oxygen species can rapidly diminish the light observed from Fluc expressing cancer cells upon the induction of apoptosis. By contrast Rluc8 maintains relatively stable light emission under the same conditions generating ROSs, particularly hydrogen peroxide [145]. These features were found to improve drug screening results by decreasing the number of false positives associated with the rapid loss of signal with native Gluc [146]. The clearance of the luciferin substrate is also of concern. In a typical experiment, D-luciferin is cleared to background in less than an hour [147]. This rapid clearance rate can be beneficial for studies over longer timescales, but simultaneously means that continuous monitoring of can be difficult, due to shifting concentrations of substrate. There are several ingenious solutions to these problems, including new luciferin molecules and alternative delivery modulus. For instance, an osmotic pump provides continuous delivery of the substrate [61,148]. Other schemes for controlled release of luciferin include liposomes and cationic derivatives [139,149].

The same facets of bioluminescence that make it an incredibly strong research tool for the macroscopic scale, inherently can limit its use for microscopic work. The photon output from all luciferase enzymes is inherently weak, and only a fraction of the emitted light typically reaches the detector; the majority of bioluminescent photons are absorbed or scattered by endogenous chromophores in blood and tissues [44,69]. Currently, researchers often couple several optical imaging strategies to gain further insight to their system, particularly using bioluminescence to quickly determine tissues of interest, followed by dissection and *ex vivo* microscopy. Improvements in bioluminescence sensitivity and depth are possible by engineering luciferases to produce more tissue penetrant (i.e., red-shifted) light. Branchini and co-workers generated one

such luciferase by conjugating small molecule fluorophores (AlexaFluor 650 and 680) onto the surface of Fluc [150]. Following administration of D-luciferin, near infrared light is produced via BRET transfer from the bioluminescent reaction to the fluorophores on the enzyme surface. This chemically modified luciferase was used to image factor Xa in human blood samples, an assay that is problematic for traditional luciferase probes owing to photon absorption by heme groups.

While applicable to a variety of sensing assays *ex vivo*, it is not amenable to long-term cell tracking *in vivo*. For these studies, luciferase mutants with red-shifted emission spectra are desirable. A handful of such mutants have been described, although the gains in sensitivity due to altered emission wavelengths are often offset by lower enzymatic turnover numbers [11,22,23,151-153]. One notable exception is an Rluc variant recently reported by the Gambhir group (Rluc8.6-535). This luciferase not only provides a nearly six-fold improvement in the fraction of red light emitted, but also exhibits greater overall photon output than native Rluc [154]. Additional improvements in luciferase function are expected as more structural information becomes available [155]. The majority of methods to alter bioluminescent spectra and function have focused on modifications to the luciferase scaffold [43,146,153,156]. An alternative strategy for generating new or brighter "colours" of bioluminescent light involves modulating the small molecule luciferins. As noted earlier, the emission spectrum is primarily dictated by the chemical structure of the small molecule. The wavelength of light is dependent on the protonation state of the light emitting species. As pH is increased, more oxyluciferin exists as the phenol, which pushes the spectrum towards the yellow emission wavelengths. Increased temperature also red-shifts light emission [20]. While these factors do not impede the use

of bioluminescence in vivo, they can confound interpretation of certain experiments because the wavelength of light dictates the percentage of tissue permeant light [11]. Novel luciferin scaffolds can help improve these dynamics.

Thus, modifying the luciferin core itself can result in altered emission spectra [85,157-159]. In a recent example, Conley, *et al.* synthesized a luciferin analogue comprising a selenium atom in the place of sulfur (Figure 1-5 A). The altered electronic density in this heterocycle resulted in significant red-shifting of the emitted light [159]. Luciferin-fluorophore conjugates that exhibit altered wavelengths of emission have also been prepared (Figure 1-5 B) [160]. Analogous to the fluorophore-luciferase conjugate, these molecules exploit BRET: the electronically excited luciferin core is capable of energy transfer to a covalently bound fluorophore. Urano and colleagues synthesized a variety of these conjugates and found that both luciferin-Cy7 and luciferin-SiR700 provided a significant enhancement in >600 nm photons. Not surprisingly, though, these bulky luciferins were poorly utilized by native luciferase, resulting in reduced overall photon production. Identifying mutant luciferases that can efficiently utilize these probes, along with more spectrally tuned luciferin-fluorophore conjugates (for maximal BRET efficiency) are important next steps.
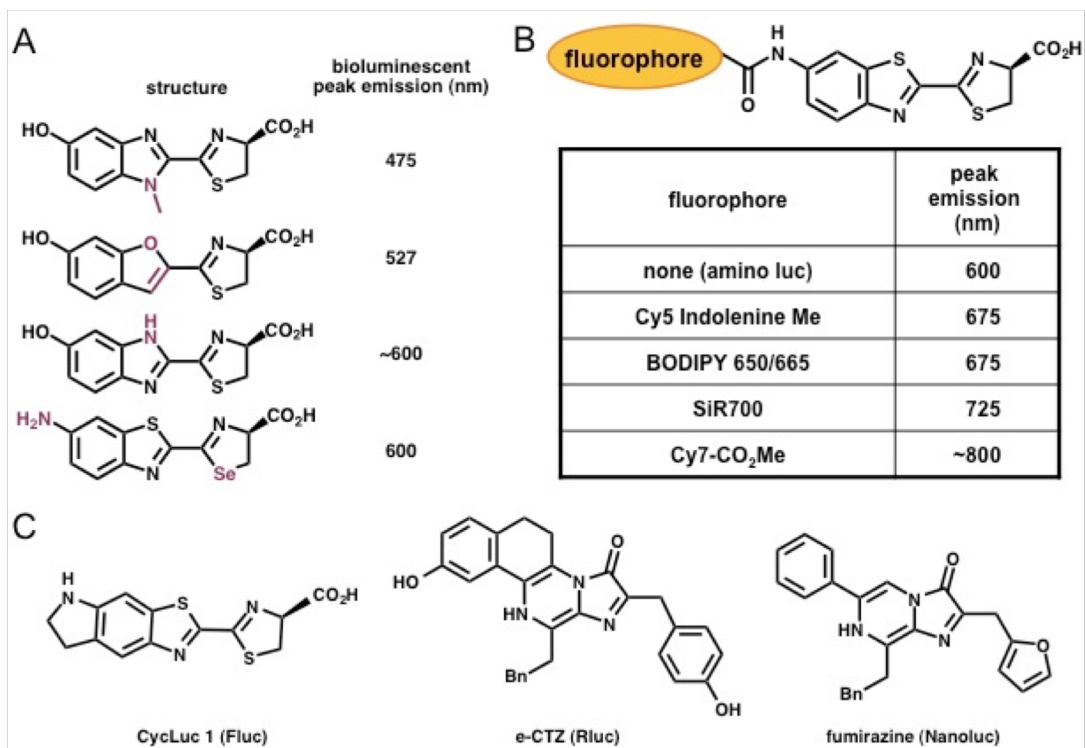
Figure 1-5 Luciferin architectures for improved bioluminescence imaging. (A) Examples of heterocyclic analogues of D-luciferin that exhibit altered bioluminescent emission spectra. (B) Luciferin-fluorophore conjugates also exhibit red-shifted emissions. (C) Chemical structures of three luciferins that exhibit robust emission with various luciferases.

Synthetic modifications to the luciferin core can not only provide altered bioluminescence spectra, but also improve the sensitivity of the imaging technique. In recent work, Miller and co-workers synthesized a cyclic aminoluciferin variant that is efficiently utilized by Fluc (Figure 1-5 C) [161]. The rigidified structure limits the non-radiative relaxation of the excited state molecule, thus improving the quantum yield of bioluminescence. We further demonstrated that this molecule has improved cell and tissue permeance in a variety of cultured cell and mouse models, resulting in more sensitive imaging [162]. More sensitive bioluminescence imaging with Rluc and Gluc is also possible using synthetic variants of coelenterazine [163,164]. In one example, a rigidified coelenterazine analogue was found to exhibit more robust light emission with Rluc(Figure 1-5 C) [165,166]. Coelenterazines with esters or benzyl groups at the phenol position also exhibit better signal-to-noise ratios in imaging studies with Rluc due to their enhanced stability (i.e., they are less prone to autooxidation). Unfortunately, these and most other coelenterazine analogues are not efficiently utilized by Gluc.

Several groups are attempting to address the need for improved coelenterazines and other luciferins that are efficiently processed by luciferases. Wood and co-workers recently designed a coelenterazine derivative (fumirazine, Figure 1-5 C) that is more stable than the native small molecule with lower rates of autoluminescence. To capitalize on these features, the authors engineered a new luciferase specific to this designer luciferin. As a starting point, they used the luciferase from the bioluminescent deep-sea shrimp *Oplophorus gracilirostris*. The native 106 kDa enzyme comprises two dimers of a large regulatory unit and a smaller catalytic core. A singular catalytic unit is capable of light-emission with coelenterazine, but in the absence of the regulatory unit, the light

emission remains dim. The authors identified the smallest domain in the enzyme that could retain catalytic activity (19 kD), and used rational mutagenesis to generate stable variants. To impart selectivity for fumirazine over coelenterazine, the group used additional rounds of mutagenesis and screened clones for stable light emission, thermostability and overall light output [36]. They eventually identified a variant, termed Nanoluc, that was over 100-fold brighter than Rluc and currently ranks among the smallest luciferases for biological imaging. Miller and co-workers used a similar approach to identify mutant versions of firefly luciferase that more efficiently catalyze light production with aminoluciferin variants [167].

The development of brighter and spectrally altered tools will continue to expand the capabilities of bioluminescence imaging *in vivo*. The ultimate goal would be to generate a diverse collection luciferase-luciferin pairs that could be used simultaneously for imaging *in vivo*. Such tools would enable multi-component cell tracking experiments, and monitoring of signal transduction in real time. So far, the majority of tools designed to expand the set of luminescent probes have focused on mutants with altered emission spectra (analogous to the fluorescent protein palette). Separating the bioluminescent pairs by color alone, though, is a lofty challenge, especially *in vivo* where the "color" of light observed by the detector is skewed by the depth of the emitter in tissue. This means that separating the blue-green-emitting Rluc from the yellow-emitting Fluc, by color, is difficult [16,168]. For this reason, multi-spectral bioluminescence imaging has largely been limited to studies *in vitro* [78,152,169]. While luciferases are not amenable to spectral resolution, they can be "biochemically" distinguished based on their specificities for distinct substrates. Sequential application of the substrates enables the desired targets

to be visualized in a single organism. This approach has already been applied to imaging mesenchymal stem cells and their interactions with breast cancer *in vivo* where the stem cells were tagged with an Fluc reporter, while breast cancer cells were monitored with Rluc [170]. Most recently, the *Vargula* (Vluc) luciferase-luciferin pair was used in tandem with Rluc and Fluc, enabling three distinct tumor cell populations to be imaged in mice (Figure 1-6) [171].

Moving beyond the naturally occurring systems, we expect that the design and implementation of orthogonal luciferase probes will be aided by new, improved and rapid syntheses of luciferin analogues [19,158,172]. We recently introduced a highly divergent luciferin synthesis that enables facile access to a variety of potential substrates [158]. Coupled with efficient means for the generation of luciferase mutants, we anticipate the development of more orthogonal bioluminescence systems [10,171,173-175].

With the continued development of new of luciferases and luciferins, researchers will soon have access to an expanded set of bioluminescent tools. In addition to the bioluminescent reactions, we expect that the current advances in bioluminescence will inspire the continued development of alternative luminescent imaging systems. Both enzyme-coupled and chemiluminescent systems are gaining traction as viable methodologies for visualizing and quantifying biological processes *in vivo* [176,177]. We anticipate that these new probes will broaden the scope of bioluminescence imaging, providing insights into macroscopic, multi-cellular behaviors ranging from immune function to tumor heterogeneity. We also expect creative new applications of bioluminescence in visualizing cell-cell contacts and other microscopic behaviors. Collectively, these studies will continue to refine our understanding of biological systems

and reveal new opportunities for therapeutic development.
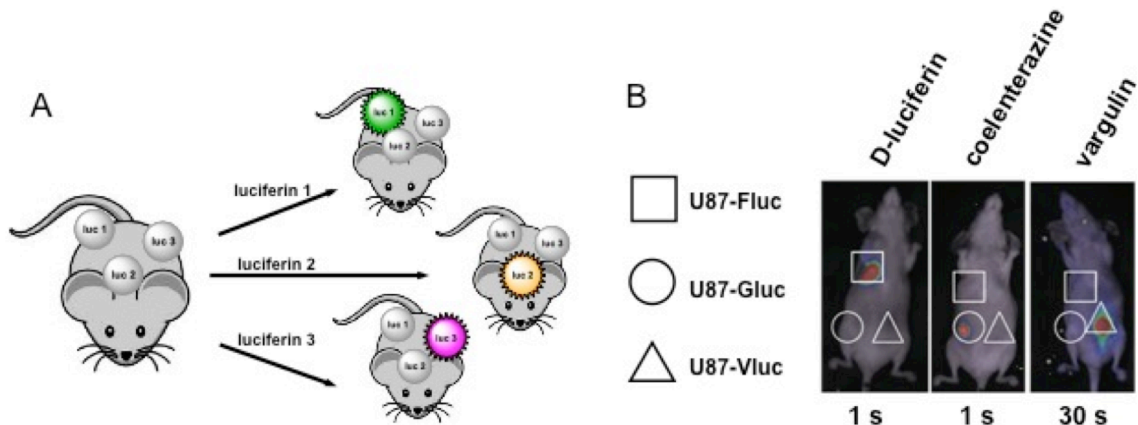
Figure 1-6 Orthogonal luciferase-luciferin pairs enable multi-component imaging *in vivo*. (A) Three unique cell types can be visualized using distinct luciferase-luciferin pairs. Sequential administration of the luciferins enables the target cells to be visualized. B. Fluc- (square), Gluc- (circle) and Vluc- (triangle) expressing glioma cells were implanted in distinct regions in a mouse model. The cells were selectively illuminated with D-luciferin, coelenterazine, and vargulin respectively, with one day separating each injection. Reprinted from ref. 171 by permission from Macmillan Publishers, Lt: Molecular Therapy - Nucleic Acids. Copyright 2013.

1.7 Objectives of this study

Despite the myriad of existing bioluminescent tools available, limitations exist in using them for imaging and quantifying multiple targets *in vivo*. To address this deficit, I aimed to develop a more generalized toolset. I envisioned that the components would be applicable for monitoring not only proteins and other biomolecules from the same toolset but also the interactions of different cell types in preclinical disease models.

My worked was inspired by applications of the fluorescent protein palette where color-coding biomolecules has helped elucidate cellular trafficking and signaling pathways. Only far-red light (>650 nm) escapes from mammalian tissue, meaning spectral differentiation with either fluorescent or bioluminescent probes in vivo is exceptionally difficult [11]. Instead, we proposed a biochemical resolution of bioluminescent signals for multicomponent imaging (Figure 1-7). Because the light emission event is the result of a luciferase-catalyzed process, there are many intimate contacts between this enzyme and its substrate. We therefore reasoned that a change in the substrate structure could be complemented with changes in the active site architecture, improving activity and engendering specificity. We believed we could screen for such "orthogonal" luciferase luciferin pairs using standard molecular biology techniques from libraries of Fluc mutants. Fluc was selected over other naturally occurring luciferases, as the target of our mutations due to its advantageous optical properties for in vivo imaging and the relative ease of synthesizing substrate analogues. Our approach would reveal unique interactions between luciferin analogues and their

particular luciferase mutants, allowing the pairs to be differentiated by administering the different luciferins over time.
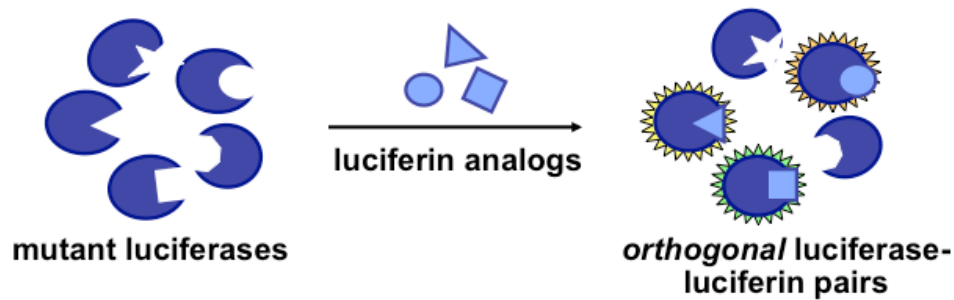
Figure 1-7 Multicomponent imaging strategy. Luciferase mutants and their matched luciferins will be identified *via* screening

To that end, I first aimed to:

1. Design and accrue various classes of luciferin analogues and demonstrate their viability for mutant luciferase screening (i.e., to validate their inherent, but not yet optimized ability to participate in the bioluminescent reaction).

2. Construct mutant Fluc libraries and rationally designed mutants, and show that the enzymes were, in fact, capable of catalyzing light emisson.

3. Design a screen to quickly evaluate the large swath of luciferase mutants against the available synthetic luciferins in the lab.

4. Improve the bioluminescence properties and specificity of the unique pairs; for this aim, I chose to apply *in vitro* evolution and to analyze several generations of the library against the most promising luciferin analogues.

5. Analyze the "orthogonal pair" hits biochemically by expressing and purifying the mutant luciferases.

This thesis reports the successful completion of aims 1-3 and the progress, to date, towards aims 4-5. Specifically, I demonstrate the analysis of candidate luciferins, the design and construction of luciferase libraries and various screening platforms, as well as the results of the initial generations of screening.

References

(1)   Contag, C. H.; Bachmann, M. H.: Advances in *in vivo* Bioluminescence Imaging of Gene Expression. *Annu. Rev. Biomed. Eng.* **2002**, *4*, 235-260.

(2)   Massoud, T. F.; Gambhir, S. S. Molecular Imaging in Living Subjects: Seeing Fundamental Biological Processes in a New Light. *Genes Dev.* **2003**, *17*, 545-580.

(3)   Duda, J.; Karimi, M.; Negrin, R. S.; Contag, C. H. Methods for Imaging Cell Fates in Hematopoiesis. *Methods Mol. Med.* **2007**, *134*, 17-34.

(4)   Chudakov, D. M.; Lukyanov, K. A. Use of Green Fluorescent Protein (GFP) and its Homologs for *in vivo* Protein Motility Studies. *Biochemistry (Mosc)* **2003**, *68*, 952-957.

(5)   Ntziachristos, V.; Ripoll, J.; Wang, L. V.; Weissleder, R. Looking and Listening to Light: the Evolution of Whole-body Photonic Imaging. *Nat. Biotechnol.* **2005**, *23*, 313-320.

(6)   Sarantopoulos, A.; Beziere, N.; Ntziachristos, V. Optical and Opto-acoustic Interventional Imaging. *Annu.Rev. Biomed. Eng.* **2012**, *40*, 346-366.

(7)   Rao, J.; Dragulescu-Andrasi, A.; Yao, H. Fluorescence Imaging *in vivo*: Recent Advances. *Curr. Opin. Biotechnol.* **2007**, *18*, 17-25.

(8)   Germain, R. N.; Robey, E. A.; Cahalan, M. D. A Decade of Imaging Cellular Motility and Interaction Dynamics in the Immune System. *Science*, **2012**, *336*, 1676-1681.

(9)   Johnsson, N.; Johnsson, K. Chemical Tools for Biomolecular Imaging. *ACS Chem. Biol.* **2007**, *2*, 31-38.

(10)   Giepmans, B. N. G.; Adams, S. R.; Ellisman, M. H.; Tsien, R. Y. The Fluorescent Toolbox for Assessing Protein Location and Function. *Science*, **2006**, 312, 217-224.

(11)   Zhao, H.; Doyle, T. C.; Coquoz, O.; Kalish, F.; Rice, B. W.; Contag, C. H. Emission Spectra of Bioluminescent Reporters and Interaction with Mammalian Tissue Determine the Sensitivity of Detection *in vivo*. *J. Biomed. Opt.* **2005**, *10*, 41210.

(12)   Viviani, V. R. The Origin, Diversity, and Structure Function Relationships of Insect Luciferases. *Cell. Mol. Life. Sci.* **2002**, *59*, 1833-1850.

(13)   Greer, L. F., 3rd; Szalay, A. A. Imaging of Light Emission from the Expression of Luciferases in Living Cells and Organisms: a Review. *Luminescence* **2002**, *17*, 43-74.

(14)   Choy, G.; O'Connor, S.; Diehn, F. E.; Costouros, N.; Alexander, H. R.; Choyke, P.; Libutti, S. K. Comparison of Noninvasive Fluorescent and Bioluminescent Small Animal Optical Imaging. *BioTechniques* **2003**, *35*, 1022-1026, 1028-1030.

(15)   Rabinovich, B. A.; Ye, Y.; Etto, T.; Chen, J. Q.; Levitsky, H. I.; Overwijk, W. W.; Cooper, L. J.; Gelovani, J.; Hwu, P. Visualizing Fewer than 10 Mouse T cells with an Enhanced Firefly Luciferase in Immunocompetent Mouse Models of Cancer. *Proc. Natl. Acad. Sci. U. S. A.* **2008**, *105*, 14342-14346.

(16)   Rice, B. W.; Cable, M. D.; Nelson, M. B. *In vivo* Imaging of Light-Emitting Probes. *J. Biomed. Opt.* **2001**, *6*, 432-440.

(17)   Luker, K. E.; Luker, G. D. Bioluminescence Imaging of Reporter Mice for Studies of Infection and Inflammation. *Antiviral Res.* **2010**, *86*, 93-100.

(18)   Huang, N. F.; Okogbaa, J.; Babakhanyan, A.; Cooke, J. P. Bioluminescence Imaging of Stem Cell-Based Therapeutics for Vascular Regeneration. *Theranostics*, **2012**, *2*, 346-354.

(19)   Prescher, J. A.; Contag, C. H. Guided by the Light: Visualizing Biomolecular Processes in Living Animals with Bioluminescence. *Curr. Opin. Chem. Bio.* **2010**, *14*, 80-89.

(20)   Hastings, J. W. Chemistries and Colors of Bioluminescent Reactions: A Review. *Gene* **1996**, *173*, 5-11.

(21)   Fraga, H. Firefly Luminescence: A Historical Perspective and Recent Developments. *Photochem. Photobiol. Sci.* **2008**, *7*, 146-158.

(22)   Branchini, B. R.; Magyar, R. A.; Murtiashaw, M. H.; Anderson, S. M.; Helgerson, L. C.; Zimmer, M. Site-Directed Mutagenesis of Firefly Luciferase Active Site Amino Acids: A Proposed Model for Bioluminescence Color. *Biochemistry* **1999**, *38*, 13223-13230.

(23)   Miloud, T.; Henrich, C.; Hammerling, G. J. Quantitative Comparison of Click Beetle and Firefly Luciferases for *in vivo* Bioluminescence Imaging. *J. Biomed. Opt.* **2007**, *12*, 054018.

(24)   Haddock, S. H.; Moline, M. A.; Case, J. F. Bioluminescence in the Sea. *Ann. Rev. Mar. Sci.* **2010**, *2*, 443-493.

(25)   Bhaumik, S.; Gambhir, S. S. Optical Imaging of Renilla Luciferase Reporter Gene Expression in Living Mice. *Proc. Natl. Acad. Sci. U. S. A.* **2002**, *99*, 377-382.

(26)   Tannous, B. A.; Kim, D. E.; Fernandez, J. L.; Weissleder, R.; Breakefield, X. O. Codon-Optimized Gaussia Luciferase cDNA for Mammalian Gene Expression in Culture and *in vivo*. *Mol. Ther.* **2005**, *11*, 435-443.

(27)   Close, D.; Xu, T.; Smartt, A.; Rogers, A.; Crossley, R.; Price, S.; Ripp, S.; Sayler, G. The Evolution of the Bacterial Luciferase Gene Cassette (lux) as a Real-Time Bioreporter. *Sensors* **2012**, *12*, 732-752.

(28)   Miyashiro, T.; Ruby, E. G. Shedding Light on Bioluminescence Regulation in Vibrio Fischeri. *Mol. Microbio.* **2012**, *84*, 795-806.

(29)   Hyde, J. A.; Weening, E. H.; Chang, M.; Trzeciakowski, J. P.; Hook, M.; Cirillo, J. D.; Skare, J. T. Bioluminescent Imaging of Borrelia Burgdorferi *in vivo* Demonstrates that the Fibronectin-Binding Protein BBK32 is Required for Optimal Infectivity. *Mol. Microbiol.* **2011**, *82*, 99-113.

(30)   Morrissey, R.; Hill, C.; Begley, M. Shining Light on Food Microbiology; Applications of Lux-Tagged Microorganisms in the Food Industry. *Trends Food Sci. Technol.* **2013**, *32*, 4-15.

(31)   Contag, C. H.; Contag, P. R.; Mullins, J. I.; Spilman, S. D.; Stevenson, D. K.; Benaron, D. A. Photonic Detection of Bacterial Pathogens in Living Hosts. *Mol. Microbiol.* **1995**, *18*, 593-603.

(32)   Hori, K.; Charbonneau, H.; Hart, R. C.; Cormier, M. J. Structure of Native Renilla Reinformis Luciferin. *Proc. Natl. Acad. Sci. U. S. A.* **1977**, *74*, 4285-4287.

(33)   White, E.; McCapra, F.; Field, G.; McElroy, W. The Structure and Synthesis of Firefly Luciferin. *J. Am. Chem. Soc.* **1961**, *83*, 2402-2403.

(34)   Day, J. C.; Tisi, L. C.; Bailey, M. J. Evolution of Beetle Bioluminescence: The Origin of Beetle Luciferin. *Luminescence* **2004**, *19*, 8-20.

(35)   Viviani, V. R.; Bechara, E. J.; Ohmiya, Y. Cloning, Sequence Analysis, and Expression of Active Phrixothrix Railroad-Worms Luciferases: Relationship Between Bioluminescence Spectra and Primary Structures. *Biochemistry* **1999**, *38*, 8271-8279.

(36)   Hall, M. P.; Unch, J.; Binkowski, B. F.; Valley, M. P.; Butler, B. L.; Wood, M. G.; Otto, P.; Zimmerman, K.; Vidugiris, G.; Machleidt, T.; Robers, M. B.; Benink, H. A.; Eggers, C. T.; Slater, M. R.; Meisenheimer, P. L.; Klaubert, D. H.; Fan, F.; Encell, L. P.; Wood, K. V. Engineered Luciferase Reporter from a Deep Sea Shrimp Utilizing a Novel Imidazopyrazinone Substrate. *ACS Chem. Biol.* **2012**, *7*, 1848-1857.

(37)   Branchini, B. R.; Behney, C. E.; Southworth, T. L.; Rawat, R.; Deheyn, D. D. Chemical Analysis of the Luminous Slime Secreted by the Marine Worm Chaetopterus (Annelida, Polychaeta). *Photochem. Photobiol*. **2013**. doi: 10.1111/php.12169. [Epub ahead of print]

(38)   Otsuji, T.; Okuda-Ashitaka, E.; Kojima, S.; Akiyama, H.; Ito, S.; Ohmiya, Y. Monitoring for Dynamic Biological Processing by Intramolecular Bioluminescence Resonance Energy Transfer System Using Secreted Luciferase. *Anal. Biochem.* **2004**, *329*, 230-237.

(39)   Berger, F.; Paulmurugan, R.; Bhaumik, S.; Gambhir, S. S. Uptake Kinetics and Biodistribution of 14C-D-Luciferin A Radiolabeled Substrate for the Firefly Luciferase Catalyzed Bioluminescence Reaction: Impact on Bioluminescence Based Reporter Gene Imaging. *Eur. J. Nucl. Med. Mol. Imaging* **2008**, *35*, 2275-2285.

(40)   Greer, L. F.; Szalay, A. A. Imaging of Light Emission from the Expression of Luciferases in Living Cells and Organisms: A Review. *Luminescence* **2002**, *17*, 43-74.

(41)   De Almeida, P. E.; Van Rappard, J. R. M.; Wu, J. C. *In vivo* Bioluminescence for Tracking Cell Fate and Function. *Am. J. Physiol.: Heart Circ. Physiol.* **2011**, *301*, H663-H671.

(42)   Sadikot, R. T.; Blackwell, T. S. Bioluminescence: Imaging Modality for *in vitro* and *in vivo* Gene Expression. *Methods Mol. Biol.* **2008**, *477*, 383-394.

(43)   Maguire, C. A.; van der Mijn, J. C.; Degeling, M. H.; Morse, D.; Tannous, B. A. Codon-Optimized Luciola Italica Luciferase Variants for Mammalian Gene Expression in Culture and *in vivo*. *Mol. Imaging* **2012**, *11*, 13-21.

(44)   Loening, A. M.; Wu, A. M.; Gambhir, S. S. Red-Shifted Renilla Reniformis Luciferase Variants for Imaging in Living Subjects. *Nat. Methods* **2007**, *4*, 641-643.

(45)   Badr, C. E.; Tannous, B. A. Bioluminescence Imaging: Progress and Applications. *Trends Biotechnol.* **2011**, *29*, 624-633.

(46)   Dothager, R. S.; Flentie, K.; Moss, B.; Pan, M. H.; Kesarwala, A.; Piwnica-Worms, D. Advances in Bioluminescence Imaging of Live Animal Models. *Curr. Opin. Biotechnol.* **2009**, *20*, 45-53.

(47)   Cao, Y.-A.; Wagers, A. J.; Beilhack, A.; Dusich, J.; Bachmann, M. H.; Negrin, R. S.; Weissman, I. L.; Contag, C. H. Shifting Foci of Hematopoiesis During

Reconstitution from Single Stem Cells. *Proc. Natl. Acad. Sci. U. S. A.* **2004**, *101*, 221-226.

(48)   Liu, H.; Patel, M. R.; Prescher, J. A.; Patsialou, A.; Qian, D.; Lin, J.; Wen, S.; Chang, Y. F.; Bachmann, M. H.; Shimono, Y.; Dalerba, P.; Adorno, M.; Lobo, N.; Bueno, J.; Dirbas, F. M.; Goswami, S.; Somlo, G.; Condeelis, J.; Contag, C. H.; Gambhir, S. S.; Clarke, M. F. Cancer Stem Cells From Human Breast Tumors are Involved in Spontaneous Metastases in Orthotopic Mouse Models. *Proc. Natl. Acad Sci. U. S. A.* **2010**, *107*, 18115-18120.

(49)   Murphy, C. T.; Moloney, G.; Hall, L. J.; Quinlan, A.; Faivre, E.; Casey, P.; Shanahan, F.; Melgar, S.; Nally, K.: Use of Bioluminescence Imaging to Track Neutrophil Migration and its Inhibition in Experimental Colitis. *Clin. Exp. Immunol.* **2010**, *162*, 188-196.

(50)   Olson, J. A.; Zeiser, R.; Beilhack, A.; Goldman, J. J.; Negrin, R. S. Tissue-Specific Homing and Expansion of Donor NK Cells in Allogeneic Bone Marrow Transplantation. *J. Immunol.* **2009**, *183*, 3219-3228.

(51)   Vocht, N. D.; Lin, D.; Praet, J.; Hoornaert, C.; Reekmans, K.; Blon, D. L.; Daans, J.; Pauwels, P.; Goossens, H.; Hens, N.; Berneman, Z.; Linden, A. V. d.; Ponsaerts, P. Quantitative and Phenotypic Analysis of Mesenchymal Stromal Cell Graft Survival and Recognition by Microglia and Astrocytes in Mouse Brain. *Immunobiology* **2013**, *218*, 696-705.

(52)   Reagan, M. R.; Kaplan, D. L. Concise Review: Mesenchymal Stem Cell Tumor-Homing: Detection Methods in Disease Model Systems. *Stem Cells*, **2011**, *29*, 920-927.

(53)   Kutschka, I.; Chen, I. Y.; Kofidis, T.; von Degenfeld, G.; Sheikh, A. Y.; Hendry, S. L.; Hoyt, G.; Pearl, J.; Blau, H. M.; Gambhir, S. S.; Robbins, R. C. *In vivo* Optical Bioluminescence Imaging of Collagen-Supported Cardiac Cell Grafts. *J. Heart Lung Transplant* **2007**, *26*, 273-280.

(54)   Gilbert, P. M.; Havenstrite, K. L.; Magnusson, K. E. G.; Sacco, A.; Leonardi, N. A.; Kraft, P.; Nguyen, N. K.; Thrun, S.; Lutolf, M. P.; Blau, H. M. Substrate Elasticity Regulates Skeletal Muscle Stem Cell Self-Renewal in Culture. *Science* **2010**, *329*, 1078-1081.

(55)   Sacco, A.; Doyonnas, R.; Kraft, P.; Vitorovic, S.; Blau, H. M. Self-Renewal and Expansion of Single Transplanted Muscle Stem Cells. *Nature* **2008**, *456*, 502-506.

(56)   Shah, K.; Weissleder, R. Molecular Optical Imaging: Applications Leading to the Development of Present Day Therapeutics. *NeuroRx* **2005**, *2*, 215-225.

(57)   Keyaerts, M.; Caveliers, V.; Lahoutte, T. Bioluminescence Imaging: Looking Beyond the Light. *Trends Mol. Med.* **2012**, *18*, 164-172.

(58)   Watts, J. C.; Giles, K.; Grillo, S. K.; Lemus, A.; Dearmond, S. J.; Prusiner, S. B. Bioluminescence Imaging of A Deposition in Bigenic Mouse Models of Alzheimer's Disease. *Proc. Natl. Acad.Sci.* **2011**, *108*, 2528-2533.

(59)   Terashima, M.; Ehara, S.; Yang, E.; Kosuge, H.; Tsao, P. S.; Quertermous, T.; Contag, C. H.; Mcconnell, M. V. *In Vivo* Bioluminescence Imaging of Inducible Nitric Oxide Synthase Gene Expression in Vascular Inflammation. *Mol. Imaging Biol.* **2011**, *13*, 1061-1066.

(60)   Moss, B. L.; Elhammali, A.; Fowlkes, T.; Gross, S.; Vinjamoori, A.; Contag, C. H.; Piwnica-Worms, D. Interrogation of Inhibitor of Nuclear Factor B/ Nuclear Factor B (I B /NF- B) Negative Feedback Loop Dynamics: From Single Cells to Live Animals *in vivo*. *J. Biol. Chem.* **2012**, *287*, 31359-31370.

(61)   Tinkum, K. L.; White, L. S.; Marpegan, L.; Herzog, E.; Piwnica-Worms, D.; Piwnica-Worms, H. Forkhead Box O1 (FOXO1), but not p53, Contributes to Robust Induction of p21 Expression in Fasted Mice. *J. Biol. Chem*. **2013**, *39*, 27999.

(62)   Moroz, E.; Carlin, S.; Dyomina, K.; Burke, S.; Thaler, H. T.; Blasberg, R.; Serganova, I. Real-Time Imaging of HIF-1alpha Stabilization And Degradation. *PLoS One* **2009**, *4*, e5077.

(63)   Naik, S.; Piwnica-Worms, D. Real-Time Imaging of Beta-Catenin Dynamics in Cells and Living Mice. *Proc. Natl. Acad.Sci. U. S. A.* **2007**, *104*, 17465-17470.

(64)   Perroy, J.; Pontier, S.; Charest, P. G.; Aubry, M.; Bouvier, M. Real-Time Monitoring of Ubiquitination in Living Cells by BRET. *Nat. Methods* **2004**, *1*, 203-208.

(65)   Ryan, D. P.; Matthews, J. M. Protein-Protein Interactions in Human Disease. *Curr. Opin. Struct. Biol.* **2005**, *15*, 441-446.

(66)   De, A. The New Era of Bioluminescence Resonance Energy Transfer Technology. *Curr. Pharm. Biotechnol.* **2011**, *12*, 558-568.

(67)   Prinz, A.; Diskar, M.; Herberg, F. W. Application of Bioluminescence Resonance Energy Transfer (BRET) for Biomolecular Interaction Studies. *Chembiochem* **2006**, *7*, 1007-1012.

(68)   Compan, V.; Baroja-Mazo, A.; Bragg, L.; Verkhratsky, A.; Perroy, J.; Pelegrin, P. A Genetically Encoded IL-1 Bioluminescence Resonance Energy Transfer Sensor to Monitor Inflammasome Activity. *J. Immunol.* **2012**, *189*, 2131-2137.

(69)   Dragulescu-Andrasi, A.; Chan, C. T.; De, A.; Massoud, T. F.; Gambhir, S. S. Bioluminescence Resonance Energy Transfer (BRET) Imaging of Protein-Protein Interactions Within Deep Tissues of Living Subjects. *Proc. Natl. Acad. Sci. U. S. A.* **2011**, *108*, 12060-12065.

(70)   Massoud, T. F.; Paulmurugan, R.; Gambhir, S. S. Molecular Imaging of Homodimeric Protein-Protein Interactions in Living Subjects. *FASEB J.* **2004**, *18*, 1105-1107.

(71)   Nyfeler, B.; Michnick, S. W.; Hauri, H. P. Capturing Protein Interactions in the Secretory Pathway of Living Cells. *Proc. Natl. Acad. Sci. U. S. A.* **2005**, *102*, 6350-6355.

(72)   Massoud, T. F.; Paulmurugan, R.; De, A.; Ray, P.; Gambhir, S. S. Reporter Gene Imaging of Protein-Protein Interactions in Living Subjects. *Curr. Opin. Biotechnol.* **2007**, *18*, 31-37.

(73)   Villalobos, V.; Naik, S.; Piwnica-Worms, D. Current State of Imaging Protein-Protein Interactions *In Vivo* with Genetically Encoded Reporters. *Annu. Rev. Biomed. Eng.* **2007**, *9*, 321-349.

(74)   Gammon, S. T.; Villalobos, V. M.; Roshal, M.; Samrakandi, M.; Piwnica-Worms, D. Rational Design of Novel Red-Shifted Bret Pairs: Platforms for Real-Time Single-Chain Protease Biosensors. *Biotechnol. Prog.* **2009**, *25*, 559-569.

(75)   Widder, E. A. Bioluminescence in the Ocean: Origins of Biological, Chemical, and Ecological Diversity. *Science* **2010**, *328*, 704-708.

(76)   Ma, N.; Marshall, A. F.; Rao, J. Near-Infrared Light Emitting Luciferase via Biomineralization. *J. Am. Chem. Soc.* **2010**, *132*, 6884-6885.

(77)   So, M. K.; Xu, C.; Loening, A. M.; Gambhir, S. S.; Rao, J. Self-Illuminating Quantum Dot Conjugates for *In Vivo* Imaging. *Nat. Biotechnol.* **2006**, *24*, 339-343.

(78)   Paulmurugan, R.; Massoud, T. F.; Huang, J.; Gambhir, S. S. Molecular Imaging of Drug-Modulated Protein-Protein Interactions in Living Subjects. *Cancer Res.* **2004**, *64*, 2113-2119.

(79)   Takakura, H.; Hattori, M.; Takeuchi, M.; Ozawa, T. Visualization and Quantitative Analysis of G Protein-Coupled Receptor-Beta-Arrestin Interaction in Single Cells and Specific Organs of Living Mice Using Split Luciferase Complementation. *ACS Chem. Biol.* **2012**, *7*, 901-910.

(80)   Reichling, J.; Kaplan, M. Clinical Use of Serum Enzymes in Liver Disease. *Dig. Dis.Sci.* **1988**, *33*, 1601-1614.

(81)   Straub, V.; De Waele, L.; Barresi, R. Enzymes: Cytosolic Proteins Calpain-3, SEPN1, and GNE, in Muscle Disease: Pathology and Genetics. *Muscle Disease: Pathology and Genetics,*; H. H. Goebel, C. S. a. R. W., Ed.; John Wiley & Sons: Oxford, 2013.

(82)   Razgulin, A.; Ma, N.; Rao, J. Strategies for *In Vivo* Imaging of Enzyme Activity: An Overview and Recent Advances. *Chem. Soc. Rev.* **2011**, *40*, 4186-4216.

(83)   Li, J.; Chen, L.; Du, L.; Li, M. Cage the Firefly Luciferin! - A Strategy for Developing Bioluminescent Probes. *Chem. Soc. Rev.* **2012**, *42*, 662-676.

(84)   Branchini, B. R. Chemical Synthesis of Firefly Luciferin Analogs and Inhibitors. *Meth. Enzymol.* **2000**, *305*, 188-195.

(85)   Meroni, G.; Santaniello, E.; Rajabi, M. D-Luciferin, Derivatives and Analogues: Synthesis and *In Vitro*/*In Vivo* Luciferase-Catalyzed Bioluminescent Activity. *Arkivoc*, **2009**, 265.

(86)   Kindermann, M.; Roschitzki-Voser, H.; Caglic, D.; Repnik, U.; Miniejew, C.; Mittl, P. R.; Kosec, G.; Grutter, M. G.; Turk, B.; Wendt, K. U. Selective and Sensitive Monitoring of Caspase-1 Activity by a Novel Bioluminescent Activity-Based Probe. *Chem. Biol.* **2010**, *17*, 999-1007.

(87)   Wehrman, T. S.; von Degenfeld, G.; Krutzik, P. O.; Nolan, G. P.; Blau, H. M. Luminescent Imaging of Beta-Galactosidase Activity in Living Subjects Using Sequential Reporter-Enzyme Luminescence. *Nat. Methods* **2006**, *3*, 295-301.

(88)   O'Brien, M. A.; Daily, W. J.; Hesselberth, P. E.; Moravec, R. A.; Scurria, M. A.; Klaubert, D. H.; Bulleit, R. F.; Wood, K. V. Homogeneous, Bioluminescent Protease Assays: Caspase-3 as a Model. *J. Biomol. Screen* **2005**, *10*, 137-148.

(89)   Dragulescu-Andrasi, A.; Liang, G.; Rao, J. *In vivo* Bioluminescence Imaging of Furin Activity in Breast Cancer Cells Using Bioluminogenic Substrates. *Bioconjugate Chem.* **2009**, *20*, 1660-1666.

(90)   O'Brien, M. A.; Moravec, R. A.; Riss, T. L.; Bulleit, R. F. Homogeneous, Bioluminescent Proteasome Assays. *Methods Mol. Bio.* **2008**, *414*, 163-181.

(91)   Leippe, D. M.; Nguyen, D.; Zhou, M.; Good, T.; Kirkland, T. A.; Scurria, M.; Bernad, L.; Ugo, T.; Vidugiriene, J.; Cali, J. J.; Klaubert, D. H.; O'Brien, M. A. A Bioluminescent Assay for the Sensitive Detection of Proteases. *Biotechniques* **2011**, *51*, 105-110.

(92)   Zhou, W.; Valley, M. P.; Shultz, J.; Hawkins, E. M.; Bernad, L.; Good, T.; Good, D.; Riss, T. L.; Klaubert, D. H.; Wood, K. V. New Bioluminogenic Substrates for Monoamine Oxidase Assays. *J. Am. Chem. Soc.* **2006**, *128*, 3122-3123.

(93)   Van de Bittner, G. C.; Dubikovskaya, E. A.; Bertozzi, C. R.; Chang, C. J. *In Vivo* Imaging of Hydrogen Peroxide Production in a Murine Tumor Model with a Chemoselective Bioluminescent Reporter. *Proc. Natl. Acad. Sci. U. S. A.* **2010**, *107*, 21316-21321.

(94)   Rush, J. S.; Beatty, K. E.; Bertozzi, C. R. Bioluminescent Probes of Sulfatase Activity. *Chembiochem* **2010**, *11*, 2096-2099.

(95)   Porterfield, W. B.; Jones, K. A.; Prescher, J. *J. Am. Chem. Soc.* **2014**, *in revision*.

(96)   Stevens, G. B.; Silver, D. A.; Zgaga-Griesz, A.; Bessler, W. G.; Vashist, S. K.; Patel, P.; Achazi, K.; Strotmeier, J.; Worbs, S.; Dorner, M. B.; Dorner, B. G.; Pauly, D.; Rummel, A.; Urban, G. A.; Krueger, M. Bioluminescence Assay for the Highly Sensitive Detection of Botulinum Neurotoxin A Activity. *Analyst* **2013**, *138*, 1-9.

(97)   Fan, F.; Binkowski, B. F.; Butler, B. L.; Stecha, P. F.; Lewis, M. K.; Wood, K. V. Novel Genetically Encoded Biosensors Using Firefly Luciferase. *ACS Chem. Biol.* **2008**, *3*, 346-351.

(98)   Kanno, A.; Yamanaka, Y.; Hirano, H.; Umezawa, Y.; Ozawa, T. Cyclic Luciferase for Real-Time Sensing of Caspase-3 Activities in Living Mammals. *Angew. Chem. Int. Ed. Engl.* **2007**, *46*, 7595-7599.

(99)   Galban, S.; Jeon, Y. H.; Bowman, B. M.; Stevenson, J.; Sebolt, K. A.; Sharkey, L. M.; Lafferty, M.; Hoff, B. A.; Butler, B. L.; Wigdal, S. S.; Binkowski, B. F.; Otto, P.; Zimmerman, K.; Vidugiris, G.; Encell, L. P.; Fan, F.; Wood, K. V.; Galban, C. J.; Ross, B. D.; Rehemtulla, A. Imaging Proteolytic Activity in Live Cells and Animal Models. *PLoS One* **2013**, *8*, e66248.

(100)   Xia, Z.; Rao, J. Biosensing and Imaging Based on Bioluminescence Resonance Energy Transfer. *Curr. Opin. Biotechnol.* **2009**, *20*, 37-44.

(101)   Prescher, J. A.; Bertozzi, C. R. Chemistry in Living Systems. *Nat. Chem. Biol.* **2005**, *1*, 13-21.

(102)   Sletten, E. M.; Bertozzi, C. R. Bioorthogonal Chemistry: Fishing for Selectivity in a Sea of Functionality. *Angew. Chem. Int. Ed. Engl.* **2009**, *48*, 6974-6998.

(103)   Abe, K.; Kumagai, T.; Takahashi, C.; Kezuka, A.; Murakami, Y.; Osawa, Y.; Motoki, H.; Matsuo, T.; Horiuchi, M.; Sode, K.; Igimi, S.; Ikebukuro, K. Detection of Pathogenic Bacteria by Using Zinc Finger Protein Fused with Firefly Luciferase. *Anal. Chem.* **2012**, *84*, 8028-8032.

(104)   Contessa, J. N.; Bhojani, M. S.; Freeze, H. H.; Ross, B. D.; Rehemtulla, A.; Lawrence, T. S. Molecular Imaging of N-Linked Glycosylation Suggests Glycan Biosynthesis is a Novel Target for Cancer Therapy. *Clin. Cancer Res.* **2010**, *16*, 3205-3214.

(105)   Shekhawat, S. S.; Ghosh, I. Split-Protein Systems: Beyond Binary Protein-Protein Interactions. *Curr. Opin. Chem. Biol.* **2012**, *15*, 789-797.

(106)   Henkin, A. H.; Cohen, A. S.; Dubikovskaya, E. A.; Park, H. M.; Nikitin, G. F.; Auzias, M. G.; Kazantzis, M.; Bertozzi, C. R.; Stahl, A. Real-Time Noninvasive Imaging of Fatty Acid Uptake *In Vivo*. *ACS Chem. Biol.* **2012**, *7*, 1884-1891.

(107)   Cairns, R. A.; Papandreou, I.; Sutphin, P. D.; Denko, N. C. Metabolic Targeting of Hypoxia and Hif1 in Solid Tumors can Enhance Cytotoxic Chemotherapy. *Proc. Natl. Acad. Sci. U. S. A.* **2007**, *104*, 9445-9450.

(108)   Moriyama, E. H.; Niedre, M. J.; Jarvi, M. T.; Mocanu, J. D.; Moriyama, Y.; Subarsky, P.; Li, B.; Lilge, L. D.; Wilson, B. C. The Influence of Hypoxia on Bioluminescence in Luciferase-Transfected Gliosarcoma Tumor Cells *In Vitro*. *Photochem. Photobiol. Sci.* **2008**, *7*, 675-680.

(109)   Saha, D.; Dunn, H.; Zhou, H.; Harada, H.; Hiraoka, M.; Mason, R. P.; Zhao, D. *In Vivo* Bioluminescence Imaging of Tumor Hypoxia Dynamics of Breast Cancer Brain Metastasis on a Mouse Model. *J. Vis. Exp.* **2011**, *56*, e3175.

(110)   Kricka, L. J. Clinical and Biochemical Applications of Luciferases and Luciferins. *Anal. Biochem.* **1988**, *175*, 14-21.

(111)   Umezawa, Y.; Ozawa, T.; Sato, M. Methods of Analysis for Chemicals that Promote/Disrupt Cellular Signaling. *Anal. Sci.* **2002**, *18*, 503-516.

(112)   Ahmadian, A.; Ehn, M.; Hober, S. Pyrosequencing: History, Biochemistry and Future. *Clin. Chim. Acta.* **2006**, *363*, 83-94.

(113)   Naumann, E. A.; Kampff, A. R.; Prober, D. A.; Schier, A. F.; Engert, F. Monitoring Neural Activity with Bioluminescence During Natural Behavior. *Nat. Neurosci.* **2010**, *4*, 513-520.

(114)   Hattori, M.; Haga, S.; Takakura, H.; Ozaki, M.; Ozawa, T. Sustained Accurate Recording of Intracellular Acidification in Living Tissues with a Photo-Controllable Bioluminescent Protein. *Proc. Natl. Acad. Sci. U.S.A.* **2013**, *110*, 9332-9337.

(115)   Hemeon, I.; Gutierrez, J. A.; Ho, M. C.; Schramm, V. L. Characterizing DNA Methyltransferases with an Ultrasensitive Luciferase-Linked Continuous Assay. *Anal. Chem.* **2011**, *83*, 4996-5004.

(116)   Taneoka, A.; Sakaguchi-Mikami, A.; Yamazaki, T.; Tsugawa, W.; Sode, K. The Construction of a Glucose-Sensing Luciferase. *Biosens. Bioelectron.* **2009**, *25*, 76-81.

(117)   Walenta, S.; Schroeder, T.; Mueller-Klieser, W. Metabolic Mapping with Bioluminescence: Basic and Clinical Relevance. *Biomol. Eng.* **2002**, *18*, 249-262.

(118)   Kim, S. B.; Sato, M.; Tao, H. Genetically Encoded Bioluminescent Indicators for Stress Hormones. *Anal. Chem.* **2009**, *81*, 3760-3768.

(119) Kabiersch, G.; Rajasärkkä, J.; Tuomela, M.; Hatakka, A.; Virta, M.; Steffen, K. Bioluminescent Yeast Assay for Detection of Organotin Compounds. *Anal. Chem.* **2013**, *85*, 5740-5745.

(120) Binkowski, B.; Fan, F.; Wood, K. Engineered Luciferases for Molecular Sensing in Living Cells. *Curr. Opin. Biotechnol.* **2009**, *20*, 14-18.

(121) Paulmurugan, R.; Gambhir, S. S. An Intramolecular Folding Sensor for Imaging Estrogen Receptor-Ligand Interactions. *Proc. Natl. Acad. Sci. U. S. A.* **2006**, *103*, 15883-15888.

(122) Kim, S. B.; Umezawa, Y.; Kanno, K. A.; Tao, H. An Integrated-Molecule-Format Multicolor Probe for Monitoring Multiple Activities of a Bioactive Small Molecule. *ACS Chem. Biol.* **2008**, *3*, 359-372.

(123) Sieracki, N. A.; Gantner, B. N.; Mao, M.; Horner, J. H.; Ye, R. D.; Malik, A. B.; Newcomb, M. E.; Bonini, M. G. Bioluminescent Detection of Peroxynitrite with a Boronic Acid-Caged luciferin. *Free Rad. Biol. & Med.* **2013**, *61*, 40-50.

(124) Van de Bittner, G. C.; Bertozzi, C. R.; Chang, C. J.: Strategy for Dual-Analyte Luciferin Imaging: *in vivo* Bioluminescence Detection of Hydrogen Peroxide and Caspase Activity in a Murine Model of Acute Inflammation. *J. Am. Chem. Soc*. **2013,** *135*, 1783-1795.

(125) Petty, R. D.; Sutherland, L. A.; Hunter, E. M.; Cree, I. A. Comparison of MTT and ATP-Based Assays for the Measurement of Viable Cell Number. *J. Biolumin. Chemilumin.* **1995**, *10*, 29-34.

(126) Kalra, J.; Anantha, M.; Warburton, C.; Waterhouse, D.; Yan, H.; Yang, Y. J.; Strut, D.; Osooly, M.; Masin, D.; Bally, M. B. Validating the use of a Luciferase Labeled Breast Cancer Cell Line, MDA435lCC6, as a Means to Monitor Tumor Progression and to Assess the Therapeutic Activity of an Established Anticancer Drug, Docetaxel (DT) Alone or in Combination with the ILK Inhibitor, QLT0267. *Cancer Biol. Ther.* **2011**, *11*, 826-838.

(127) Kasahara, N.; Kikuchi, T.; Doi, J.; Teratani, T.; Fujimoto, Y.; Uemoto, S.; Yasuda, Y.; Kobayashi, E. Luminescence-Based Assay to Screen Preservation Solutions for Optimal Ability to Maintain Viability of Rat Intestinal Grafts. *Transplant Proc.* **2013**, *45*, 2486-2490.

(128) Kodack, D. P.; Chung, E.; Yamashita, H.; Incio, J.; Duyverman, A. M. M. J.; Song, Y.; Farrar, C. T.; Huang, Y.; Ager, E.; Kamoun, W.; Goel, S.; Snuderl, M.; Lussiez, A.; Hiddingh, L.; Mahmood, S.; Tannous, B. A.; Eichler, A. F.; Fukumura, D.; Engelman, J. A.; Jain, R. K. PNAS Plus: Combined Targeting of HER2 and VEGFR2 for Effective Treatment of HER2-Amplified Breast Cancer Brain Metastases. *Proc. Natl. Acad. Sci.* **2012**, *109*, E3119-E3127.

(129) Kolibab, K.; Derrick, S. C.; Jacobs, W. R.; Morris, S. L. Characterization of an Intracellular ATP Assay for Evaluating the Viability of Live Attenuated Mycobacterial Vaccine Preparations. *J. Microbiol. Methods.* **2012**, *90*, 245-249.

(130) McMillin, D. W.; Delmore, J.; Negri, J. M.; Vanneman, M.; Koyama, S.; Schlossman, R. L.; Munshi, N. C.; Laubach, J.; Richardson, P. G.; Dranoff, G.; Anderson, K. C.; Mitsiades, C. S. Compartment-Specific Bioluminescence Imaging Platform for the High-Throughput Evaluation of Antitumor Immune Function. *Blood* **2012**, *119*, e131-138.

(131) McMillin, D. W.; Delmore, J.; Weisberg, E.; Negri, J. M.; Geer, D. C.; Klippel, S.; Mitsiades, N.; Schlossman, R. L.; Munshi, N. C.; Kung, A. L.; Griffin, J. D.; Richardson, P. G.; Anderson, K. C.; Mitsiades, C. S. Tumor Cell-Specific Bioluminescence Platform to Identify Stroma-Induced Changes to Anticancer Drug Activity. *Nat. Med.* **2010**, *16*, 483-489.

(132) Auld, D. S.; Thorne, N.; Nguyen, D.-T.; Inglese, J. A Specific Mechanism for Nonspecific Activation in Reporter-Gene Assays. *ACS Chem. Biol.* **2008**, *3*, 463-470.

(133) Thorne, N.; Auld, D. S.; Inglese, J. Apparent Activity in High-Throughput Screening: Origins of Compound-Dependent Assay Interference. *Curr. Opin. Chem. Biol.* **2010**, *14*, 315-324.

(134) Inglese, J.; Johnson, R. L.; Simeonov, A.; Xia, M.; Zheng, W.; Austin, C. P.; Auld, D. S. High-Throughput Screening Assays for the Identification of Chemical Probes. *Nat. Chem. Biol.* **2007**, *3*, 466-479.

(135) Ho, P.; Yue, K.; Pandey, P.; Breault, L.; Harbinski, F.; McBride, A. J.; Webb, B.; Narahari, J.; Karassina, N.; Wood, K. V.; Hill, A.; Auld, D. S. Reporter Enzyme Inhibitor Study to Aid Assembly of Orthogonal Reporter Gene Assays. *ACS Chem. Biol.* **2013**, *8*, 1009-1017.

(136) Venisnik, K. M.; Olafsen, T.; Gambhir, S. S.; Wu, A. M. Fusion of Gaussia Luciferase to an Engineered Anti-Carcinoembryonic Antigen (CEA) Antibody for *In Vivo* Optical Imaging. *Mol. Imaging Biol.* **2007**, *9*, 267-277.

(137) Kelkar, M.; De, A. Bioluminescence Based *In Vivo* Screening Technologies. *Curr. Opin. Pharmacol.* **2012**, *12*, 592-600.

(138) El-Sayed, R.; Eita, M.; Barrefelt, A.; Ye, F.; Jain, H.; Fares, M.; Lundin, A.; Crona, M.; Abu-Salah, K.; Muhammed, M.; Hassan, M. Thermostable Luciferase from Luciola Cruciate for Imaging of Carbon Nanotubes and Carbon Nanotubes Carrying Doxorubicin Using *In Vivo* Imaging System. *Nano Lett.* **2013**, *13*, 1393-1398.

(139) Dubikovskaya, E. A.; Thorne, S. H.; Pillow, T. H.; Contag, C. H.; Wender, P. A. Overcoming Multidrug Resistance of Small-Molecule Therapeutics Through Conjugation with Releasable Octaarginine Transporters. *Proc. Natl. Acad. Sci. U. S. A.* **2008**, *105*, 12128-12133.

(140)   Bovenberg, M. S.; Degeling, M. H.; Tannous, B. A. Enhanced Gaussia Luciferase Blood Assay for Monitoring of *In Vivo* Biological Processes. *Anal. Chem.* **2013**, *84*, 1189-1192.

(141)   Thompson, J. F.; Hayes, L. S.; Lloyd, D. B. Modulation of Firefly Luciferase Stability and Impact on Studies of Gene Regulation. *Gene* **1991**, *103*, 171-177.

(142)   Leclerc, G. M.; Boockfor, F. R.; Faught, W. J.; Frawley, L. S. Development of a Destabilized Firefly Luciferase Enzyme for Measurement of Gene Expression. *Biotechniques* **2000**, *29*, 590-591, 594-596, 598 passim.

(143)   Koksharov, M. I.; Ugarova, N. N. Random Mutagenesis of Luciola Mingrelica Firefly Luciferase. Mutant Enzymes with Bioluminescence Spectra Showing Low pH Sensitivity. *Biochemistry Moscow* **2008**, *73*, 862-869.

(144)   Ugarova, N. N. Stabilization of Luciola Mingrelica Firefly Luciferase by Genetic Engineering Methods. *Moscow Univ. Chem. Bull.* **2010**, *65*, 139-143.

(145)   Czupryna, J.; Tsourkas, A. Firefly Luciferase and RLuc8 Exhibit Differential Sensitivity to Oxidative Sress in Apoptotic Cells. *PLoS One* **2011**, *6*, e20073.

(146)   Degeling, M. H.; Bovenberg, M. S.; Lewandrowski, G. K.; de Gooijer, M. C.; Vleggeert-Lankamp, C. L.; Tannous, M.; Maguire, C. A.; Tannous, B. A. Directed Molecular Evolution Reveals Gaussia Luciferase Variants with Enhanced Light Output Stability. *Anal. Chem.* **2013**, *85*, 3006-3012.

(147)   Evans, M. S.; Chaurette, J. P.; Adams, S. T., Jr.; Reddy, G. R.; Paley, M. A.; Aronin, N.; Prescher, J. A.; Miller, S. C. A Synthetic Luciferin Improves Bioluminescence Imaging in Live Mice. *Nat. Methods* **2014**, *11*, 393-395.

(148)   Gross, S.; Abraham, U.; Prior, J. L.; Herzog, E. D.; Piwnica-Worms, D. Continuous Delivery of D-Luciferin by Implanted Micro-Osmotic Pumps Enables True Real-Time Bioluminescence Imaging of Luciferase Activity *In Vivo*. *Mol. Imaging* **2007**, *6*, 121-130.

(149)   Kheirolomoom, A.; Kruse, D. E.; Qin, S.; Watson, K. E.; Lai, C. Y.; Young, L. J.; Cardiff, R. D.; Ferrara, K. W. Enhanced *In Vivo* Bioluminescence Imaging Using Liposomal Luciferin Delivery System. *J. Control Release* **2010**, *141*, 128-136.

(150)   Branchini, B. R.; Ablamsky, D. M.; Rosenberg, J. C. Chemically Modified Firefly Luciferase is an Efficient Source of Near-Infrared Light. *Bioconjug. Chem.* **2010**, *21*, 2023-2030.

(151)   Branchini, B. R.; Ablamsky, D. M.; Rosenman, J. M.; Uzasci, L.; Southworth, T. L.; Zimmer, M. Synergistic Mutations Produce Blue-Shifted Bioluminescence in Firefly Luciferase. *Biochemistry*, **2007**, *46*, 13847-13855.

(152)   Branchini, B. R.; Southworth, T. L.; Khattak, N. F.; Michelini, E.; Roda, A. Red- and Green-Emitting Firefly Luciferase Mutants for Bioluminescent Reporter Applications. *Anal. Biochem.* **2005**, *345*, 140-148.

(153)   Caysa, H.; Jacob, R.; Muther, N.; Branchini, B.; Messerle, M.; Soling, A. A Redshifted Codon-Optimized Firefly Luciferase is a Sensitive Reporter for Bioluminescence Imaging. *Photochem. Photobiol. Sci.* **2009**, *8*, 52-56.

(154)   Loening, A. M.; Dragulescu-Andrasi, A.; Gambhir, S. S. A Red-Shifted Renilla Luciferase for Transient Reporter-Gene Expression. *Nat. Methods* **2010**, *7*, 5-6.

(155)   Sundlov, J. A.; Fontaine, D. M.; Southworth, T. L.; Branchini, B. R.; Gulick, A. M. Crystal Structure of Firefly Luciferase in a Second Catalytic Conformation Supports a Domain Alternation Mechanism. *Biochemistry* **2012**, *51*, 6493-6495.

(156)   Li, X.; Nakajima, Y.; Niwa, K.; Viviani, V. R.; Ohmiya, Y. Enhanced Red-Emitting Railroad Worm Luciferase for Bioassays and Bioimaging. *Protein Sci.* **2010**, *19*, 26-33.

(157)   Woodroofe, C. C.; Meisenheimer, P. L.; Klaubert, D. H.; Kovic, Y.; Rosenberg, J. C.; Behney, C. E.; Southworth, T. L.; Branchini, B. R. Novel Heterocyclic Analogues of Firefly Luciferin. *Biochemistry* **2012**, *51*, 9807-9813.

(158)   McCutcheon, D. C.; Paley, M. A.; Steinhardt, R. C.; Prescher, J. A. Expedient Synthesis of Electronically Modified Luciferins for Bioluminescence Imaging. *J Am Chem Soc* **2010**.

(159)   Conley, N. R.; Dragulescu-Andrasi, A.; Rao, J.; Moerner, W. E. A Selenium Analogue of Firefly D-Luciferin with Red-Shifted Bioluminescence Emission. *Angew. Chem. Int. Ed.* **2012**, *51*, 3350-3353.

(160)   Kojima, R.; Takakura, H.; Ozawa, T.; Tada, Y.; Nagano, T.; Urano, Y. Rational Design and Development of Near-Infrared-Emitting Firefly Luciferins Available *In Vivo*. *Angew. Chem. Int. Ed.* **2012**, *52*, 1175-1179.

(161)   Reddy, G. R.; Thompson, W. C.; Miller, S. C. Robust Light Emission from Cyclic Alkylaminoluciferin Substrates for Firefly Luciferase. *J. Am. Chem. Soc.* **2010**, *132*, 13586-13587.

(162)   Evans, M. S.; Chaurette, J. P.; Adams, S. T., Jr.; Reddy, G. R.; Paley, M. A.; Aronin, N.; Prescher, J. A.; Miller, S. C. A Synthetic Luciferin Improves Bioluminescence Imaging in Live Mice. *Nat. Methods,* **2014**, *11*, 393-395.

(163)   Morse, D.; Tannous, B. A. A Water-Soluble Coelenterazine for Sensitive *In Vivo* Imaging of Coelenterate Luciferases. *Mol. Ther.* **2012**, *20*, 692-693.

(164) Levi, J.; De, A.; Cheng, Z.; Gambhir, S. S. Bisdeoxycoelenterazine Derivatives for Improvement of Bioluminescence Resonance Energy Transfer Assays. *J. Am. Chem. Soc.* **2007**, *129*, 11900-11901.

(165) Shimomura, O.; Musicki, B.; Kishi, Y. Semi-Synthetic Aequorins with Improved Sensitivity to Ca2+ Ions. *Biochem. J.* **1989**, *261*, 913-920.

(166) Inouye, S.; Shimomura, O. The Use of Renilla Luciferase, Oplophorus Luciferase, and Apoaequorin as Bioluminescent Reporter Protein in the Presence of Coelenterazine Analogues as Substrate. *Biochem. Biophys. Res. Commun.* **1997**, *233*, 349-353.

(167) Harwood, K. R.; Mofford, D. M.; Reddy, G. R.; Miller, S. C. Identification of Mutant Firefly Luciferases that Efficiently Utilize Aminoluciferins. *Chem. Biol.* **2011**, *18*, 1649-1657.

(168) Mezzanotte, L.; Que, I.; Kaijzel, E.; Branchini, B.; Roda, A.; Lowik, C. Sensitive Dual Color *In Vivo* Bioluminescence Imaging Using a New Red Codon Optimized Firefly Luciferase and a Green Click Beetle Luciferase. *PLoS One*, **2011**, *6*, e19277.

(169) Kwon, H. J.; Ohmiya, Y.; Yasuda, K. Dual-Color System for Simultaneously Monitoring Intracellular Ca2+ and ATP Dynamics. *Anal. Biochem.* **2012**, *430*, 45-47.

(170) Wang, H.; Cao, F.; De, A.; Cao, Y.; Contag, C.; Gambhir, S. S.; Wu, J. C.; Chen, X. Trafficking Mesenchymal Stem Cell Engraftment and Differentiation in Tumor-Bearing Mice by Bioluminescence Imaging. *Stem Cells* **2009**, *27*, 1548-1558.

(171) Maguire, C. A.; Bovenberg, M. S.; Crommentuijn, M. H.; Niers, J. M.; Kerami, M.; Teng, J.; Sena-Esteves, M.; Badr, C. E.; Tannous, B. A. Triple Bioluminescence Imaging for *In Vivo* Monitoring of Cellular Processes. *Mol. Ther. Nucleic Acids* **2013**, *2*, e99.

(172) Woodroofe, C. C.; Meisenheimer, P. L.; Klaubert, D. H.; Kovic, Y.; Rosenberg, J. C.; Behney, C. E.; Southworth, T. L.; Branchini, B. R. Novel Heterocyclic Analogues of Firefly Luciferin. *Biochemistry* **2012**, *51*, 9807-9813.

(173) Woodroofe, C. C.; Shultz, J. W.; Wood, M. G.; Osterman, J.; Cali, J. J.; Daily, W. J.; Meisenheimer, P. L.; Klaubert, D. H. N-Alkylated 6'-Aminoluciferins are Bioluminescent Substrates for Ultra-Glo and Quantilum Luciferase: New Potential Scaffolds for Bioluminescent Assays. *Biochemistry* **2008**, *47*, 10383-10393.

(174) Cai, D.; Cohen, K. B.; Luo, T.; Lichtman, J. W.; Sanes, J. R. Improved Tools for the Brainbow Toolbox. *Nat. Methods* **2013**, *10*, 540-547.

(175) Wendt, M. K.; Molter, J.; Flask, C. A.; Schiemann, W. P. *In Vivo* Dual Substrate Bioluminescent Imaging. *J. Vis. Exp.* **2011,** *56*, e3245.

(176)   Yuan, H.; Chong, H.; Wang, B.; Zhu, C.; Liu, L.; Yang, Q.; Lv, F.; Wang, S. Chemical Molecule-Induced Light-Activated System for Anticancer and Antifungal Activities. *J. Am. Chem. Soc.* **2012**, *134*, 13184-13187.

(177)   Gross, S.; Gammon, S. T.; Moss, B. L.; Rauch, D.; Harding, J.; Heinecke, J. W.; Ratner, L.; Piwnica-Worms, D. Bioluminescence Imaging of Myeloperoxidase Activity *In Vivo*. *Nat. Med.* **2009**, *15*, 455-461.

CHAPTER 2: Analysis of luciferin analogs for orthogonal multicomponent imaging

2.1 Introduction

The luciferase reaction first garnered the attention of organic chemists in the 1960s [1-4]. Emil White used organic synthesis to tease apart the light-emitting species by supplying various chemical entities to ground-up firefly light organs and observing which, if any, catalyzed light emission [3-5]. His pioneering work, and that of others, identified D-luciferin as the native substrate for Fluc, but just as importantly, helped to elucidate, "what makes a luciferin" beyond those found in nature. In short, the most key elements to the successful generation of light include:

- an aromatic core structure [6,7] ,

- electron density at the 6′ position [8,9] ,

- a D-stereocenter [2] , and

- a carboxylate with an alpha proton off the thiazoline ring [10-12]

The aromatic core serves as the chromophore and thus dictates the wavelength of light emission. Existing literature suggests that the identity and extent of the π system can be flexible [7,13]. Photon emission is promoted by an electron dense residue at the 6′ position of D-luciferin [6]. In addition, there must be a carboxylate available for adenylation during the light emitting reaction (Figure 2-1) [14]; the mechanism also necessitates an accessible proton at C-4 for enzymatic abstraction and subsequent reaction with molecular oxygen [15]. D-Stereochemistry is also required for

bioluminescence (L-luciferin does get adenylated but does not become oxidized to emit light) [16].
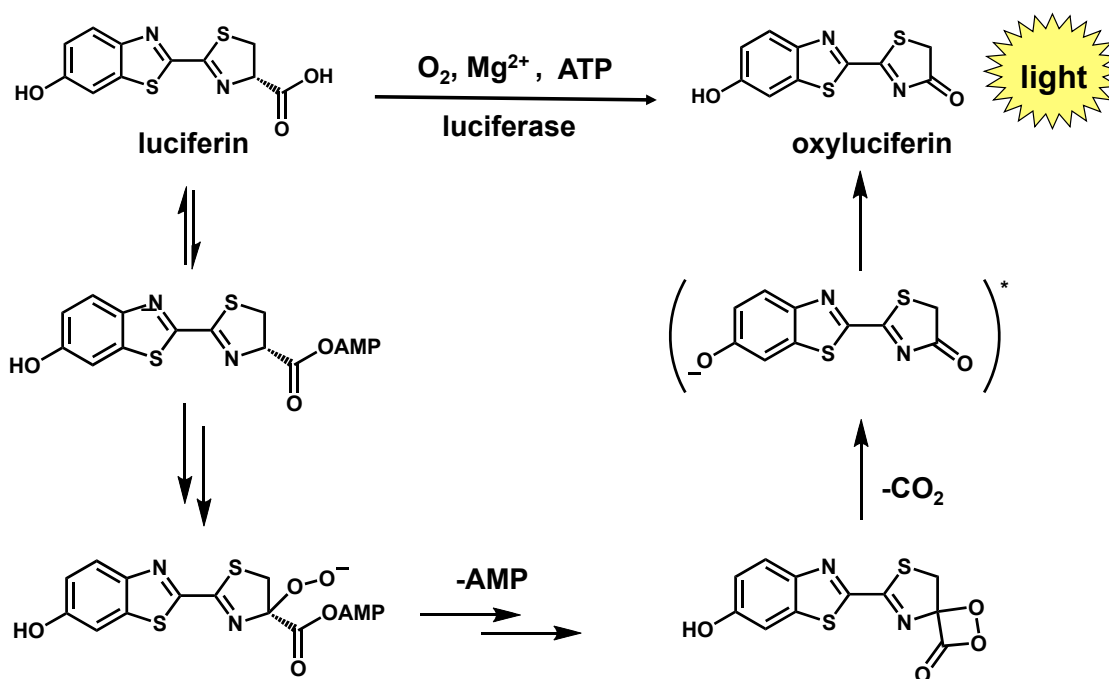
Figure 2-1 Bioluminescent light emission reaction mechanism. Luciferin is activated as the adenyl mixed anhydride. H-atom abstraction and subsequent addition of molecular oxygen ultimately provides the high-energy dioxetanone intermediate. Breakdown of this intermediate releases CO_2 and the excited state product. Relaxation of oxyluciferin to the ground state results in the emission of a photon of light.

Collectively, these findings guided our designs and particularly helped established which parameters in the luciferin scaffold were essential to light emission and which ones would be amenable to adaptation for orthogonal probe development. Auxiliary steric bulk is tolerated to varying degrees in different positions on both the benzothiazole and thiazoline ring [6,9,17]. Molecules that act as competitive inhibitors also gave a sense of the Fluc active site, and where re-engineering of the enzyme could better accommodate these modifications [6,18,19]. A sample of light-emitting luciferins and their non-emitting brethren are illustrated in Figure 2-2.

After assessing the available data on the topic, we converged on three classes of potential orthogonal luciferins, including those with modified electronic and steric properties as well as alternative aromatic cores (Figure 2-3) [20,21]. We preserved the D-stereochemistry, a carboxylate and sp^3 carbon at C4 in all the molecules (refer to Figure 2-3 A for D-luciferin numbering). Incidentally, this allowed us to access all analogs *via* a facile condensation reaction between D-cysteine and cyanobenzothiazoles, analogous to the proposed last step of D-luciferin biosynthesis [22]. This reaction has been used in multiple luciferin syntheses over the decades, but these approaches were unnecessarily long and harsh [1,3,6,26]. Dave McCutcheon in our lab developed a synthesis of D-luciferin was both shorter and milder, and also tolerated steric modifications to the benzothiazole core, heteroatom substitutions, and other aromatic scaffolds as starting materials. This adaptable synthesis provided access to the three classes of luciferin analogs in which we were most interested. Initially, he used the method to generate several luciferin analogs with nitrogen atoms substituted for sulfur atoms (Figure 2-3 B)

[20]. Due to their similarities to D-luciferin, these luciferins were expected to be respectable light emitters, but not necessarily as potent. Thus, they were perhaps good candidates for emission improvements with mutant luciferases.
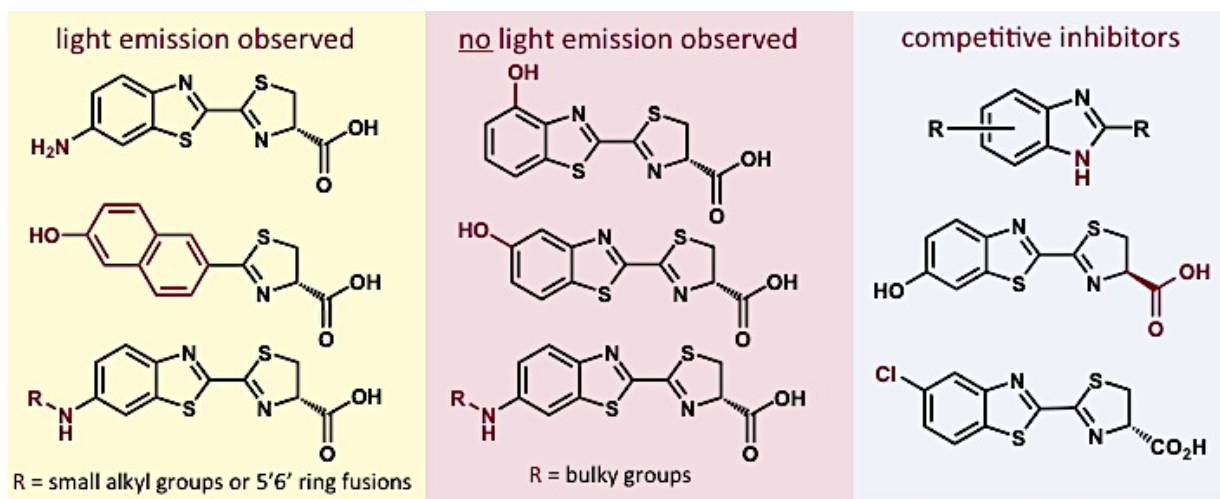
Figure 2-2 Characteristics of previously reported light-emitting luciferin analogs and related "dark" luciferins, along with competitive inhibitors of D-luciferin. R=alkyl or aryl substituents in most cases.
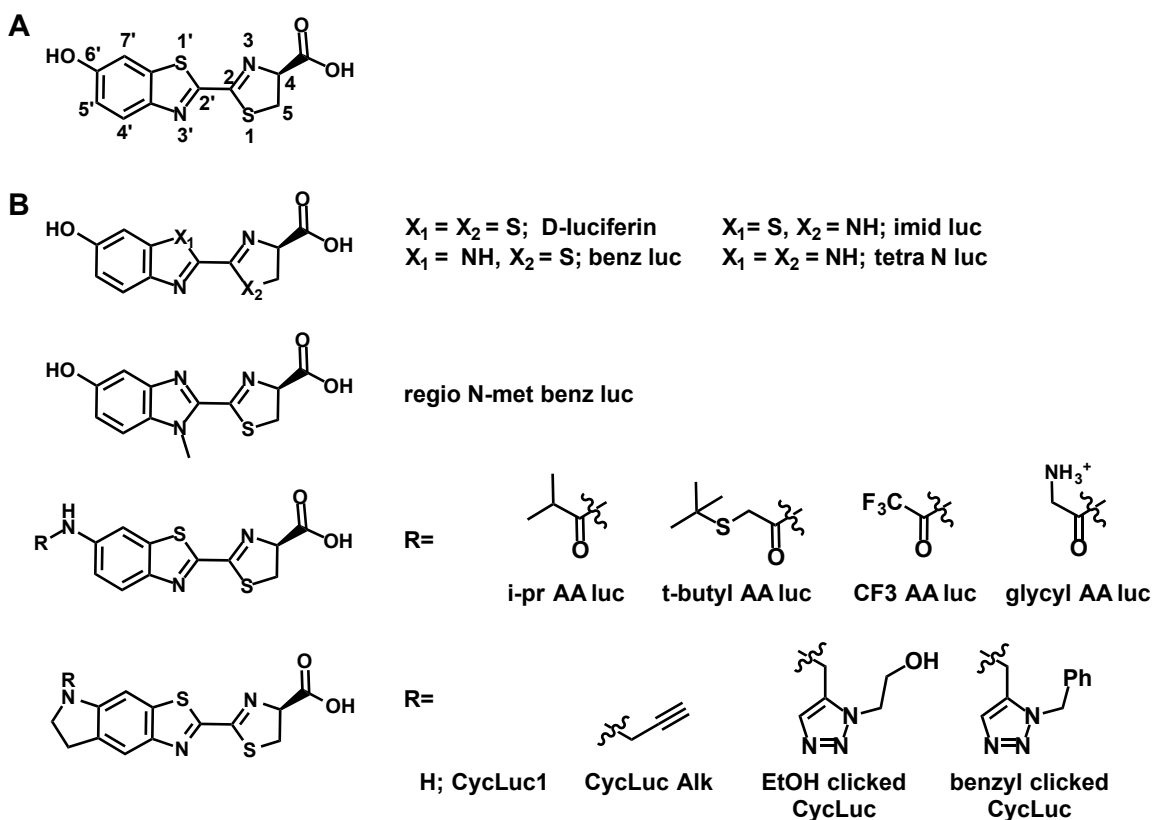
Figure 2-3 Luciferins investigated in this chapter. (A) Numbering scheme for D-luciferin and related analogs. (B) Structures of luciferin analogs used for orthogonal probe development in this chapter and the names that will be used to refer to them.

2.2 *In vitro* evaluation of nitrogenous luciferins

Two main types of experiments were required to assess the suitability of these compounds as potential orthogonal luciferins. First, we needed to verify that the analogs were capable of producing luciferase-catalyzed light, but were less-suited for this task than D-luciferin to promote orthogonality. These data would provide insight into the molecular interactions between the analogs and residues in the Fluc active site. I proposed to tackle this by examining the behavior of analogs with Fluc and mutants, as well as modeling their binding with conventional docking studies [23]. Second, we needed to verify that the analogs were cell-permeable and otherwise suited for *in vivo* work. I proposed to investigate this directly by testing the luciferin analogs with Fluc-expressing mammalian cell lines, as predicting such features from "drug-likeness" can be misleading [9,24,25].

To address the first set of experiments and assess the luminescence of the analogs under controlled conditions, recombinant Fluc was required. The *luc2* gene was cloned into a pET28 vector, and protein expression in *E. coli* was induced with IPTG (500 μM). A 1-L expression was carried out at 22 °C for 16 h. Lower temperatures were necessary in order to keep Fluc soluble [27]. Successful expression of Fluc in the soluble fraction of *E. coli* was confirmed by gel electrophoresis. After Ni-NTA purification and concentration, 30 mg of Fluc were isolated and found to be >95% pure (Figure 2-4). Enzyme activity was confirmed with D-luciferin using standard bioluminescence assays (Figure 2-5). The emission from our recombinant Fluc was comparable to that previously reported [28].
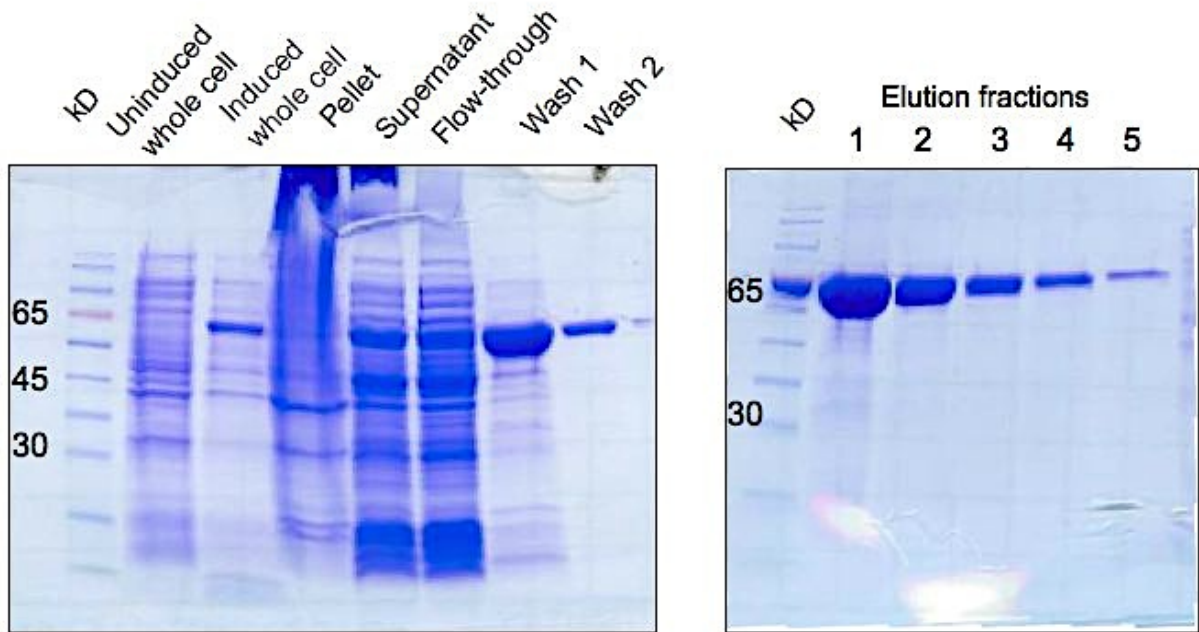
Figure 2-4 Recombinant Fluc product analyzed via gel electrophoresis. The Fluc band at 63 kDa was observed in acrylamide gel stained with Coomasie blue.

A

B
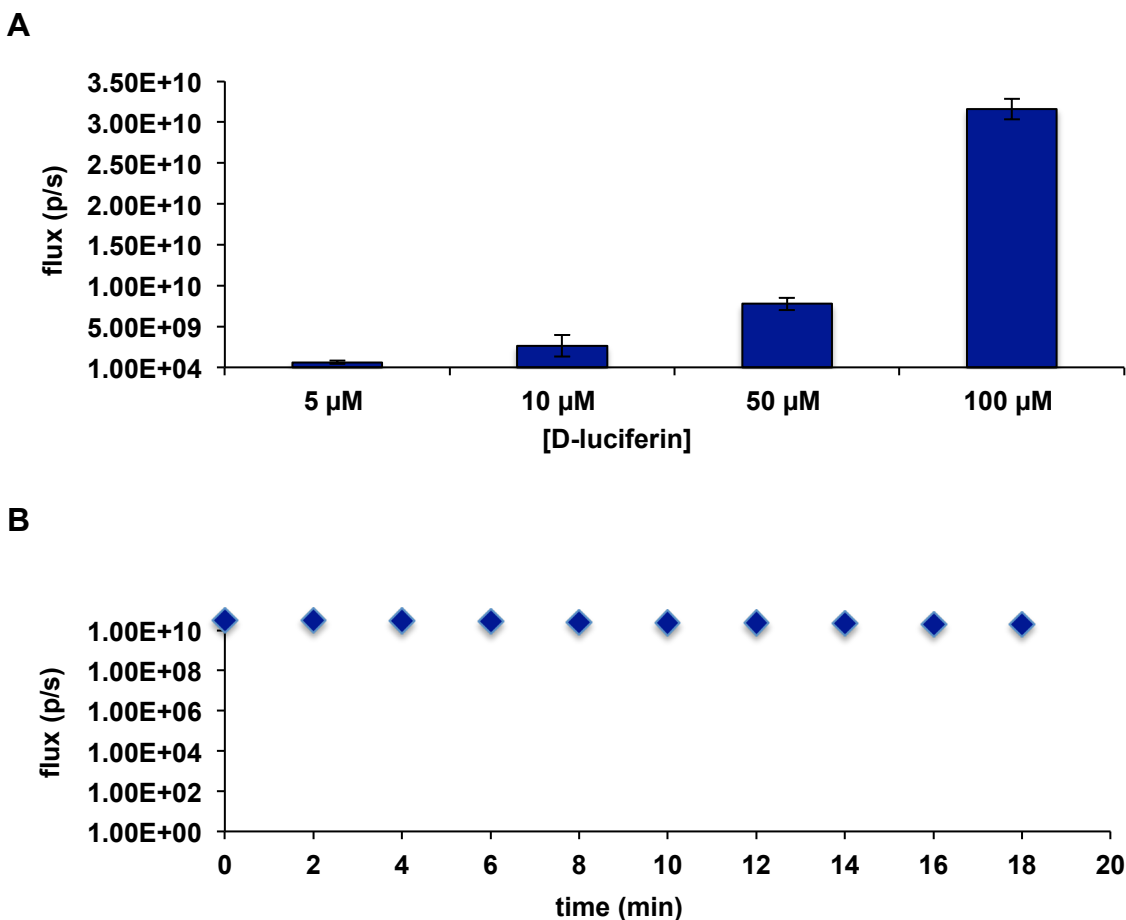
Figure 2-5 Recombinant Fluc emits light with D-luciferin. (A) Fluc (1 µg) was assayed in the presence of increasing concentrations of D-luciferin. (B) Light emission from an Fluc sample (1 µg) D-luciferin, ATP, and acetyl CoA (100 µM) was observed over time.

In collaboration with Dave McCutcheon, light emission assays were performed using Fluc, required cofactors and the first cavalcade of luciferin analogs: the nitrogenous heterocycles benz luc, imid luc, regio N-met luc and tetra N luc [20] (Figure 2-6 B). Among the best substrates, including the benz luc and regio N-met benz luc, dose dependent light emission was observed, while no light was observed in the absence of enzyme. While emission was observed for approximately half of the luciferin analogs, the signal intensities were universally weaker (~100 fold or greater) than that observed from D-luciferin. These data suggested that all the molecules tested were potential orthogonal

luciferins and that several clearly possess the ability to produce light. These molecules seemed to be promising starting points for identifying complementary luciferases [20].

In order to assess the viability of the nitrogenous analogs as *in vivo* probes, HEK 293 cells stably expressing Fluc were incubated with benz luc or regio N met luc, and the light emission was quantified. The dose dependency observed in the *in vitro* enzymatic assay was maintained as expected, and the steady-state emissions suggested that the compounds were capable of diffusing across the mammalian cell membrane, an important requirement for *in vivo* imaging (Figure 2-7).

These first assays and luciferins demonstrated that our synthetic approach and analyses were valid, and we further investigated a more diverse panel of luciferin architectures.
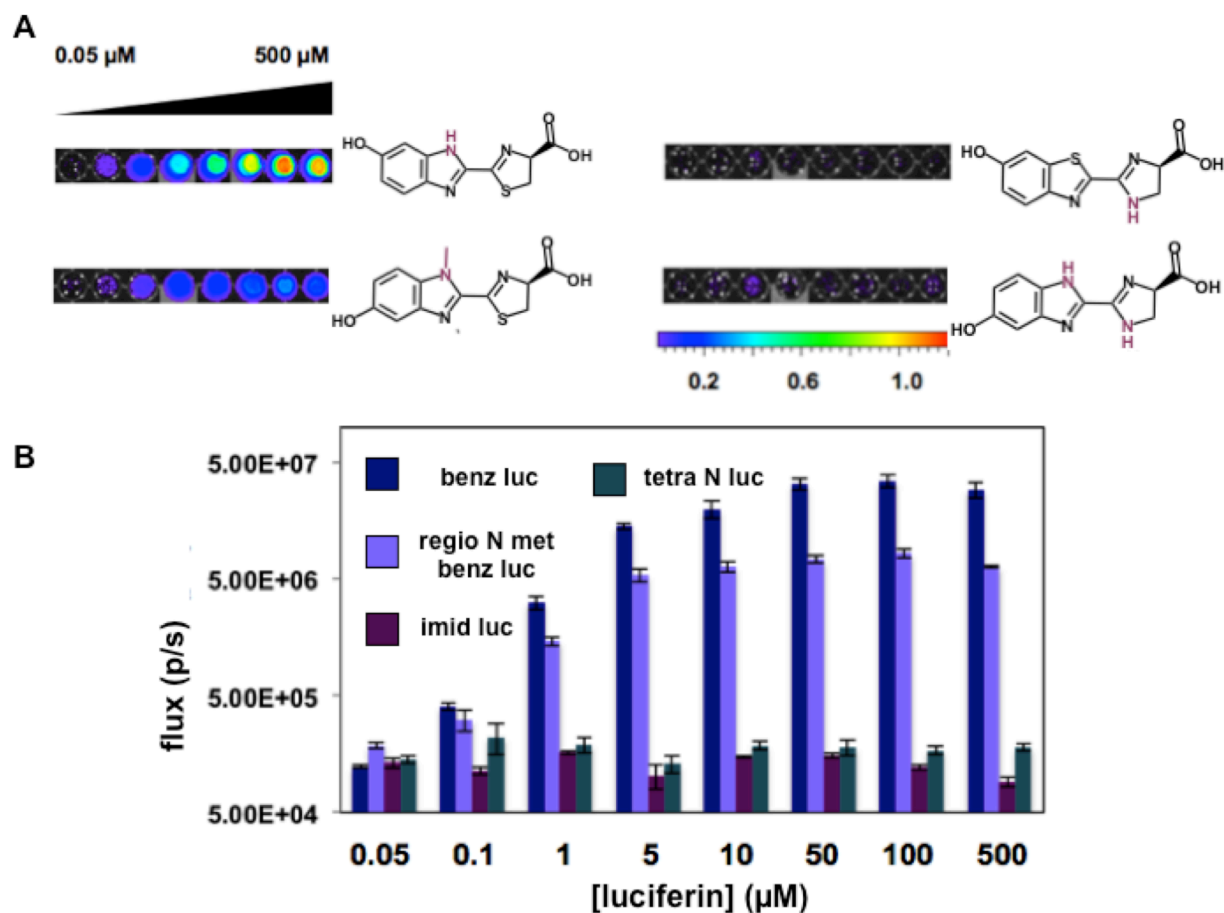
Figure 2-6 Light production from luciferin analogs. (A) Bioluminescence images from analogs benz luc, imid luc, regio N-met luc and tetra N luc (0.05−500 μM) incubated with Fluc or no enzyme. (B) Quantification of the light emission from images from (A) Error bars represent the standard error of the mean for three independent experiments.
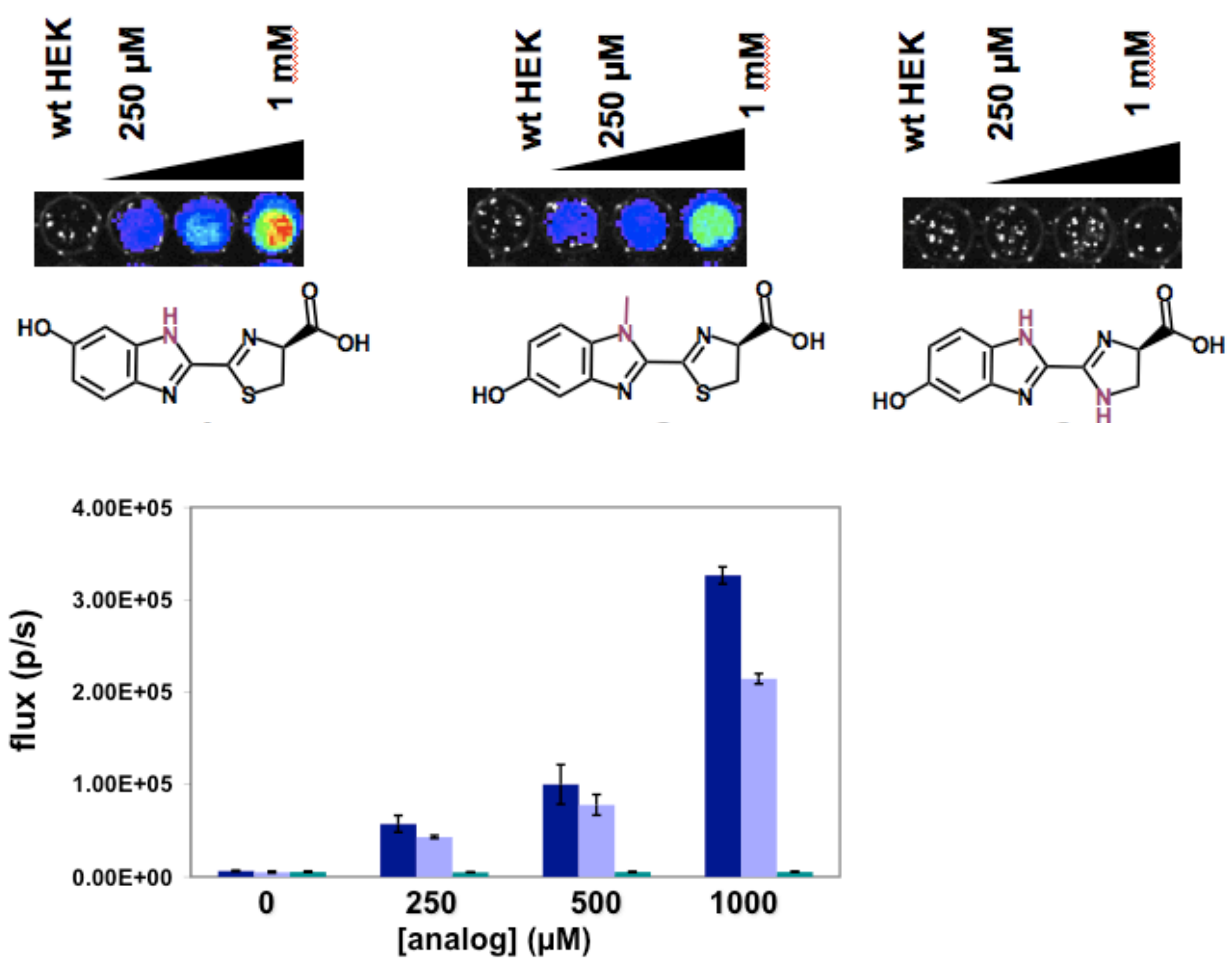
Figure 2-7 Some luciferin analogs emit light in a dose dependent fashion in the presence of luciferase-expressing mammalian cells. HEK 293 cells stably expressing *luc2* were incubated with 250, 500 and 1000 μM of each luciferin analog at room temperature for five minutes. Luminescence was collected and quantified on IVIS camera. Error bars represent the standard deviation of the mean for three replicate samples.

2.3 Analysis of 6´ amino acyl luciferins *in vitro*

To expand beyond the electronically modified luciferins, we also looked to synthetically accessible steric modifications, particularly around the benzothiazole core (Figure 2-3). The 6´ position of D-luciferin has been heavily researched due to the ease of accessing derivatives at this position and inspired by inquiry into the mechanism of light emission [29]. Indeed, 6´acylated aminoluciferins [30] and alkyl aminoluciferins [8] have both been shown to have robust light emission. The crystal structure indicates significant space extending off this position (Figure 2-8). Biochemical experiments with larger residues appended at the 6´ position (e.g., a PEG-chain) support this model [31]. Thus, we envisioned a series of 6´ amino acyl luciferins would be a reasonable starting point for orthogonal probe development (Figure 2-3 B, row 3.)
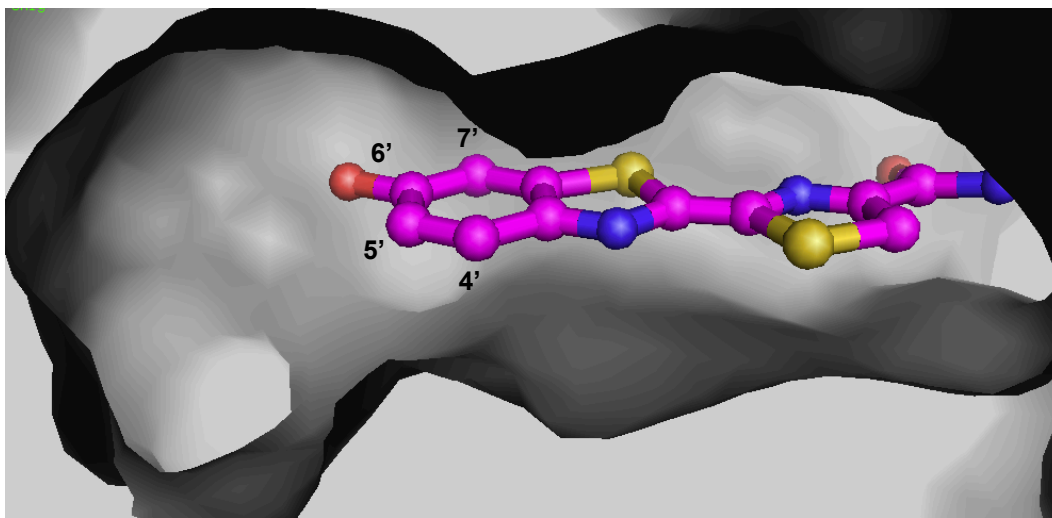
Figure 2-8 Space surrounding the 6´ position of D-luciferin in the co-crystal structure. (PDB: 4G36).

I initially investigated some amino acyl derivatives *in silico* using the Glide module of Maestro from the Schrödinger molecular modeling software suite. The Fluc

structure (PDB:4G36) was pre-processed with protein prepwizard to generate hydrogen atoms that would have been missing from the crystal structure [32]. The software modules Prime and EpiK were used to incorporate and minimize the energy of missing amino acid sidechains, and to determine the biologically relevant protonation state of all protonatable groups [32]. After this, a global energy minimization was performed using the OPLS 2005 force field. From this new minimized structure, a Glide receptor grid was generated. Concurrently, the CF3 AA, i-pr and t-butyl luc analogs (Figure 2-3) were built using the existing DSLA ligand from the crystal structure. DSLA is a non-hydrolyzable analog of the activated AMP ester invoked in the light emission reaction. This analog has been used as a co-crystallizing agent in several structures [32,33].

Each new luciferin analog was docked statically to the receptor and compared to DSLA. As expected, all analogs were all able to access the luciferin-binding site in a manner analogous to D-luciferin. The GlideScore (a unitless measure of predicted binding ability) suggested binding of these substrates would be on par with the native substrate, with some potential additional contacts. CF3 AA luc, in particular, was predicted to have nearly 1 kcal/mol more lipophilic contacts over other analogs (Table 2-1). However, the error of these GlideScores compared to empirical ΔG of binding can vary significantly, so empirical validation would be required to support such claims [34].

Table 2-1 Ligand docking with Glide to WT Fluc receptor.

ligand	docking score	glide gscore	glide lipo	glide hbond
CF3 AA luc	-14.291	-14.291	-5.155	-0.44
i-pr AA luc	-13.654	-13.654	-4.482	-0.932
t-butyl AA luc	-13.124	-13.124	-4.628	-0.39
D-luciferin (DSLA)	-11.532	-11.532	-4.308	-0.247

In addition, because enzymes are not static structures, we were curious how the picture might change if the analogs were given more flexibility to move in the active site or influence the position of surrounding Fluc residues. In order to assess this potential, OPLS200 force field energy minimizations were run on the structure with each analog to see how much the protein would have to move to accept the structure. I visualized the interaction as the surface of the ligand against the surface of the binding pocket (Figure 2-9). In this view, it's clear that all three ligands should be tolerated by the active site similarly. t-Butyl AA luc (yellow) protrudes from the binding site the furthest, but is accommodated nearly as well because active site residues can swing away preventing steric clash. i-Pr AA luc (red) and CF3 AA luc (blue) have very similar energy-minimized conformations, but CF3 AA luc is predicted to have favorable interactions with several active site residues and a more similar footprint to D-luciferin. These results highlight the importance of not only total steric bulk, but also ligand flexibility and electrostatic contacts.

These *in silico* investigations required experimental validation.   Dave McCutcheon synthesized the 6´-amino acyl probes using a similar approach to that of the nitrogenous luciferins. A 6´ amino precursor analog was subjected to various acylating conditions to give CF3 AA luc, t-butyl AA luc and i-pr AA luc. Gratifyingly, each luciferin was demonstrated to have dose-dependent light emission with Fluc (Figure 2-10). The GlideScoring correctly predicted CF3 AA luc as the most potent light emitter. In contrast to the predictions, though, t-butyl AA luc was significantly brighter than i-pr AA luc across all doses, despite its proposed steric clash.   Also in conflict with the calculations, CF3 AA luc and i-pr AA luc, while having basically the same footprint in the active site, showed nearly three orders of magnitude difference in their light emission across multiple doses. This was likely due to the decreased electron density for
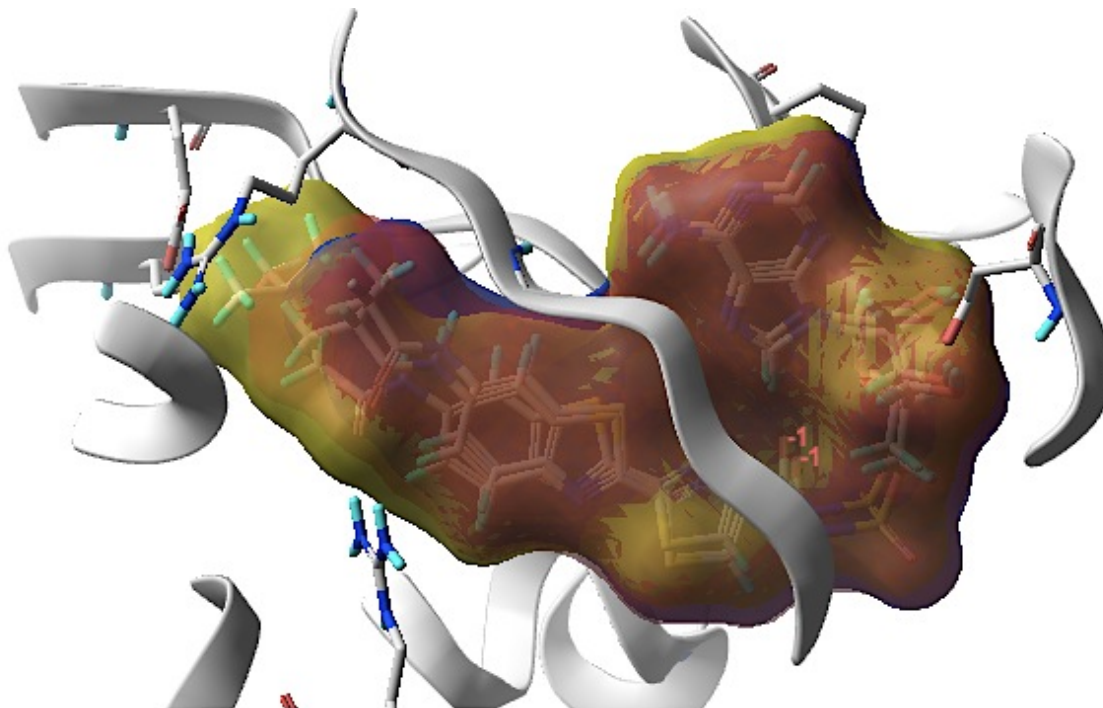
Figure 2-9 Space filling model of energy minimized and merged 6´ acyl aminoluciferin conformations in the active site of Fluc (PDB: 436G). Structure processed with the protein prep wizard and energy minimized with the OPLS 2005 force field.
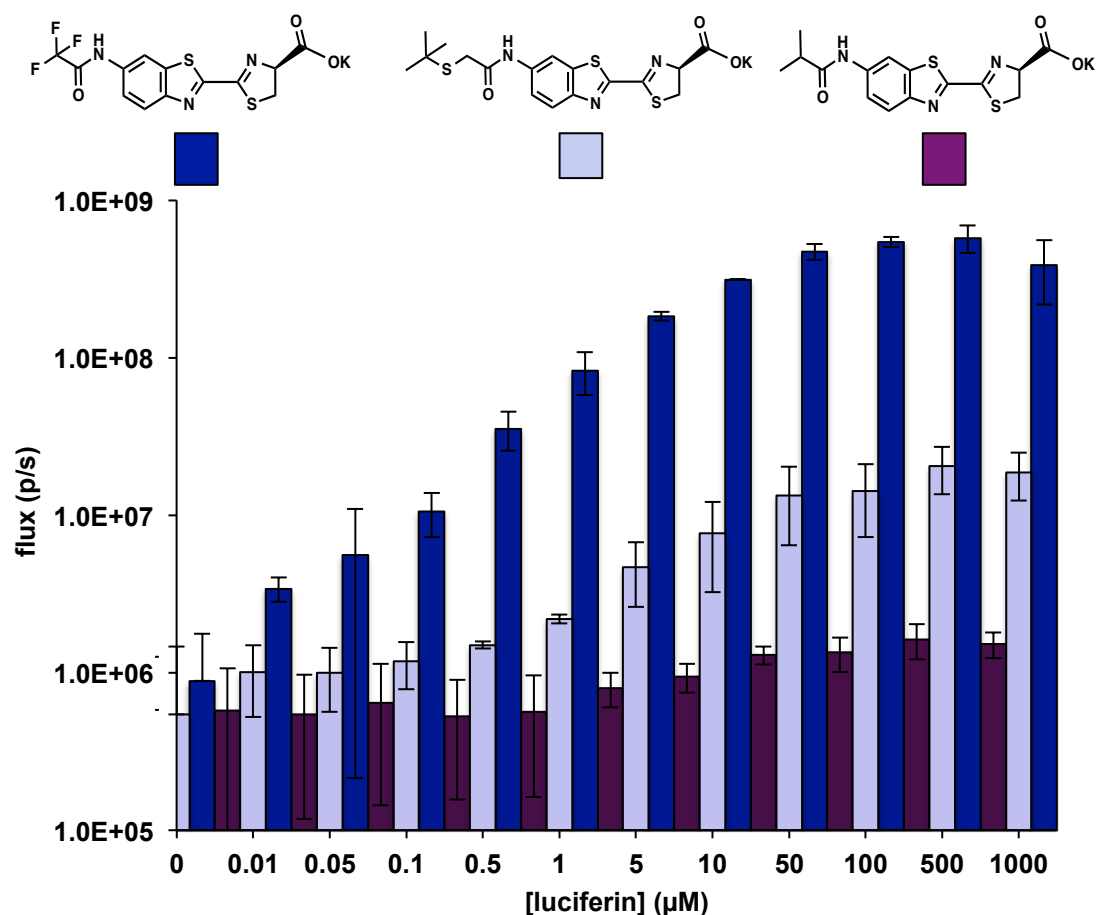
Figure 2-10 6′ Acyl aminoluciferins demonstrate dose-dependent light emission. Quantification of bioluminescence from of CF3 AA luc (dark blue), t-butyl AA luc (light blue) and i-pr AA luc (raspberry) from 0.01−1000 μM when incubated with Fluc. Error bars represent the standard error of the mean from three independent replicates.

ipr AA luc at the 6′ position. These differences also highlight the difficulties in predicting enzymatic activity.

The 6′ acyl aminoluciferins were attractive due to their ease of synthesis to provide a variety of sterically modified luciferins. Computations also predicted good binding for all the derivatives. i-Pr AA luc is particularly ripe for *in vitro* evolution owing to its appropriate size and shape but as yet unoptimized emission. Conversely, as one of the most robust luciferin analogs identified to date, we feel that an enzyme enhanced for

use with CF3 AA luc would have a chance to obtain orthogonality with WT Fluc and D-luciferin, something that more poorly emitting luciferins may never achieve.

2.4 Development and expansion of a novel cyclic luciferin scaffold

If the reduced light emission with the acylated series of luciferins arose from electronic rather than steric considerations, alkylated amino luciferins would offer a more viable starting point. These types of probes have also been validated in the literature. For example, in 2010, Miller and coworkers reported a bright, stable 6′ alkyl cyclic amino luciferin, (CycLuc1) [9]. Our lab immediately recognized the potential utility of this luciferin due to its robust light emission at low concentrations *in vitro*. We also hypothesized that the greater carbon:heteroatom ratio would be advantageous (see the structure in Figure 2-3). Melanie Evans confirmed that the minimal luciferin needed to produce visible signal in mice from implanted tumors was lowered nearly 100-fold from 5 mM to 500 µM. In addition, collaborators at the University of Massachusetts Medical School demonstrated that CycLuc1 readily penetrates the brain through the blood brain barrier and access brain tissue [35].

To further investigate the mechanisms behind CycLuc1's improved *in vivo* performance, I analyzed the relative light emission from CycLuc1 and D-luciferin in various tissue-culture assays. Fluc-expressing 4T1, DB7 and CMT-64 tumor cells were treated with varying concentrations of both luciferins. All the cell lines yielded higher bioluminescent signals with D-luciferin, except at low substrate concentrations, where CycLuc1 is favored (Figure 2-11). When implanted in mice, these same cells produced

greater photon flux with CycLuc1, even in tumors that were located near the surface and/or proximal to the site of substrate injection [35]. This suggests that the delivery of D-luciferin to Fluc-expressing cells *in vivo* is limiting, and that the cell permeability, lower K_m [36] and bioavailability of CycLuc1 play important roles in its superior *in vivo* performance. CycLuc1 outperformed D-luciferin over a wider range of concentrations in 4T1 and CMT-64; these cell lines are known to be highly mucinous which likely presents a barrier to the passive diffusion of D-luciferin (Figure 2-11 A-C) [37]. This provides further evidence to the role of *in vivo* bioavailability in differentiating the two substrates. Another potential contributor to the improved *in vivo* performance of CycLuc1 is a redshift in the emitted photons to more tissue-penetrating wavelengths. When the same cells were imaged through a Cy5.5 (675 nm) emission filter emulating signal attenuation in mammalian tissue, CycLuc1 had a greater percentage of its light in the crucial range, even though D-luciferin emitted a greater number of total photons (Figure 2-11 D and E).

Finally, using recombinant Fluc, I found some evidence that CycLuc1 may enable longer longer-lived emission. I followed the light emitting reaction at time points long after the typical "glow" period for D-luciferin (1-20 min). CycLuc1's emission continued to rise during this period while that of D-luciferin trailed off. CycLuc1 maintained its steady-state emission for nearly one hour (Figure 2-12). In the substrate-limited environment of the implanted tumor, such a subtle effect may become much more pronounced, but additional studies are needed to evaluate the molecular basis for this observation.
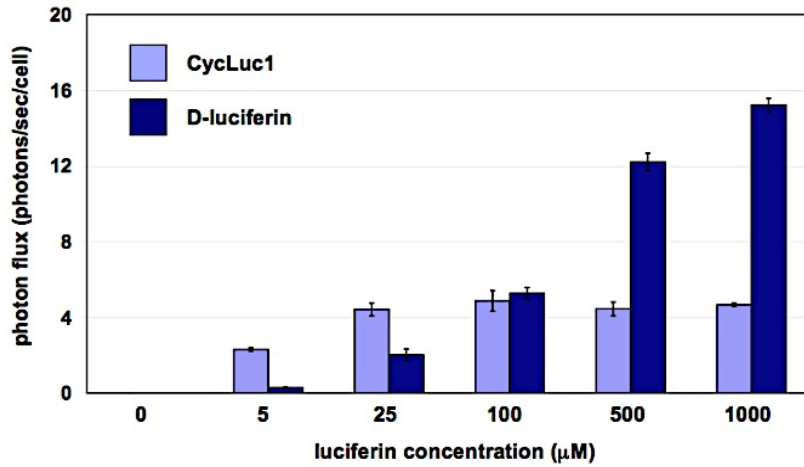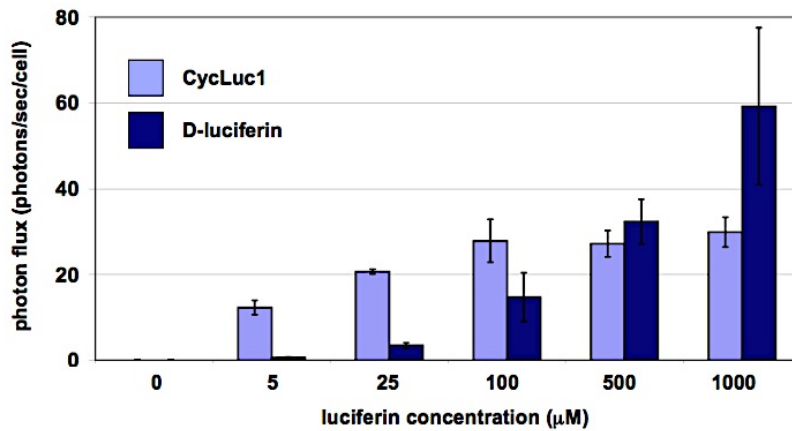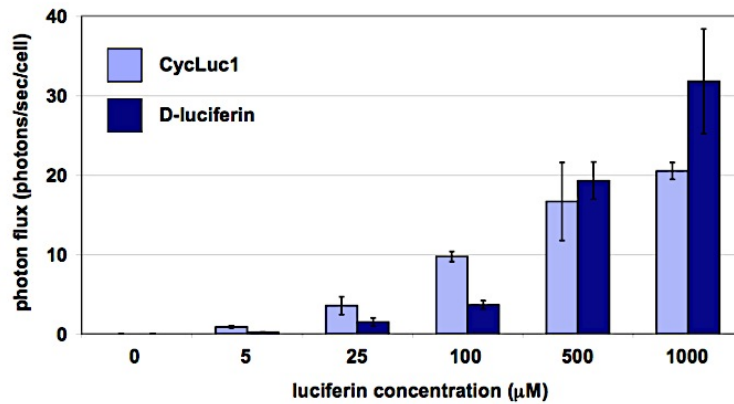
Figure 2-11. Bioluminescence imaging of (A) DB7-luc, (B) 4T1-luc2, and (C) CMT-64-luc cells treated with the indicated concentration of CycLuc1 (light blue bars) or D-luciferin (dark blue bars).

D
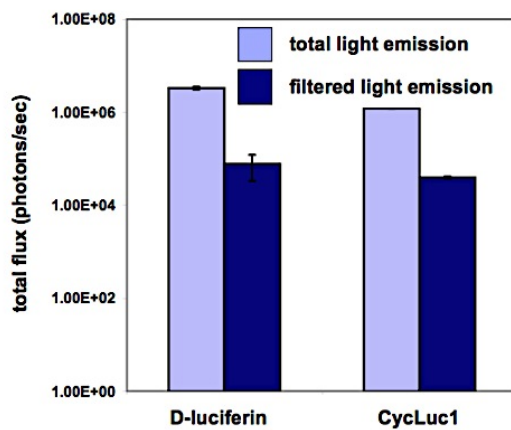
E
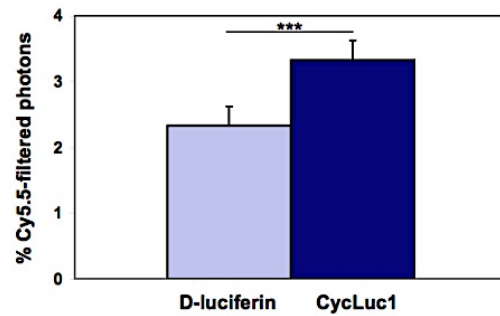
Figure 2-11 cont'd (D) Light output from 50,000 4T1-luc cells treated with 1 mM D-luciferin or CycLuc1. Photons were collected either with an open filter (light blue bars) or after passage through a Cy5.5 filter (dark blue bars). The percent filtered light captured in each case is shown in (E), ***P < 0.001 (t-test). For (A)-(E), error bars represent the standard error of the mean for three independent experiments.
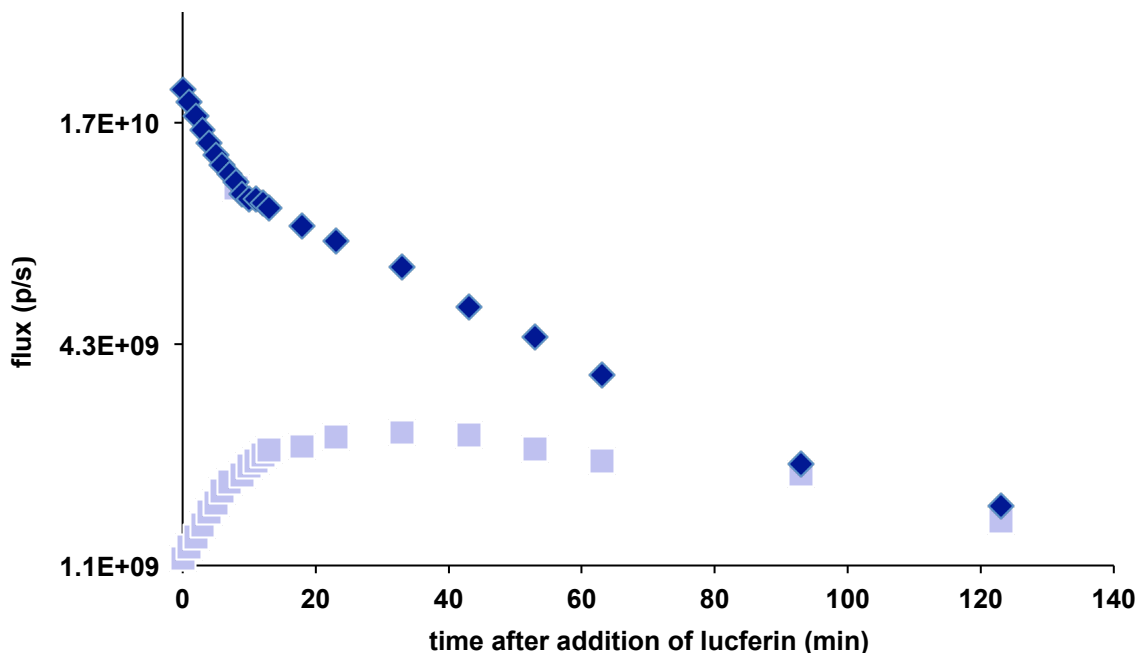
Figure 2-12 Prolonged light emission observed with CycLuc1. Luciferin (100 µM) was added to buffer containing equimolar acetyl CoA and an excess of ATP. Light emission was monitored over time. D-luciferin (dark blue) lost emission while CycLuc1 (light blue) gained intensity.

CycLuc1, in addition to having improved pharmacokinetics, offered unique advantages for designing steric modifications and rapid analog generation. While the parental scaffold was perhaps too bright with WT Fluc, to obtain orthogonality, it could be readily modified. In particular, we were interested in elaboration of the scaffold using mild late-stage diversification to provide a new class of orthogonal luciferins. Rachel Steinhardt, Jessica O'Neill and Brittany Ripley developed a modular "click"-based approach using a propargylated luciferin (CycLuc Alk) (Figure 2-3). The terminal alkyne moiety of CycLuc Alk can be further elaborated with a variety of organic azides using the "click" reaction. The resulting "clicked" CycLucs (Figure 2-3) were assayed for their light emission with Fluc (Figure 2-13). At 100 µM, the EtOH and benzyl "clicked" products produced roughly equivalent numbers of photons (68 and 55% respectively)

compared to parental CycLuc1, despite vastly bulkier substituents. This result further supports extra "room" and flexibility of the active site surrounding the 6′ position, as predicted by our docking and modeling.

The clicked CycLuc1 series of molecules are still a research arm in the lab, but the lack of initial differential in light emission (only the EtOH clicked CycLuc1 had a statistically relevant difference in light emission to D-luciferin) has limited their utility for orthogonal luciferin development. The beauty of the modular "click" approach is that we should be able to access a wide variety of scaffolds. It is possible that even bulkier azido reagents could be used to differentiate the products.
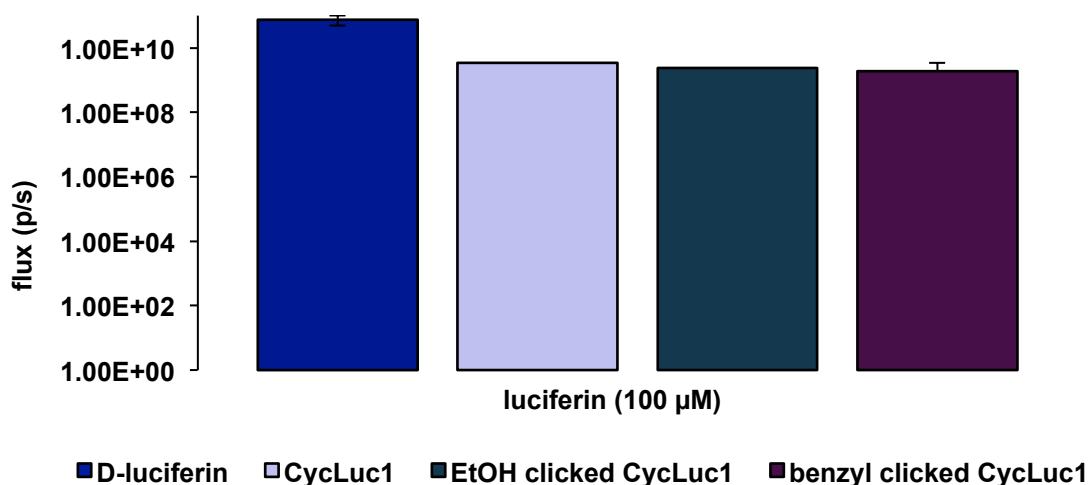
Figure 2-13 Light emission was preserved among CycLuc1 derivatives. CycLuc Alk was "clicked" with azido ethanol and benzyl azide. The resulting luciferins were assayed against recombinant Fluc. Neither CycLuc1 (light blue) nor benzyl click luc (berry) emitted statistically less light than D-luciferin, and none of the three CycLucs' emission was significantly different from any other.

2.5 Identification of luciferase mutants that emit light with luciferin analogs

Having identified both the nitrogenous and 6′ acylated aminoluciferins as viable luciferin analog classes, we also examined the enzyme in parallel. To successfully identify orthogonal pairs, we needed to establish that Fluc could withstand significant mutations to the active site and surrounding amino acids while maintaining its catalytic activity. As a complement to the body of literature available in our design for the luciferin analogs, there has also been significant inquiry into the Fluc structure. For example, some of the residues necessary to catalyze light emission, modulate the wavelength of released photons, and provide stability to the protein structure are known. It has also been established that many of these active site residues can withstand mutation to varying degrees. Branchini and coworkers identified many of the key active site amino acids in the late 1990s and early 2000s [38-42] (Table 2-2). In particular, they reported that several residues may be substituted to afford mutants that provide up to one-fourth of the wild-type activity but exhibit red-shifted bioluminescence emissions [38]. These mutations were included to optimize two "colors" of click beetle luciferases whose spectra were sufficiently resolved to image two targets *in vitro* [43]. These data also suggested that mutations to the putative active site were tolerated reasonably well, and that distant substitutions could also modulate the interaction between the substrate and the enzyme.

Table 2-2. A selection of known Fluc mutant and their bioluminescent activities.

Enzyme	flash height (RLU/mg)	integrated (RLU/mg)	rise time (s ± 0.15)	decay time (min ± 0.1)	Reference #
WT	100	100	0.5	0.2	
H245De	0.3	2.6	59.2	11.7	42
H245A	22	80	0.9	0.9	
H245Ff	4.2	21	1.5	0.8	
H244F	18.4	48	1.0	1.6	
R218A	3.6	30	1.2	4.4	
H245A	26.4	80	0.9	0.9	
G246A	44	104	0.8	0.2	
F247A	4	57	0.9	7.8	
F247L	89	307	0.6	1.3	
F247Y	71	84	0.4	0.2	
F250G	7.5	23	2	3.4	
F250S	21.7	25	0.5	0.2	
T251A	29	156	0.6	2.9	43
G315A	0.15	20.4	1.4	62.3	
G316A	31.7	5.7	0.3	0.1	
G341A	0.16	3	1.1	14.3	
L342A	56	730	0.8	9.4	
T343A	1.1	19.5	1.8	8.9	
S347A	16.7	97.2	0.6	2.4	
A348V	41	150	0.6	4.6	
I351A	139	547	0.5	0.5	
K529A	0.06	12.5	0.6	106	
R218K	33	165	0.62	7.02	
R218Q	5.1	40.5	0.99	4.85	44
R337K	40.6	49.5	0.41	0.12	
R337Q	3.3	20.5	0.51	0.9	

Further insight into desirable mutants to pursue was garnered from crystal structure data. In 2006 and more recently in 2012, structures from insect luciferases with a luciferin-AMP analog (DSLA) were reported in two different catalytic conformations. These structures revealed the involvement of previously implicated residues alongside a few previously unidentified ones. In particular, Arg218 and Thr251 appeared to make

close and stereoelectronically mediated contacts with DSLA. The positive charge of Arg218 had been implicated in the mechanism biochemically, and its placement in the crystal structure could either help stabilize the presumed 6′ phenolate of D-luciferin during the reaction mechanism or perhaps provide a cation-π interaction [39]. Thr251, for its part, seemed poised to donate a hydrogen bond to a nitrogen atom in the thiazoline ring. A mutation of T251A in this position has since been exploited to improve light emission with CycLuc1, and its N-methyl derivative CycLuc2 [36]. These residues looked to be important in our search for orthogonal luciferase-luciferin pairs.

In assessing the relative contributions of the mutant enzyme, I used L-luciferin as a model probe. L-luciferin, the enantiomer of D-luciferin, has been previously shown not to be a substrate of Fluc. However, it can bind the active site and be adenylated. It necessarily maintains all other criteria of a viable luciferin. These features also made L-luciferin an attractive starting point for a rationally designed orthogonal pair, to complement some of the other analogs mentioned earlier. I proposed that a minimalist active site remodeling could be accomplished by trading the places of the R218 and T251 residues because of their defined roles and that their sidechains should be locked into opposite sides of the active site by alpha helices (Figure 2-15). This sort of flip-flop of important catalytic residues in order to invert stereospecifity has precedent in vanillyl alcohol oxidase [44] and in the activation of ion channels by using salt bridges as a molecular switch [45]. In both cases, we were gratified to see that the authors actually use a switch in charges at the targeted residues for mutagenesis.

A

T251

R218

B
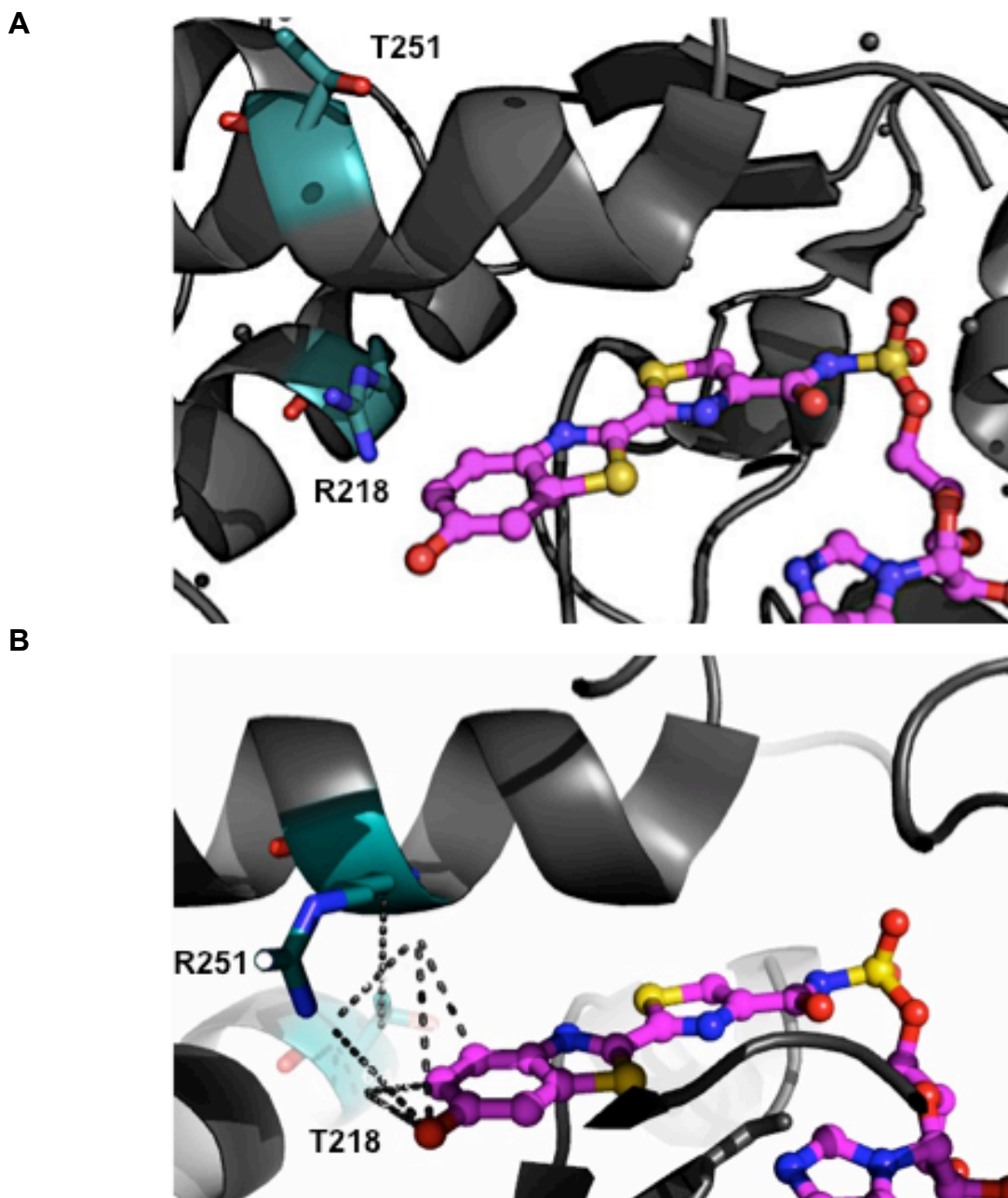
R251

T218

Figure 2-14 Residues Arg218 and Thr251 are in close proximity to luciferin binding site. (A) Pymol rendering of interactions between R218, T251 and D-luciferin in WT Fluc (PDB: 4G36). (B) Proposed flip-flopped active site with T218 and R251 (PDB: 2DIS). Dashed lines represent positions in the active site within an H-bond distance of D-luciferin including both R218 and T251. These residues therefore made sense to target for mutagenesis.

To test the hypothesis that R218T and T251R mutations would enable Fluc to catalyze light emission with L-luciferin, it was first necessary to install the mutations into the Fluc gene. Using Quikchange mutagenesis, I first generated the R218T mutation in the *luc2* gene of a pcDNA Luc2-IRES-eGFP construct, (donated by the Contag laboratory at Stanford) followed by T251R. To optimize protein production in *E. coli*, these mutated Fluc genes were then subcloned into the protein expression vector pET28. Small cultures were inoculated with freshly transformed BL21DE3 cells. After several hours when the cultures had reach mid-log phase, the absorbances were normalized to $OD_{600} \approx 0.6$ and protein expression was initiated with the addition of 500 μM IPTG. Expression was induced for 1 h at 37 °C. Cells were subsequently harvested, resuspended in bioluminescence buffer, and lysed by sonication. The cell lysates were imaged in the presence of each luciferin (100 μM) and 1 mM ATP.
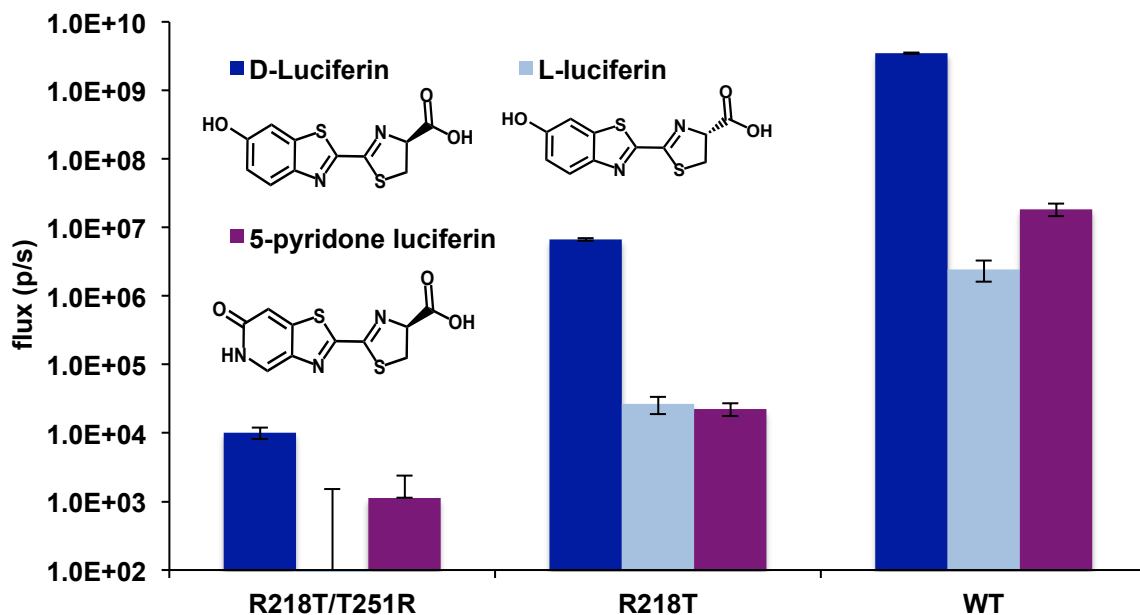
Figure 2-15 R218T and R218T/T251R Fluc mutants catalyze light emission with D- but not L- luciferin. Induced *E. coli* cell lysate was assayed with 1 mM ATP and 100 μM either D-luciferin (dark blue), L-luciferin (light blue) or 5-pyridone luciferin (raspberry) in either R218T/T251R, R218T or WT Fluc cell lines.

Weak emission was observed from the double mutant expressing bacteria (Figure 2-15). Additionally, there was little difference in either mutant's acceptance of L vs. D-luciferin (less than 1% L:D in all Flucs; data not shown). This small level of emission was likely reporting on the enantiopurity of the L-luciferin as a substrate, because any small contamination from D-luciferin present will emit brightly. The analysis was further complicated by slowly increasing light emission for L-luciferin, even in WT Fluc (Figure 2-16). We assume this was due to intracellular racemases in the *E. coli* lysate interconverting the L-luciferin; there is also evidence that Fluc itself can interconvert the two stereochemistries via the CoA thioester intermediate [46]. Collectively, the data suggested that L-luciferin may have been a more difficult starting point for our orthogonal pairs than we had predicted. In the future, screening for activity with L-luciferin in mammalian cells, or other Fluc sources, could limit the racemization issue. In addition, a control could be engineered to subtract the residual emission from D-luciferin contamination. Recent work from the Kato lab also demonstrated that in a related system (the thiolation of ketoprofen by other insect luciferases), positions I350 and M397 (I351 and M397 in Fluc) determine whether or not the preferred R substrate is accepted. It is reasonable to target these residues to being to change the stereospecificity of the enzyme [47].
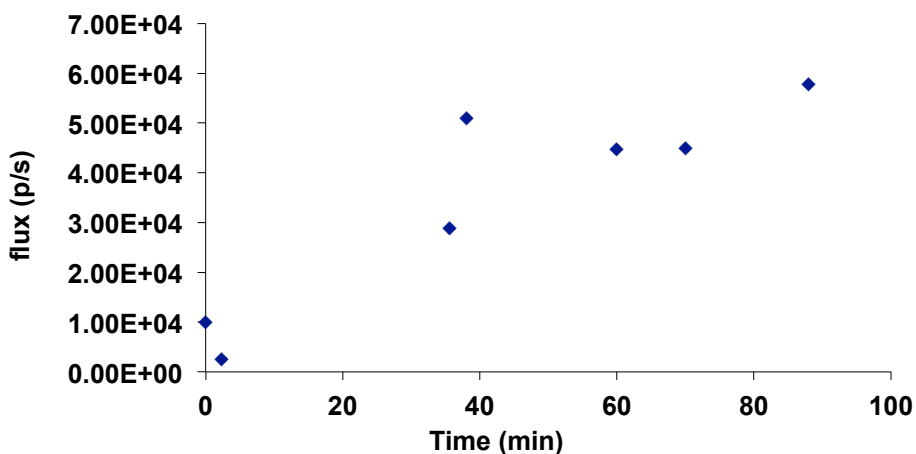
Figure 2-16 L-Luciferin light emission increases over time. WT Fluc *E. coli* cell lysate was incubated with 100 μM L-lucferin at 37 °C and light emission was recorded periodically.

Surprisingly, we did observe significant light emission from the R218T Fluc mutant with both D-luciferin and a 5 N-methyl pyridone variant (included because it does not have a proton at the 6´ position) (Figure 2-14). Both results indicated better catalytic potential from the mutant than we would have hypothesized given the previous literature on that position [39] (Table 2-2). In fact, R218S has even been used as an "inactive enzyme" negative control [48]. In order to analyze this analog and mutant luciferase in a more relevant model for the eventual applications, we decided to test them in cell culture. The pcDNA3.1(+) plasmids were transfected into HEK293 cells using lipofectamine 2000. These cells were drug selected with 500 μg/mL G418 (geneticin) to ensure stable expression of the luciferase. When the cell lines were treated with 100 μM to 1 mM of D-luciferin and N-methyl pyridone luciferin, both compounds exhibited dose-dependent light emission (Figure 2-17 A). Note: the cell lysate assays used the unmethylated pyridone luciferin, but NMR studies from Brendan Zhang suggest that both of these

substrates exist in the same tautomeric state so comparisons between the studies should be valid.) The emission from R218T was equal to that of WT Fluc for both D-luciferin and N-methyl 5-pyridone luciferin. As with CycLuc1, these data could be explained by increased cell permeability. Alternatively, if the mammalian cells expressed more copies of R218T Fluc than WT Fluc in the HEK 293 cell lines I used, this would also explain the discrepancy.

I also surveyed the light emission from R218T and WT Fluc HEK cell lines against many of the previously described luciferins, particularly those with 6′ modifications. Light emission over the background was observed for CF3 AA luc and glycyl AA luc, as well as the three CycLucs (CycLuc1, EtOH clicked CycLuc1 and benzyl clicked CycLuc1) and for D-luciferin itself (Figure 2-17 B). In all cases, the light emission for the WT Fluc vs. the R218T mutant was not substantially different. While further studies with purified R218T Fluc would be needed to confirm this, most likely these results arise from differential expression levels of the protein. Many models of protein folding penalize the "burying" of charges within the active site. pcDNA3.1(+) is a "leaky" expression vector, whereas pET28 works through activation of the *lac* operon with a lactose analog, resulting in a harsh induction of protein. It is possible that R218T Fluc can build up more gradually in the mammalian cell, and does not have that opportunity in the bacterial expression conditions. The unique properties of R218T Fluc as well as additional point mutants published in the literature and produced by others in the lab, made us confident that the biological space that luciferase occupies is ripe for additional development and that new active site residues can imbue this system with novel capabilities.
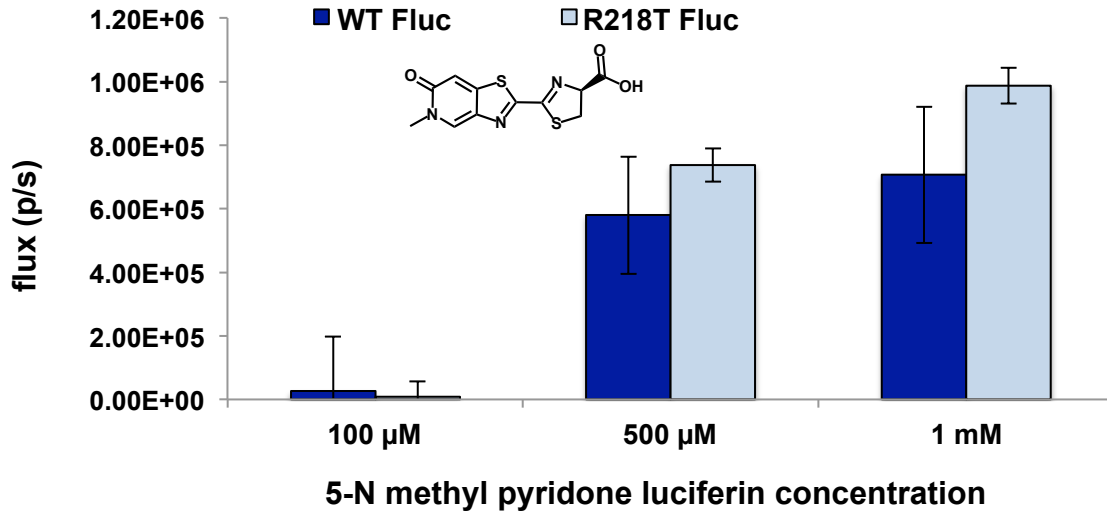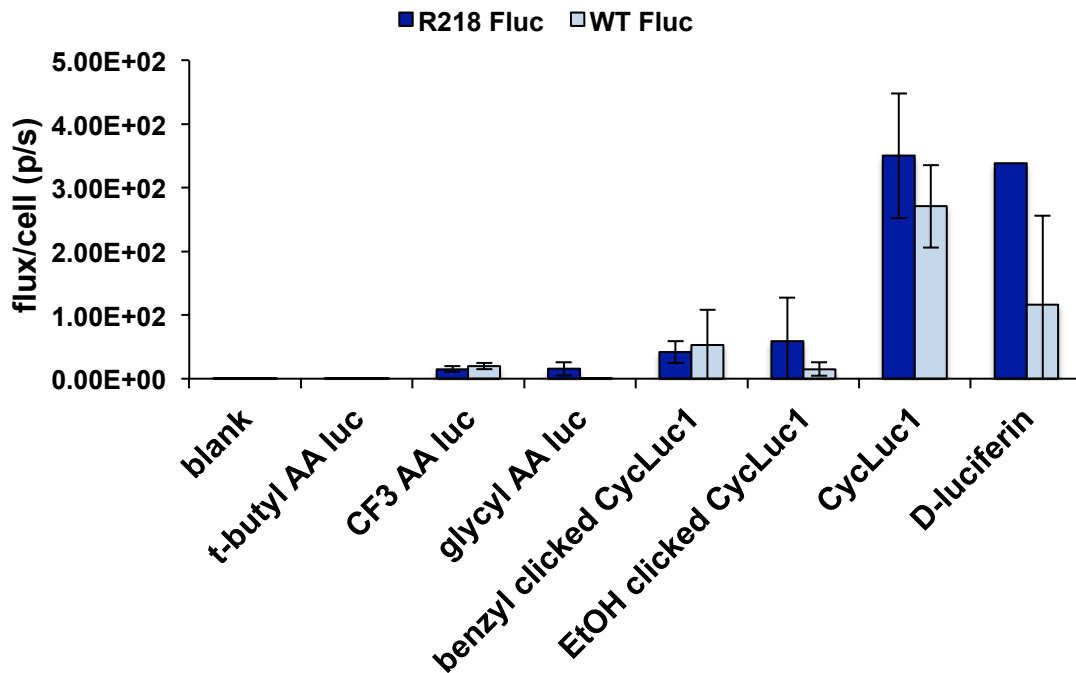
Figure 2-17 WT and R218T Fluc expressing mammalian cells emit light with luciferin analogs comparably. HEK 293 cells stably expressing WT Fluc or R218T Fluc were incubated with (A) 250, 500 and 1000 µM of 5 N-met pyridone luciferin (B) 100 µM of the listed analogs room temperature for 5 min. Bioluminescence was collected and quantified on IVIS camera. Error bars represent the standard deviation of the mean for three samples.

2.6 Conclusions and future directions

In this chapter, I demonstrated successful bioluminescent light emission from the nitrogenous luciferins, 6′ amino acyl luciferins, and CycLuc1 and clicked derivatives. These observations, and those of others demonstrate that the luciferin scaffold is hearty and adaptable [4,6]. Whether steric or electronic perturbations are made, or even alternative aromatic cores are used, as long as certain key features are maintained, a surprising number of structures are all capable of emitting light with the native enzyme, not to mention Fluc mutants. That said, it is also gratifying that it does not appear that the Fluc active site is exceedingly promiscuous. It can perceive the subtle difference in steric bulk and electronics between a CF_3 group and that of an isopropyl group in the context of the N-acyl analogs. If the active site accepted all variations on a general type, we would worry whether true specificity could actually be achieved.

Our current bioluminescence-based analysis does leave something to be desired. While we were able to learn a lot about the interactions of Fluc and our synthesized analogs, this text underplays the synthetic effort involved to produce them in the quantity and purity needed to commence screening efforts. Unfortunately, at this point we do not have a clear idea of whether a given molecule can produce photons before it has been made. Many molecules may "look like luciferins," but due to problems arising from a lack of planarity/aromaticity, poor electron-density in the ring, or other issues, they will remain "dark" no matter how long we look for their luciferase partner. Conversely, there are other luciferins that could be unfairly passed over in a purely bioluminescent assay because although they have some inherent ability to undergo the reaction and emit light, their interface with WT Fluc might be so poor that we do not detect any photon flux. This

case represents an unfortunate problem, because it is these possible, but not as yet optimized, luciferins that hold the most promise for truly orthogonal systems.

In the future, we would like to have better metrics for evaluating our luciferin analogs before they enter the screen, or more ideally, before they are ever synthesized. Our current collaboration with the Furche laboratory at UCI is investigating whether a parameter called "oscillator strength" (a unitless measure of the likelihood that an atom or molecule can absorb or emit electromagnetic during its transitions between energy levels) is sufficient to predict the potential of a molecule to act as a luciferin. If so, we will have an incredibly powerful predictor of candidates for screening before a flask is ever lifted for its synthesis. To establish such a calculation, we need methods of analyzing its predictive accuracy (for the same reason that we have used bioluminescence with the WT Fluc as a proxy thus far) before relying on the method too heavily. As an empirical check on the method, Colin Rathbun, Rachel Steinhardt, Dave McCutcheon and Will Porterfield are synthesizing a palette of known and novel luciferin analogs. These molecules are being analyzed via oscillator strength calculations, chemiluminescence and bioluminescence assays. Because chemiluminescence is fundamentally the same chemical process as bioluminescence, with a high-energy intermediate extruding CO_2 to give an excited state product, it can be used to model the potential light emission from a given luciferin without the influence of the enzyme [49,50]. An ideal luciferin candidate for screening would have poor bioluminescence but robust chemiluminescence and oscillator strength. To complement their work, I have collaborated with the Mobley lab to dock these luciferins in the binding site of the WT Fluc DSLA crystal structure in the same manner as the 6′ amino acyl luciferins; the

docking scores can approximate K_m values (listed in table 4-2). Combined with predictions of the a proposed luciferin's ability to emit light, these values help preselect compounds for the screen. Until such calculations have been fully validated, though, the *in vitro* and tissue culture experiments described in this chapter will remain a mainstay of the lab. As it is, they have already been shown to be incredibly valuable in developing the nitrogenous, acyl and alkyl amino classes of luciferin analogs the screening of whom will be discussed in the following two chapters.

2.7 Methods and materials

General methods section

Buffer reagents were purchased from Fisher Scientific. BLI buffer (100 mM Tris-HCl, 150 mM NaCl, 5 mM $MgCl_2$, 1.5% (w/v) bovine serum albumin, pH 7.8) was prepared and sterile-filtered; between uses it was kept at 4 ºC. Chemically competent bacteria were prepared according to standard protocols. Restriction enzymes and T4 DNA ligase were purchased from New England Biolabs. Platinum PFX (Invitrogen) was used for Quikchange mutagenesis while Dreamtaq (Fermentas) was used for standard PCR applications. All PCR reactions were confirmed by ethidium bromide agarose gel analysis before performing down-stream reactions. Plasmid contstruction was confirmed with sequencing provided by Genewiz, San Diego. For cultures and protein expression, LB and LB agar granulated mixes were purchased from BD Difco. IPTG, PMSF and DTT were purchased from Gold Biosciences.

Subcloning, expression and purification of Fluc

The Fluc gene was amplified by PCR using MP022 and MP027 primers encoding for *Nco*I and *Not*I sites and subcloned into pET28a(+). Colonies were screened with D-luciferin and analyzed by BLI; colonies that emitted light were isolated with Qiagen kit for sequencing. The resulting plasmid was transformed into BL21-DE3 cells. One liter of expression culture was grown to $OD_{600}=0.8$ and induced with 500 µM IPTG and transferred to a 22 ºC shaker O/N. Cells were harvested by centrifugation (10 krpm, 15 min) and resuspended in 40 mL lysis buffer (50 mM Tris-HCl, 500 mM NaCl, 1 mM

DTT, 0.5% (v/v) Tween-20, 1 mM PMSF, pH 7.4). Cells were then lysed by sonication (7 rounds, 70% output, 1 min pulsing at 70% frequency, 3 min rests), and the lysate was clarified by centrifugation (14 krpm, 1 hr). The resulting extracts were purified by Ni^{2+} affinity chromatography and eluted with 100 mM imidazole buffer. Bioluminescence was assayed with D-luciferin to establish that enzyme was functional (see below). Glycerol (10% final concentration) was added to the purified luciferase, which was stored at -20 ºC until use.

<u>Construction of lucifease point mutants</u>

Quikchange mutagenesis (Stratagene, La Jolla) using two sets of primer pairs was used make point mutations in the Fluc gene in pcDNA 3.1+ Primer pairs 1, and then 2, were used sequentially to construct the to install first R218T followed by T251R. The genes were then subcloned into pET28a(+) by standard techniques. Colonies were assessed for light emission by application of 5 mM D-luciferin and bioluminescence was captured with IVIS Lumina (Xenogen) system.   Dark colonies selected for overnight culture, miniprep and sequencing.

Quikchange mutagenic primers
MP015 Luc2 R218T Fwd   5´ CACCGCACCGCTTGTGTCACCTTCAGTCATGC 3´
MP016 Luc2 R218T Rvs   5´ GCATGACTGAAGGTGACACAAGCGGTGCGGTG 3´

MP-017 Luc2 T251R fwd 5´ GCTTCGGCATGTTCCGAACGCTGGGCTACTTG 3´
MP-018 Luc2 T251E Rvs 5´ CAAGTAGCCCAGCGTTCGGAACATGCCGAAGC 3´

<u>*In vitro* bioluminescence assays with native and analog luciferases</u>

Bioluminescence assays with all luciferin compounds were carried out in triplicate, using solid black, flat-bottom, 96-well plates (BD Bioscience). Assay wells contained purified Fluc (0 or 2 μg), luciferin substrate (0-1 mM), ATP (Sigma, 1 mM), coenzyme-A

trilithium salt, Calbiochem, 1 mM), and BLI reaction buffer (20 mM Tris-HCl, 0.5 mg/ml BSA, 0.1 mM EDTA, 1 mM TCEP, 2 mM MgSO4) pH 7.6), totaling 100 μl. Additionally, all non-enzyme assay components were premixed in the wells prior to Fluc addition. Images for all assays were acquired as described above.

Cell lysate BLI assays with native and analog luciferases

Plasmids encoding for Fluc of interest in pET28(a) vector were transformed into BL21 DE3 cells, and grown on kanamycin plates (40 µg/mL) overnight. One colony was selected to inoculate 5 mL LB broth (40 µg/mL kanamycin) for 4-6 h. until $OD_{600} \approx .4$ at which point protein expression was induced with 500 µM IPTG for 1 h. Cells were then harvested by centrifugation, resuspended in BLI reaction buffer and lysed by sonication 1 mM ATP

Cell culture bioluminescence assays with native analog luciferases

HEK293 cells were cultured in DMEM supplemented with fetal calf serum (FCS, 10%), penicillin (10 units/mL), and streptomycin (10 µg/mL) in a CO_2 (5%) humidified incubator at 37 °C. Approximately 2.5×10^5 cells were seeded in 4-cm^2 plates overnight. Cells were transfected with pLuc2-IRES-eGFP by lipofection (Lipofectamine 2000, Invitrogen) according to manufacturer directions. Between 12-24 h. after transfection, cells were replated on 96-well black well plates for bioluminescence assays. Cells were incubated with D-luciferin, benz luc or regio N met benz luc at 0, 250, 500 µM for 5 min. at room temperature. Bioluminescence was acquired as above. Cell lines were later

selected by exposure to G418 (600 µg/ml) over two weeks. 5 N-Met pyridone luc was assayed at 0, 100, 500 and 1000 µM for 5 min at rt.

Molecular modeling

These studies were performed with the Schrödinger 2013-3 molecular modeling software suite. The 4G36 structure from the PDB was imported and processed through the protein prep wizard to generate hydrogen atoms missing from the crystal structure. Thereafter, the software modules Prime and EpiK were used to incorporate and minimize the energy of amino acid sidechains missing from the crystal structure and to determine the biologically relevant protonation state of all sidechains. After this, a global energy minimization was performed using the OPLS2000 force field.

References

(1)   Suzuki, N.; Sato, M.; Nishikawa, K.; Goto, T. Synthesis and Spectral Properties Of 2-(6′-Hydroxybenzothiazol-2′-Yl)-4-Hydroxythiazole, a Possible Emitting Species in the Firefly Bioluminescence. *Tetrahedron Lett.* **1969**, *10*, 4683-4684.

(2)   Seliger, H. H.; Mc, E. W.; White, E. H.; Field, G. F. Stereo-Specificity and Firefly Bioluminescence, a Comparison of Natural and Synthetic Luciferins. *Proc. Natl. Acad. Sci. U.S.A.* **1961**, *47*, 1129-1134.

(3)   White, E. H.; McCapra, F.; Field, G. F. The Structure and Synthesis Of Firefly Luciferin. *J. Am. Chem. Soc.* **1963**, *85*, 337-343.

(4)   White, E. H.; Wörther, H.: Analogs of Firefly Luciferin. 3. *J. Org. Chem*, **1966**, 31; 1484-1488.

(5)   Seliger, H. H.; McElroy, W. Chemiluminescence of Firefly Luciferin without Enzyme. *Science* **1962**, *138*, 683-685.

(6)   Meroni, G.; Santaniello, E.; Rajabi, M. D-Luciferin, Derivatives and Analogues: Synthesis and *in Vitro/in Vivo* Luciferase-Catalyzed Bioluminescent Activity. *Arkivoc* **2009**, 265-288.

(7)   Branchini, B. R.; Hayward, M. M.; Bamford, S.; Brennan, P. M.; Lajiness, E. J. Naphthyl- and Quinolylluciferin: Green and Red Light Emitting Firefly Luciferin Analogues. *Photochem. Photobiol.* **1989**, *49*, 689-695.

(8)   Woodroofe, C. C.; Shultz, J. W.; Wood, M. G.; Osterman, J.; Cali, J. J.; Daily, W. J.; Meisenheimer, P. L.; Klaubert, D. H. N-Alkylated 6´-Aminoluciferins Are Bioluminescent Substrates for Ultra-Glo and Quantilum Luciferase: New Potential Scaffolds for Bioluminescent Assays. *Biochemistry* **2008**, *47*, 10383-10393.

(9)   Reddy, G. R.; Thompson, W. C.; Miller, S. C. Robust Light Emission from Cyclic Alkylaminoluciferin Substrates for Firefly Luciferase. *J. Am. Chem. Soc.* **2010**, *132*, 13586-13587.

(10)   Hopkins, T. A.; Seliger, H. H.; White, E. H.; Cass, M. H. The Chemiluminescence of Firefly Luciferin: a Model for the Bioluminescent Reaction and Identification of the Product Excited State. *J. Am. Chem. Soc.* **1967**, *89*, 7148-7150.

(11)   Suzuki, N.; Goto, T. Studies on Firefly Bioluminescence 2. Identification of Oxyluciferin as a Product in Bioluminescence of Firefly Lanterns and in Chemiluminescence of Firefly Luciferin. *Tetrahedron* **1972**, *28*, 4075-&.

(12)   Airth, R. L.; Rhodes, W. C.; McElroy, W. The Function Of Coenzyme A in Luminescence. *Biochim. Biophys. Acta* **1958**, *27*, 519-532.

(13)   Jathoul, A. P.; Grounds, H.; Anderson, J. C.; Pule, M. A. A Dual-Color Far-Red to Near-Infrared Firefly Luciferin Analogue Designed for Multiparametric Bioluminescence Imaging. *Angew. Chem. Int. Ed. Engl.* **2014**, 48, 13059-13063.

(14)   Fraga, H.; Esteves da Silva, J. C.; Fontes, R. Identification of Luciferyl Adenylate and Luciferyl Coenzyme A Synthesized by Firefly Luciferase. *ChemBioChem.* **2004**, *5*, 110-115.

(15)   Shimomura, O.; Goto, T.; Johnson, F. H. Source of Oxygen in the CO_2 Produced in the Bioluminescent Oxidation of Firefly Luciferin. *Proc. Natl. Acad. Sci. U.S.A.* **1977**, *74*, 2799-2802.

(16)   Lembert, N.: Firefly Luciferase Can Use L-Luciferin to Produce Light. *The Biochem. J.* **1996**, *317*, 273-277.

(17)   Woodroofe, C. C.; Meisenheimer, P. L.; Klaubert, D. H.; Kovic, Y.; Rosenberg, J. C.; Behney, C. E.; Southworth, T. L.; Branchini, B. R. Novel Heterocyclic Analogues of Firefly Luciferin. *Biochemistry* **2012**, *51*, 9807-9813.

(18)   Branchini, B. R.: Chemical Synthesis of Firefly Luciferin Analogs And Inhibitors. *Meth. Enzymol.*, **2000**, *305*; 188-195.

(19)   Craig, F. F.; Simmonds, A. C.; Watmore, D.; McCapra, F.; White, M. R. Membrane-Permeable Luciferin Esters for Assay of Firefly Luciferase in Live Intact Cells. *The Biochem. J.* **1991**, *276* 637-641.

(20)   McCutcheon, D. C.; Paley, M. A.; Steinhardt, R. C.; Prescher, J. A. Expedient Synthesis of Electronically Modified Luciferins for Bioluminescence Imaging. *J. Am. Chem. Soc.* **2012**, *18,* 7604-7607.

(21)   Porterfield, W. B.; Jones, K. A.; Prescher, J. A. *J. Am. Chem. Soc.* **2014**, *in revision*.

(22)   Oba, Y.; Yoshida, N.; Kanie, S.; Ojika, M.; Inouye, S. Biosynthesis of Firefly Luciferin in Adult Lantern: Decarboxylation of L-Cysteine is a Key Step for Benzothiazole Ring Formation in Firefly Luciferin Synthesis. *PLoS One* **2013**, *8*, e84023.

(23)   Lienhard, G. E. Enzymatic Catalysis and Transition-State Theory. *Science* **1973**, *180*, 149-154.

(24)   Petit, J.; Meurice, N.; Kaiser, C.; Maggiora, G. Softening the Rule Of Five--where to Draw the Line? *Bioorg. Med. Chem.* **2012**, *20*, 5343-5351.

(25)   Pollastri, M. P. Overview on the Rule of Five. *Curr. Protoc. Pharmacol.* **2010**, *Chapter 9*, 12.

(26)   Toya, Y.; Takagi, M.; Nakata, H.; Suzuki, N.; Isobe, M.; Goto, T.: A Convenient Synthetic Method of 2-Cyano-6-methoxybenzothiazole,–A Key Intermediate for the Synthesis of Firefly Luciferin. *Bull. Chem. Soc. Japan*, **1992**, *65*, 392-395.

(27)   Yousefi-Nejad, M.; Hosseinkhani, S.; Khajeh, K.; Ranjbar, B. Expression, Purification and Immobilization of Firefly Luciferase on Alkyl-Substituted Sepharose 4B. *Enzyme and Microbial Technology* **2007**, *40*, 740-746.

(28)   Promega. Technical Specifications, Quantilum luciferase.

(29)   White, E. H.; Wörther, H.; Seliger, H. H.; McElroy, W. D. Amino Analogs of Firefly Luciferin and Biological Activity Thereof. *J. Am. Chem. Soc.* **1966**, *88*, 2015-2019.

(30)   Shinde, R.; Perkins, J.; Contag, C. H. Luciferin Derivatives for Enhanced *in Vitr*o and *in vivo* Bioluminescence Assays. *Biochemistry* **2006**, *45*, 11103-11112.

(31)   Chandran, S. S.; Williams, S. A.; Denmeade, S. R. Extended-Release PEG-Luciferin Allows for Long-Term Imaging of Firefly Luciferase Activity *in vivo*. *Luminescence* **2009**, *24*, 35-38.

(32)   Sundlov, J. A.; Fontaine, D. M.; Southworth, T. L.; Branchini, B. R.; Gulick, A. M. Crystal Structure of Firefly Luciferase in a Second Catalytic Conformation Supports a Domain Alternation Mechanism. *Biochemistry* **2012**, *51*, 6493-6495.

(33)   Nakatsu, T.; Ichiyama, S.; Hiratake, J.; Saldanha, A.; Kobashi, N.; Sakata, K.; Kato, H. Structural Basis for the Spectral Difference in Luciferase Bioluminescence. *Nature* **2006**, *440*, 372-376.

(34)   Friesner, R. A.; Murphy, R. B.; Repasky, M. P.; Frye, L. L.; Greenwood, J. R.; Halgren, T. A.; Sanschagrin, P. C.; Mainz, D. T. Extra Precision Glide: Docking and Scoring Incorporating a Model of Hydrophobic Enclosure for Protein-Ligand Complexes. *J. Med. Chem.* **2006**, *49*, 6177-6196.

(35)   Evans, M. S.; Chaurette, J. P.; Adams, S. T., Jr.; Reddy, G. R.; Paley, M. A.; Aronin, N.; Prescher, J. A.; Miller, S. C. A Synthetic Luciferin Improves Bioluminescence Imaging in Live Mice. *Nat. Methods,* **2014**, *11*, 393-395.

(36)   Harwood, K. R.; Mofford, D. M.; Reddy, G. R.; Miller, S. C. Identification of Mutant Firefly Luciferases that Efficiently Utilize Aminoluciferins. *Chem. Biol.* **2011**, *18*, 1649-1657.

(37)   Cooney, C. A.; Jousheghany, F.; Yao-Borengasser, A.; Phanavanh, B.; Gomes, T.; Kieber-Emmons, A. M.; Siegel, E. R.; Suva, L. J.; Ferrone, S.; Kieber-Emmons, T.; Monzavi-Karbassi, B. Chondroitin Sulfates Play a Major Role in Breast Cancer Metastasis: a Role for CSPG4 and CHST11 Gene Expression in Forming Surface P-Selectin Ligands in Aggressive Breast Cancer Cells. *Breast Cancer Res.* **2011**, *13*, R58.

(38)   Branchini, B. R.; Magyar, R. A.; Murtiashaw, M. H.; Anderson, S. M.; Helgerson, L. C.; Zimmer, M.: Site-Directed Mutagenesis of Firefly Luciferase Active Site Amino Acids: a Proposed Model for Bioluminescence Color. *Biochemistry*, **1999**, *38*, 13223-13230.

(39)   Branchini, B. R.; Magyar, R. A.; Murtiashaw, M. H.; Portier, N. C.: The Role Of Active Site Residue Arginine 218 in Firefly Luciferase Bioluminescence. *Biochemistry*, **2001**, *40*, 2410-2418.

(40)   Branchini, B. R.; Murtiashaw, M. H.; Magyar, R. A.; Portier, N. C.; Ruggiero, M. C.; Stroh, J. G. Yellow-Green and Red Firefly Bioluminescence from 5,5-Dimethyloxyluciferin. *J. Am. Chem. Soc.* **2002**, *124*, 2112-2113.

(41)   Branchini, B. R.; Magyar, R. A.; Murtiashaw, M. H.; Anderson, S. M.; Zimmer, M. Site-Directed Mutagenesis of Histidine 245 in Firefly Luciferase: a Proposed Model of The Active Site. *Biochemistry* **1998**, *37*, 15311-15319.

(42)   Branchini, B. R.; Southworth, T. L.; Murtiashaw, M. H.; Boije, H.; Fleet, S. E. A Mutagenesis Study of the Putative Luciferin Binding Site Residues of Firefly Luciferase. *Biochemistry* **2003**, *42*, 10429-10436.

(43)   Branchini, B. R.; Southworth, T. L.; Khattak, N. F.; Michelini, E.; Roda, A. Red- And Green-Emitting Firefly Luciferase Mutants for Bioluminescent Reporter Applications. *Anal. Biochem.* **2005**, *345*, 140-148.

(44)   van Den Heuvel, R. H.; Fraaije, M. W.; Ferrer, M.; Mattevi, A.; van Berkel, W. J. Inversion of Stereospecificity of Vanillyl-Alcohol Oxidase. *Proc. Natl. Acad. Sci. U.S.A.* **2000**, *97*, 9455-9460.

(45)   Moroni, A.; Thiel, G. Flip-flopping salt bridges gate an ion channel. *Nat. Chem. Biol*. **2006**, *2*, 572-573.

(46)   Nakamura, M.; Maki, S.; Amano, Y.; Ohkita, Y.; Niwa, K.; Hirano, T.; Ohmiya, Y.; Niwa, H. Firefly Luciferase Exhibits Bimodal Action Depending on The Luciferin Chirality. *Biochem. Biophys. Res. Commun.* **2005**, *331*, 471-475.

(47)   Kato, D.; Hiraishi, Y.; Maenaka, M.; Yokoyama, K.; Niwa, K.; Ohmiya, Y.; Takeo, M.; Negoro, S. Interconversion of Ketoprofen Recognition in Firefly Luciferase-Catalyzed Enantioselective Thioesterification Reaction Using from *Pylocoeria miyako* (Pml) and *Hotaria parvura* (Hpl) just by Mutating Two Amino Acid Residues. *J. Biotechnol.* **2013**, *168*, 277-283.

(48)   Murooka, T. T.; Deruaz, M.; Marangoni, F.; Vrbanac, V. D.; Seung, E.; Andrian, U. H. v.; Tager, A. M.; Luster, A. D.; Mempel, T. R.: HIV-Infected T Cells Are Migratory Vehicles for Viral Dissemination. *Nature* **2012**, 1-7.

(49)   Marques, S. M.; Esteves da Silva, J. C. Firefly Bioluminescence: a Mechanistic Approach of Luciferase Catalyzed Reactions. *IUBMB Life* **2009**, *61*, 6-17.

(50)   Merenyi, G.; Lind, J.; Eriksen, T. E. Luminol Chemiluminescence: Chemistry, Excitation, Emitter. *J. Biolum. Chemilum.* **1990**, *5*, 53-56.

CHAPTER 3: Screening a library of luciferase mutants

3.1 Introduction

One of the biggest unknowns in any screen is the question of "is it possible?" While *in vitro* evolution has been incredibly successful at finding the necessary sequences to perform a task of interest, this is no guarantee that a sequence exists for a particular application. Selections are long and hard. The fitness landscape that connects proteins with fold and function to those nearly infinitum series of functionless amino acid sequences is vast and flat. Most mutations are deleterious. We are miserable at predicting what pathway connects the few oases with purpose in the desert of empty biological space. This has been stated eloquently by Frances Arnold:

> "Despite major advances, a molecular-level understanding of why one protein performs a certain task better than another remains elusive. This is perhaps not surprising when we remember that a protein often undergoes conformational changes during function and exists as a dynamic ensemble of conformers that are only slightly more stable than their unfolded and non-functional states and that might themselves be functionally diverse. Mutations far away from active sites can influence protein function. Engineering enzymatic activity is particularly difficult because very small changes in structure or chemical properties can have big effects on catalysis. Thus, predicting the amino acid sequence, or changes to an amino acid sequence, that would generate a specific behavior remains a challenge... [1]"

That said, the combined published work on luciferin analogs and mutations in the luciferin-binding site, in parallel with our own work tells us that the fitness landscape surrounding Fluc is rich and varied and could potentially be adapted with relative ease towards new substrates and functions. While the crystal structures of enzymes and other proteins provide insight, and targeted mutagenesis can be successful, a large proportion

of "change-of-function" studies arrive at their structure through random mutagenesis [2]. This may be due to the process' inherent ability to survey multiple subtle changes in the fitness landscape [3] while seemingly rational changes can generate harsher jags in that topography.

In vitro evolution has been used to improve the function of many enzymes, including evolved versions of Fluc with improved thermostability [4] pH sensitivity, [5] and K_m and V_{max} values [6]. Most importantly, the screening of small libraries of Fluc mutants have afforded luciferase variants that do not emit light with D-luciferin, but can be turned-on with certain optimized luciferin analogs [7]. Conversely, combinations of random mutagenesis and substrate engineering have been used to rescue light emission from related monooxygenases (enzyme family in which Fluc belongs) found in worms [8] and even *Drosophila* [8,9]. These data collectively, along with the limited success in our efforts at rational mutagenesis, convinced me that random mutagenesis and a screen of the luciferases and luciferins against one another would yield orthogonal pairs most efficiently.

I set about to design a luciferase library that would maximize the effect of mutations, while not sacrificing the integrity of the enzymatic scaffold. The latter often results in misfolded or otherwise inactive proteins. At the same time, I worked to develop a screen that identified mutants with interesting activities: for example, the ability to process unique luciferins or to discriminate between two luciferins. We also looked for improved binding affinities for an analog scaffold of interest. This latter feature is most akin to *in vitro* evolution, selecting variants that exhibit improved features compared to earlier "versions" of the enzyme. The screen needed to be sensitive enough to detect

small changes in relative light emission levels, but also robust and reproducible even when using minimal amounts of the luciferin compounds. I also hoped that the screen would be minimally time and labor intensive, so that all members of the lab could be employed as screeners compounds became available.

Improvements to either specificity or affinity would aid our search for orthogonal luciferase-luciferin pairs because the shifts in substrate preference (even if imperfect) could be evolved into complete orthogonality over several generations of the library. Analogously, finding Fluc variants that were particularly bright emitters with a given luciferin, were likely to contain mutations that made them specific for that substrate and could then be screened against other such optimized pairs. Both approaches would be benefitted by facile access to additional generations of libraries, so I also aimed to optimize each subcloning step to simplify the workflow on subsequent improvements to the initial hits.

3.2 Construction of the library

The mechanisms of luciferase-catalyzed light emission are still debated, but overall, the enzyme generates an activated luciferin–AMP intermediate from bound molecules of luciferin and ATP (Figure 2-1). Subsequent oxidation of this molecule results in the production of light [10,11]. Previous studies have demonstrated that the light emission is dependent on amino acid residues within both the luciferin and ATP binding pockets, as well as distant locations [12]. The activities of known mutants are provided in Table 2-2. Based on these findings, we decided to create libraries where the mutations spanned defined regions for a higher level of mutagenesis. The luciferin-

binding site (R1), the ATP cofactor binding site (R2), as well as the collective region

spanning both shorter sections (R1R2) presented attractive targets for random

mutagenesis. The targeted regions of Fluc are shown in Figure 3-1.
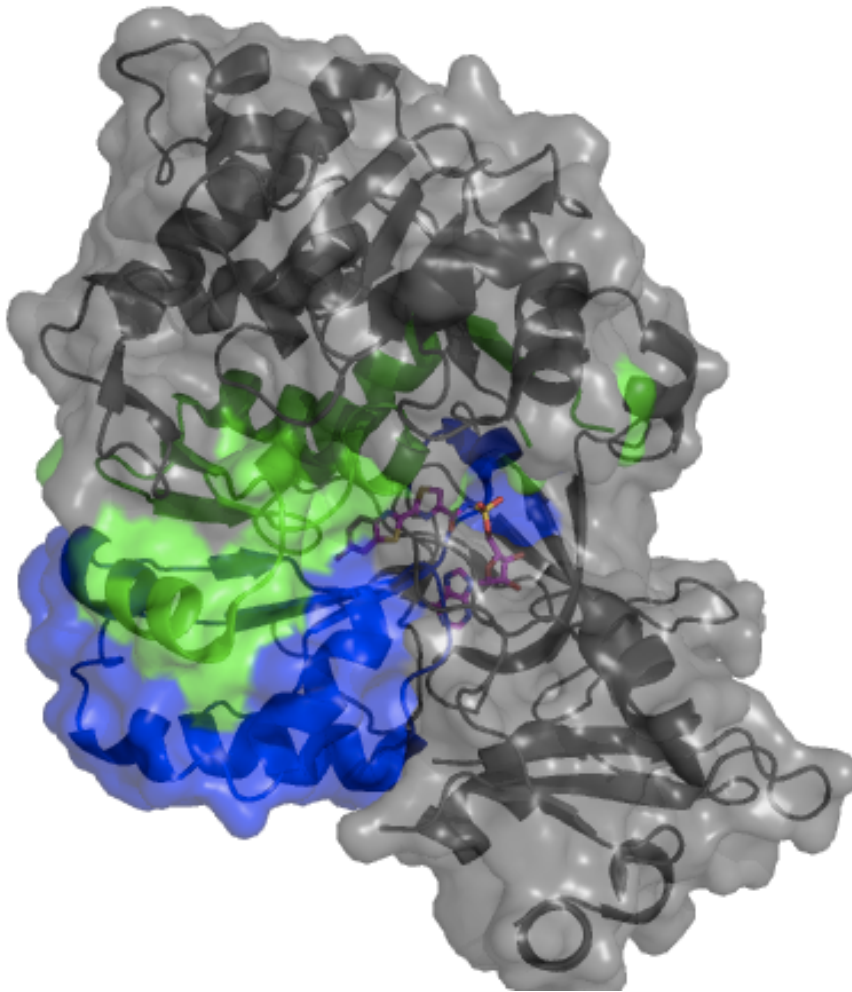
Figure 3-1 Regions of Fluc targeted for mutagenesis: these included the luciferin-binding site from Gly199 to Arg275 (green) and ATP-binding site from Arg275 to Thr346 (blue).
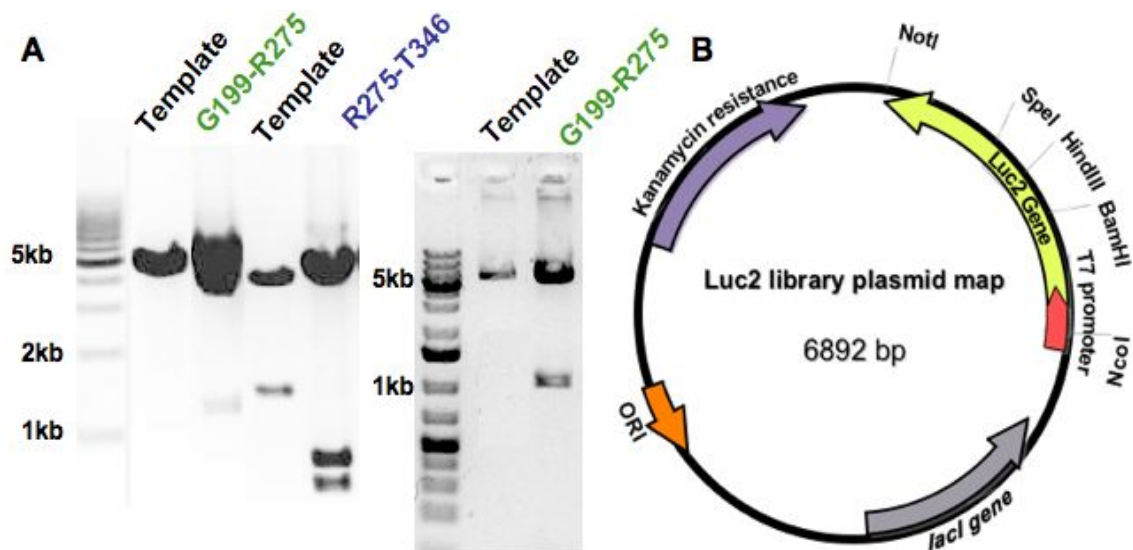
Figure 3-2 Generation of parental vectors for mutant luciferase libaries. (A) Plasmid map of Luc2- pET28a(+) highlighting "silent" restriction sites. (B) Gel analysis of digested Luc2-pET plasmid in which the resulting additional band demonstrates the presence of a new restriction enzyme site.

In order to confine mutations in R1 and R2, we needed to identify regions of the luciferase gene that could be modified for specific insertion of library DNA. With these general positions identified, the gene sequence was scanned for positions where a mutation could introduce a new restriction endonuclease recognition site, without altering the amino acid sequence. Such "silent" restriction sites would enable access to the targeted gene regions. G199, R275 and T346 were all identified as potential positions to install "silent" *Bam*HI, *Hind*III and *Spe*I restriction sites, respectively. These sites were introduced using Quikchange mutagenesis in the pcDNA3.1 vector. Successful introduction of these sites was verified via digestion analysis (Figure 3-2 A). The modified Fluc genes were also introduced into the pET28a(+) bacterial expression plasmid for future screening work (Figure 3-2B). When transformed into bacteria and
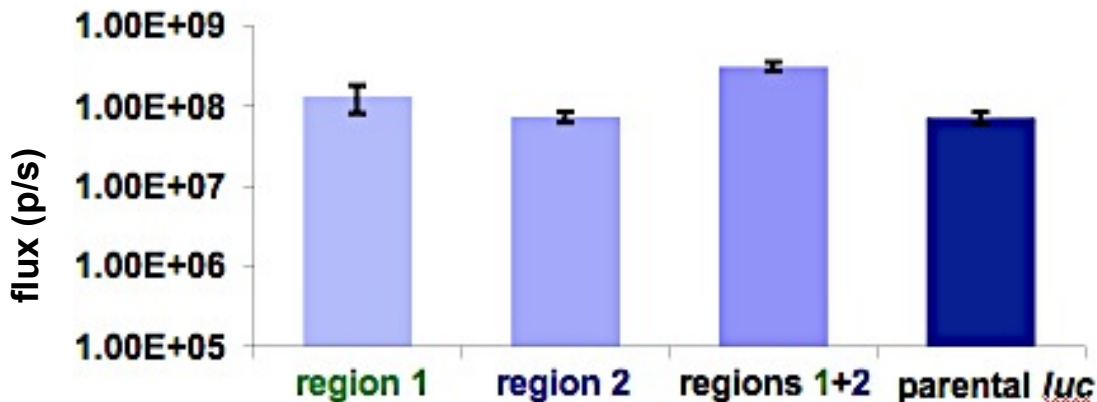
Figure 3-3 "Silent site" luciferase constructs emit light similarly to to the parental *luc* construct. Overnight cultures were induced with 500 µM IPTG for one hour, (37 °C) then they were normalized for $OD_{600} = 3.2$. D-Luciferin (50 µM) was added to 100 µL of culture. After a 5 min incubation at rt, light emission was quantified on an IVIS Ilumina CCD camera.

assessed for light emission with 100 µM D-luciferin, their light emission was comparable to bacteria transformed with *luc2* (Figure 3-3). This result suggested that our constructs were valid starting points for further diversification.

With the "silent" sites installed, it was necessary to produce mutated fragments of luciferase DNA to construct the targeted libraries. In order to generate mutant DNA, many techniques have been developed to take advantage of the natural propensity of DNA polymerases to make errors during replication [13]. Mutagenesis with dNTP analogs is a particularly useful method for introducing errors into a gene of interest, and in some cases, error rates of twenty percent have been reported while minimizing frame shifting insertions and deletions [14]. This approach utilizes unnatural DNA analogs (8-oxo-dGTP and dPTP) in early rounds of PCR, and the level of mutation can be easily "tuned" by adjusting the concentrations of the unnatural analogs. We generated libraries of DNA fragments for our two shortest libraries using this technique. Gel analysis

revealed a decreasing yield of randomized DNA inserts with increasing analog

concentration (Figure 3-4), suggesting successful mutagenesis because the polymerase

has trouble incorporating large quantities of unnatural dNTPs.
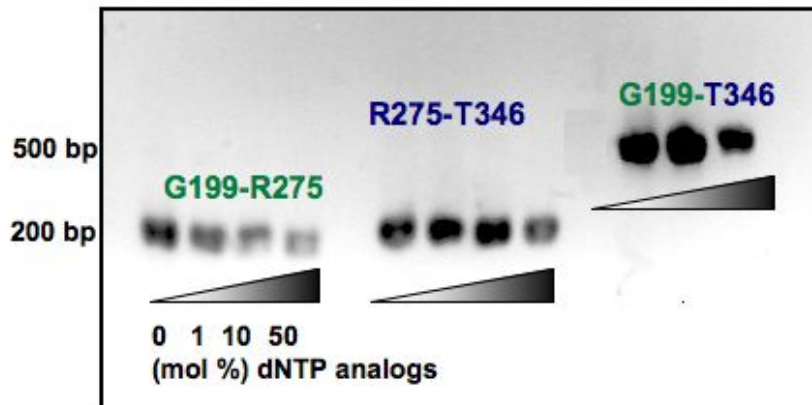
Figure 3-4 Agarose gel stained with ethidium bromide shows products of analog dNTP mutagenesis for the R1, R2 and R1R2 regions of the *luc2* gene. Error-prone PCR was performed with 0, 2, 20 or 100 μM each of dPTP and 8-oxo dGTP and 200 μM each of the natural nucleotides. Twenty rounds of amplification were performed.

In addition to targeting critical regions of luciferase, we also aimed to generate a

library with mutations spanning the entire gene. Amino acids far from the active site of

luciferase have been shown to impact the thermostability, bioluminescence emission

spectra and pH sensitivity of the enzyme [5,15,16]. Such key residues are often difficult

to predict based on sequence or structure analysis alone, and are usually revealed only by

random mutagenesis screening. Due to the vast length of the *luc2* gene (1653 bp), a

milder mutagenic technique for creating library DNA was selected [17]. Amplifying the

gene in the presence of 1 mM $MnCl_2$ and 7 mM $MgCl_2$ produced sequences with an error

rate of 0.4-1.6% (based on 750 bp sequencing reads). Because R1R2 was a relatively

long region encoding for many key residues, this milder technique was also employed to generate a second R1R2 library, thus ensuring that if the analog mutagenesis proved to harsh, we would have an alternative. As expected, the error rate was much lower than that of the analog strategy. For the R1 library, only the transformations of plasmid DNA prepared with the lowest dNTP analog concentration (1 mol%) produced viable colonies. This result underscores how key this region is to proper folding and protein production. The ATP binding site, by contrast, appears to be remarkably tolerant of mutation given the residual light emission, despite very high (up to 20%) amino acid substitution (Table 3-1; For raw sequence data, see Appendix 1). When 5 mM D-luciferin was directly applied to the colonies containing R1 library members, a majority emitted light, albeit with reduced intensity than colonies expressing natuive Fluc (Figure 3-5 A; Table 3-1, entry 1). Conversely, under the same conditions, only one-quarter of the R2 library members emitted light over background (Figure 3-5 B; Table 3-1 line 2). As we suspected, the R1R2 region required the milder mutagenic conditions to generate functional enzymes. Gratifyingly, the mutations revealed *via* sequencing were representative of these light emission observations: the more mutations correlated with lower percentages of light emitting colonies (Table 3-1). In addition, these mutations were distributed throughout each targeted region. Finally, in unbiased sequencing (no selection for light emission properties with a given luciferin), each sequence was unique. Collectively, these properties suggested wide library diversity.

Table 3-1 Quantification of luciferase mutants from each generation 1 library.

library	number of clones analyzed	light emitting sequences (%)	number of observed bp mutations	amino acid alterations (total amino acids)
R1 (G199-R275)	12	70	0-2	1 (76)
R2 (R275-T346)	7	25	6-15	9 (71)
R1R2 (G199-T346)	12	35	4-16	5 (147)
Fluc (full length)	15	85	0-8*	2* (550)

 * extrapolated to full length enzyme from 750 bp sequence
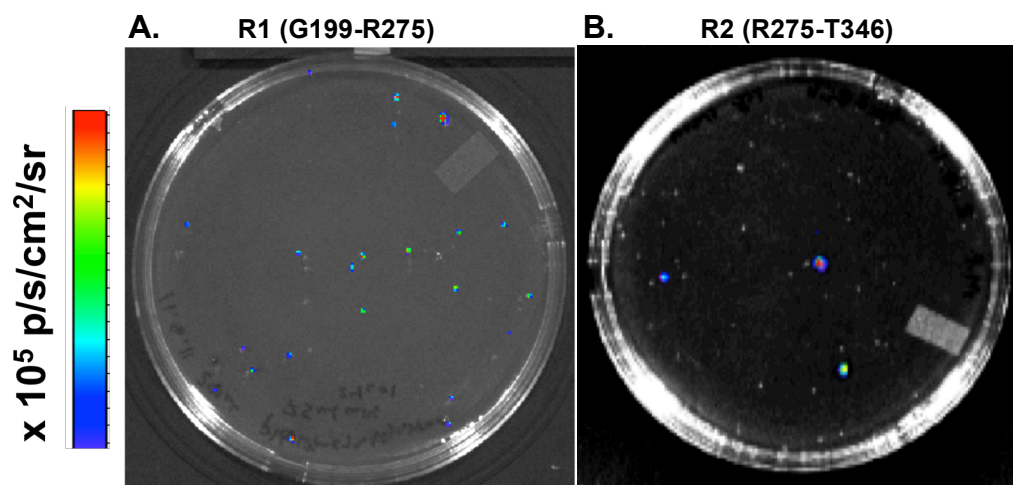
Figure 3-5 Bioluminescent image of (A) R1 and (B) R2 library members screened on an agar plate. D-Luciferin (5 mM) was directly applied to the individual colonies prior to image acquisition.

3.3 Design of the screen

With several luciferase libraries in hand, we were poised to begin screening the sequences for productive light emission both with D-luciferin and unnatural luciferin analogs. There were several factors to consider for the screens themselves: how to segregate the library members, how to administer the compound and assay for light emission, and ultimately, how to identify the sequences of the "hits." To begin addressing these issues, we first measured the light emission associated with D-luciferin from R1 and R2 library members and imaging with our IVIS camera.

I first decided to investigate an assay using pooled luciferase mutants arrayed over 96-well plates. The benefit here is that a defined amount of D-luciferin or an analog could be delivered to each well, and light emission measured in a manner controlled for both cell count and substrate volume. We found that 250 pg of library DNA transformed one *E. coli* bacterium (on average) and that we could control the numbers of colonies in each well by dilution (from 1-20 distinct colonies). While this result was gratifying, the observed luminescence was quite low (Figure 3-6 A). Through several rounds of optimization, we found conditions that provided robust light emission while minimizing the amount of compound used. We induced the overexpression of protein with IPTG, concentrated the cultures, and lysed the cells with hen egg-white lysozyme (HEWL) (Figure 3-6 B). A control experiment was performed under these optimized conditions to demonstrate that when the parental *luc2* vector was screened in concert with D-luciferin, the light emission remained constant across the wells (Figure 3-6 C). This result

reassured us that differential emission under our optimized conditions was a reflection of the new architectures of the active site rather than inconsistencies in cell lysis or substrate delivery.
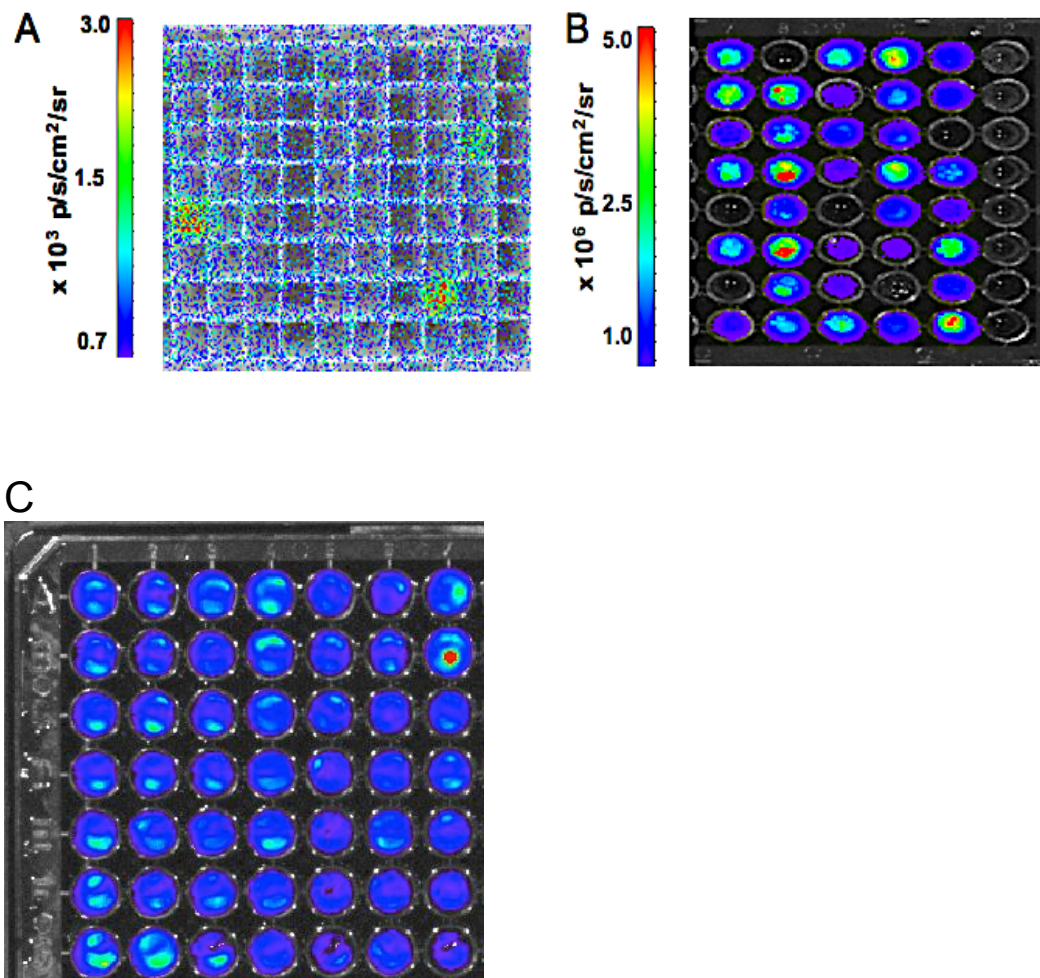
Figure 3-6 Bioluminescence images of solution-phase screening conditions. (A) Preliminary screening conditions involved 500 µL of uninduced culture, (XL1 cells,) 20 µM D-luciferin and a 5 min incubation, rt. (B) Screening conditions were optimized for robust light emission which included BL21 cells induced with 100 µM IPTG, then concentrated and lysed with HEWL. (C) BL21 cells expressing WT Fluc were exposed to the same screening conditions and imaged with 50 µM D-luciferin, ATP and coenzyme A. Average emission = $1.87 +/- .61 * 10^8$ p/s, where the error is the standard deviation of the mean for n=49 wells.

3.4 Screening with nitrogenous luciferin analogs

The first class of analog luciferins available for screening were the nitrogenous analogs benz luc, regio N met benz luc and CF3 AA luc (Figure 2-3). Benz luc and regio N met benz luc were attractive for screening due to their complimentary levels of light emission with native Fluc and ease of synthesis. I began the process of screening for orthogonal luciferin-luciferase pairs by transforming R1 library DNA into *E. coli*, diluting the transformants over a deep-well plate, and growing the cultures overnight. After a 1 h induction of protein expression with 100 μM IPTG, the cultures were divided into replicate plates, harvested, lysed, and imaged with D-luciferin (positive control), benz luc, imid luc or regio N-met benz luc. Different patterns of light emission were observed for the different analogs. Most importantly, the brightest wells for various
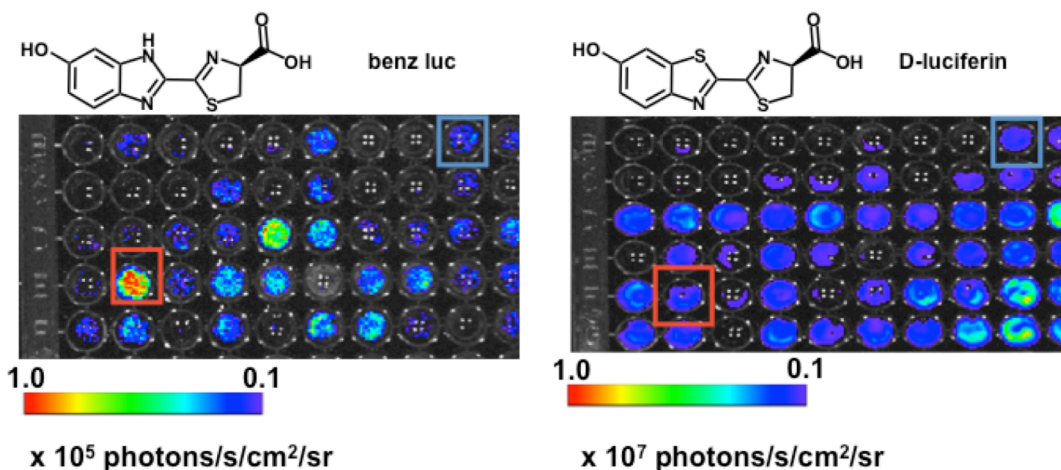
Figure 3-7 Differential light emission patterns from D-luciferin and an analog. Benz luc (200 μM) and D-luciferin (50 μM) in R1 screening. Wells highlighted in red included the following mutations: I226V, H246R, G249S. Wells highlighted in blue contained WT Fluc.

analogs were not the same ones for D-luciferin (Figure 3-7). Cultures of light emitting wells were grown overnight, and DNA harvested from those cultures were sequenced. In cases where a single sequence was present, we noted a number of mutations in the region corresponding to the active site. For benz luc, changes in aliphatic residues were mostly observed, including I226V, F243L, V262A, and I257L. I257L was pulled out of the screen from four separate wells—suggesting potential importance in substrate binding. H246R, G249S were also identified (Figure 3-7). The absolute light emission from these analogs, though, consistently remained an order or magnitude or more beneath the respective emission for the same sequences observed with D-luciferin. This discrepancy made us pursue the possibility of screening the nitrogenous analogs against one another, where true orthogonality might be more easily obtained. Immediately, we found that the patterns of light emission were complementary and on the same relative light emission scale (Figure 3-8).
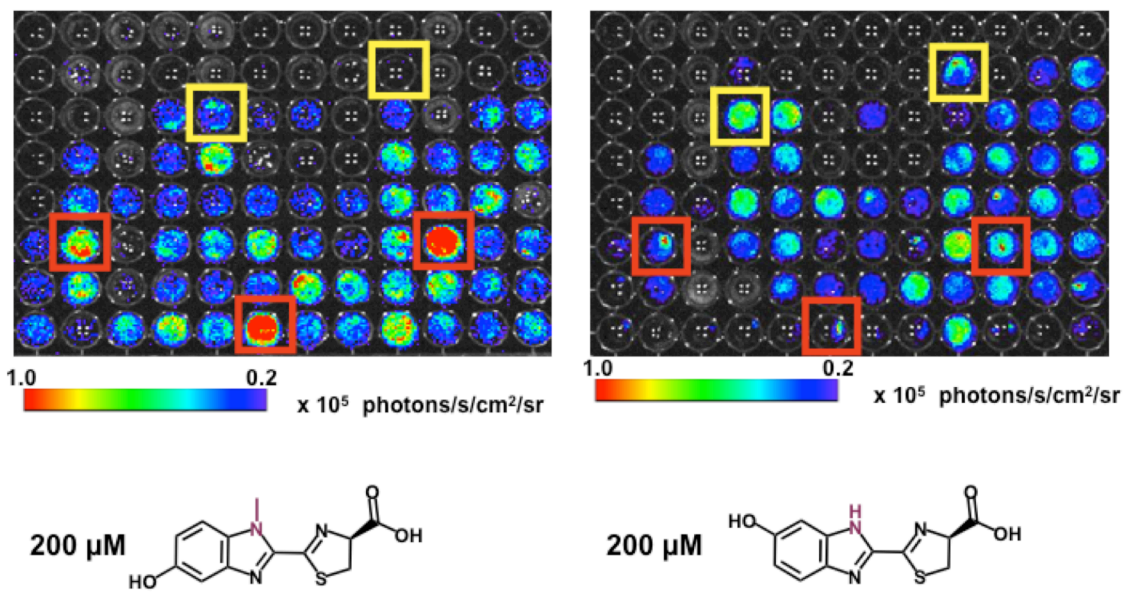
Figure 3-8 Light emission data for nitrogenous luciferin analogs from solution screen. Cultures from deep-well plates were induced, lysed, replica plated and imaged with 200 μM benz luc (right) or regio N-met benz luc (left). Yellow and red boxes highlight wells containing potential hit sequences for benz luc and regio N-met benz luc respectively, subject to further analyses.

Upon rescreening, though, the initial screening results were difficult to reproduce. In particular, the light emission differentials between benz and regio N-met bez seemed to decrease over time; sometimes preferences seemed to reverse. The 96-well images of regio N-met benz luc also began to mirror that of benz luc over time. These data suggested that we were losing the orthogonality and consistency of the analogs within the screen. Dave McCutcheon ultimately discovered that regio N-met benz luc was demethylating in buffer forming benz luc in the process. While the inability to confirm or move forward with these mutants was disappointing, we were pleased to find that our screen could read out potential orthogonal pairs.

3.5 Investigation of F250S as a specific Fluc mutant for CF3 AA luc

The next series of analogs that were synthetically accessible and viable light emitters were the 6´ acyl aminoluciferins. These included a variety of appendages including trifluoro, isopropyl and t-butyl thio ether. I had already established that these luciferins had many desirable properties (Chapter 2.3). In terms of its nascent light emission characteristics with native Fluc, CF3 AA luciferin was best paired with benz luciferin. In solution screening, it was fairly easy to find luciferases that had reasonable selectivity for CF3 AA luc over benz luc, but not vice versa (Figure 3-9). One simple explanation was that we were recapitulating the same 10-fold difference in emission levels between the two analogs when treated with WT Fluc, but variations in the ratio of CF3 AA luc to benz luc emission suggested alternate mechanisms.

We wanted to investigate the biochemical reasons for these differences in a controlled environment. One of the sequences pulled from the screen that appeared to be especially specific for CF3 AA luc was F250S, a mutant previously reported in the literature. This particular mutation has been linked to blue-light emitting Fluc variants [16]. The color of light emission in luciferin-luciferase systems is primarily dictated by the chromophore of the luciferin. The enzyme holds the excited state product such that the energy dissipates as a photon of light rather than heat. If there is room for the molecule to vibrate and lose energy prior to relaxing to the ground state, red-shifted emission is observed. The fact that F250S mutants had blue-shifted emission might, then, signal a tighter binding interaction with the excited state product. I expressed and purified the F250S mutant in *E. coli* in order to evaluate it more critically. I treated 1 μg F250S Fluc with a range of concentrations of D-luciferin, CF3 AA luc and benz luc in the

presence of necessary cofactors to generate dose response curves (Figure 3-10 A). I was able to recapitulate the preference between CF3 AA luc and benz luc from the screen, but extremely low emission from the latter complicated the analysis (Figure 3-10 B). The dose response curve did suggest, though, that CF3 AA luc binds F250S Fluc better than either benz luc or D-luciferin (based on apparent K_m values). The $K_m$app values for both analogs were about 10-fold smaller compared to D-luciferin. The significant product inhibition observed also supports a tight-binding mechanism. Similar trends were observed in the flexible docking of each of these ligands. In order to see the most favorable interactions, F250S and WT Fluc were minimized in the presence of the appropriate luciferins with the OPLS2005 force field. CF3 AA luc, benz luc and D-luciferin (DSLA) are all predicted to bind both WT and F250S Fluc, but CF3 AA luc and F250S are predicted to have an ~1 kcal more favorable interaction than the others (Figure 3-11). From these data, it appears that the release of steric penalties for CF3 AA luc upon going from WT-bound to F250S-bound is responsible for engendering the selectivity observed *in vitro* (Figure 3-10 B). That said, this difference is not sufficient to differentiate between CF3 AA luc and benz luc. In the future, a library of F250S containing mutant luciferases could be screened for additional compensatory mutations to improve the catalytic turnover and increase the total light output to D-luciferin and the Fluc. Collectively, these investigations validated our ability to improve binding and specificity in a screening approach, even in the absence of true orthogonality.
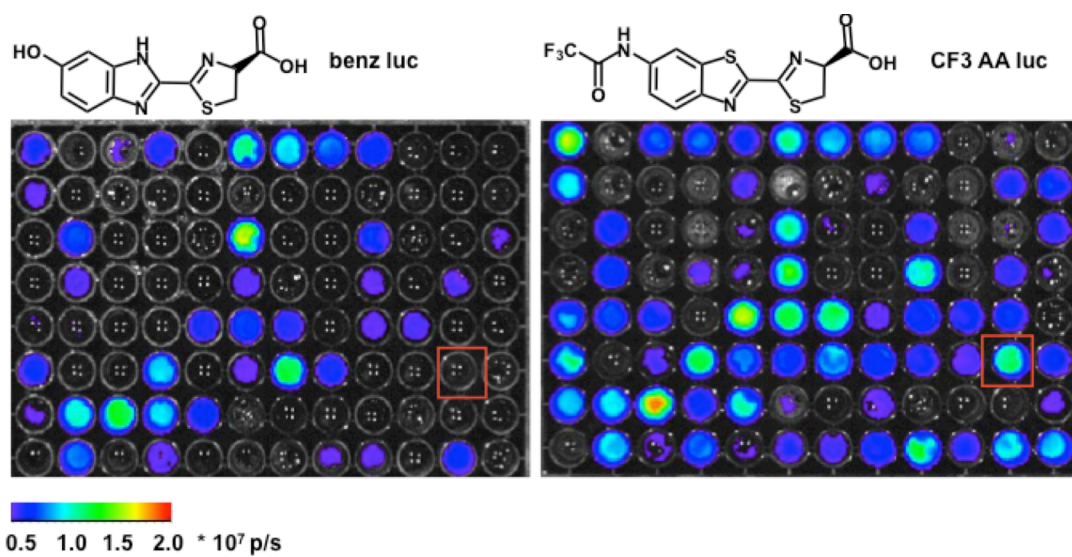
Figure 3-9 Light emission data for benz luc vs. CF3 AA luc from in solution screen. Cultures from deep-well plates were induced, lysed, replica plated and imaged with 200 µM benz luc (left) and CF3 AA luc (right). Red boxes highlight wells containing potential "hit" for CF3 AA luc: F250S.

A
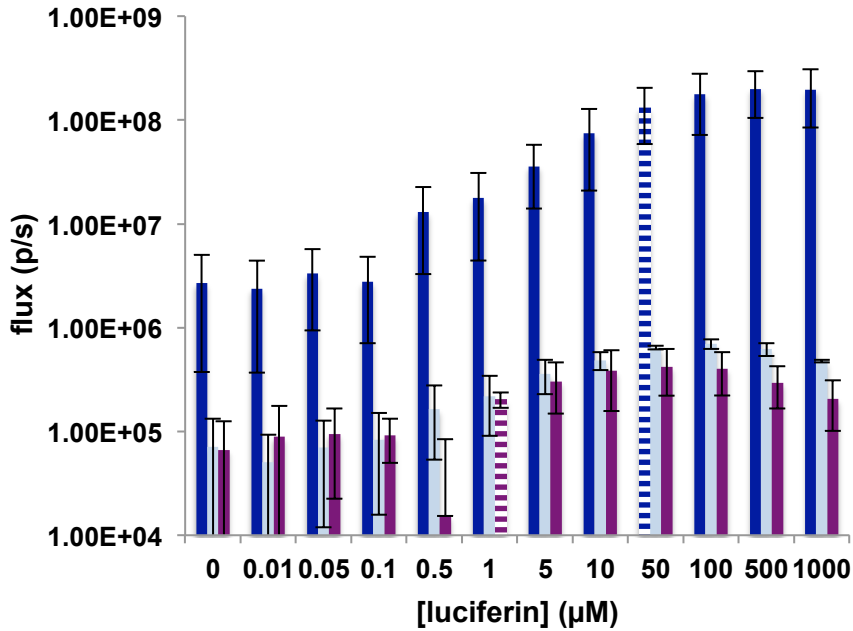
B
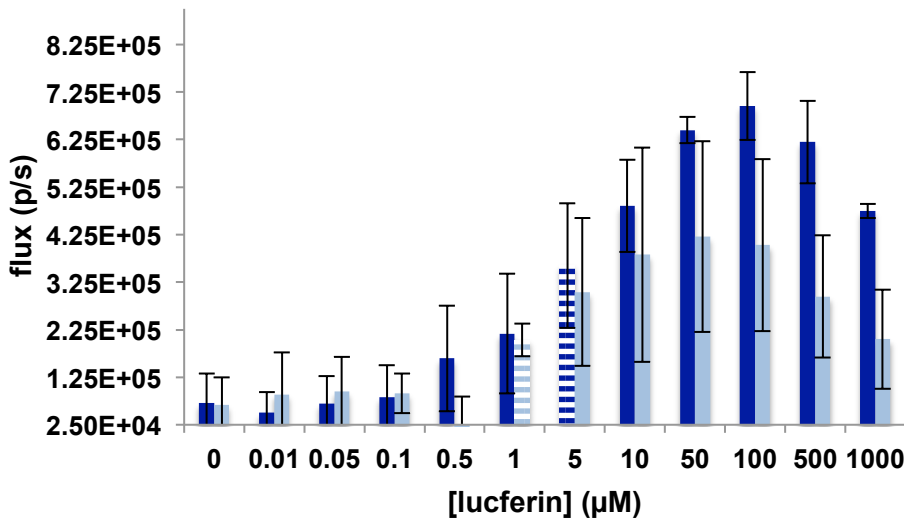
Figure 3-10 F250S Fluc exhibits tighter binding to CF3 AA luciferin than D-luc. (A) The bioluminescence from recombinantly expressed F250S luciferase was recorded over a range of luciferin concentrations. The $K_m$app (highlighted with stripes) for CF3 AA luciferin (raspberry) was estimated to be 5 μM, while that of D-luciferin was judged to be 50 μM (dark blue). (B) With a more focused axis, slight differences between the light emission from CF3 AA luc (dark blue) a benz luc (light blue) were observed. For (A) - (B) error bars represent the standard error of the mean for three independent experiments.

WT Fluc

Name▼	GScore	DockScore	Similarity	Penalties	LipophilicEvdW	HBond	Sitemap	RotPenal	Electro
DSLA	-13.40	-13.40	1.00	0.00	-6.18	-4.42	-0.92	0.12	-2.00
CF3 AA luc	-13.56	-13.56	0.71	0.40	-6.35	-4.32	-1.38	0.09	-2.00
Benzimidazole luc	-13.28	-13.28	0.74	0.00	-5.89	-4.16	-1.37	0.14	-2.00

F250S Fluc

Name	GScore	DockScore	Similarity	Penalties	LipophilicEvdW	HBond	Sitemap	Electro▲	RotPenal
DSLA	-11.43	-11.43	1.00	0.00	-6.46	-2.11	-1.07	-1.91	0.12
CF3 AA luc	-12.48	-12.48	0.69	0.00	-6.76	-2.38	-1.60	-1.84	0.09
Benzimiadole	-11.51	-11.51	0.71	0.00	-6.05	-2.23	-1.54	-1.82	0.14

Figure 3.11 Docking scores show improvement in selectivity for CF3 AA luc with F250S over WT. While globally GScores were reduced from WT (top) to F250S (bottom), due to of H-bonds, CF3 AA suffered a steric penalty with WT (highlighted red) and was show to have some steric clash relieved in the mutant F250S Fluc as penalties fell from 0.40 to 0.00 (boxed in red).

3.6 Difficulties with the screen and solution phase rescreening efforts

As screening progressed, we continued identify promising mutants that suggested that we were selecting enzymes with remodeled active sites. Over time, though, a number of liabilities from our screening process became apparent. It was impossible to guarantee one sequence in each well and bacterial growth in the deep-well plates was inconsistent, likely due to poor aeration. Some days, no transformants survived the overnight growth and the LB media remained clear. Increases in the nutrient richness of the media helped this problem, but also promoted non-specific contamination, resulting in wells full of turgid, malodorous bacteria samples devoid of bioluminescence. Attempts to isolate the source of contamination through miniprep and sequencing were inconclusive.

I tried multiple means of improving either the consistency of plating (to ensure close to one colony per well), growth conditions, or light emission. These efforts included examining various additives to the growth media, changing the temperature and speed of mixing in order to promote aeration and transferring colonies grown on agar plates into media. Even the time-consuming method of transforming on plate and picking individual colonies for each well did not guarantee robust growth and light emission or clean sequencing. Our best results arose from growing colonies on large rectangular agar plates at a density such that 1-5 colonies could be transferred using a comb. Alternatively, "flipping" the agar face down atop wells containing media, followed by an additional 8-10 hours of growth prior to induction and analysis was also successful.

Despite these difficulties, I continued to screen for orthogonality between a host of luciferins including benz luc, the 6′ acyl aminoluciferins and a new 7′ aldehyde substituted luciferin (formyl luc). When a number of single sequence mutants had been pulled out, I retransformed each mutant back into BL21s and measured the emission with all luciferin analogs available in the lab in induced cell lysate. Each luciferin analog had its own light emission profile across the Fluc mutants, but no orthogonal pairs were identified from the batch (Figure 3-12). I decided that screening should continue but needed to be buoyed by further mutagenesis. Since the current screening platform had failed to identify an orthogonal pairs, was inconsistent, a faster, more consistent, screening method was necessary to collect a sufficient assortment of beneficial mutations on which to base additional generations of the library.
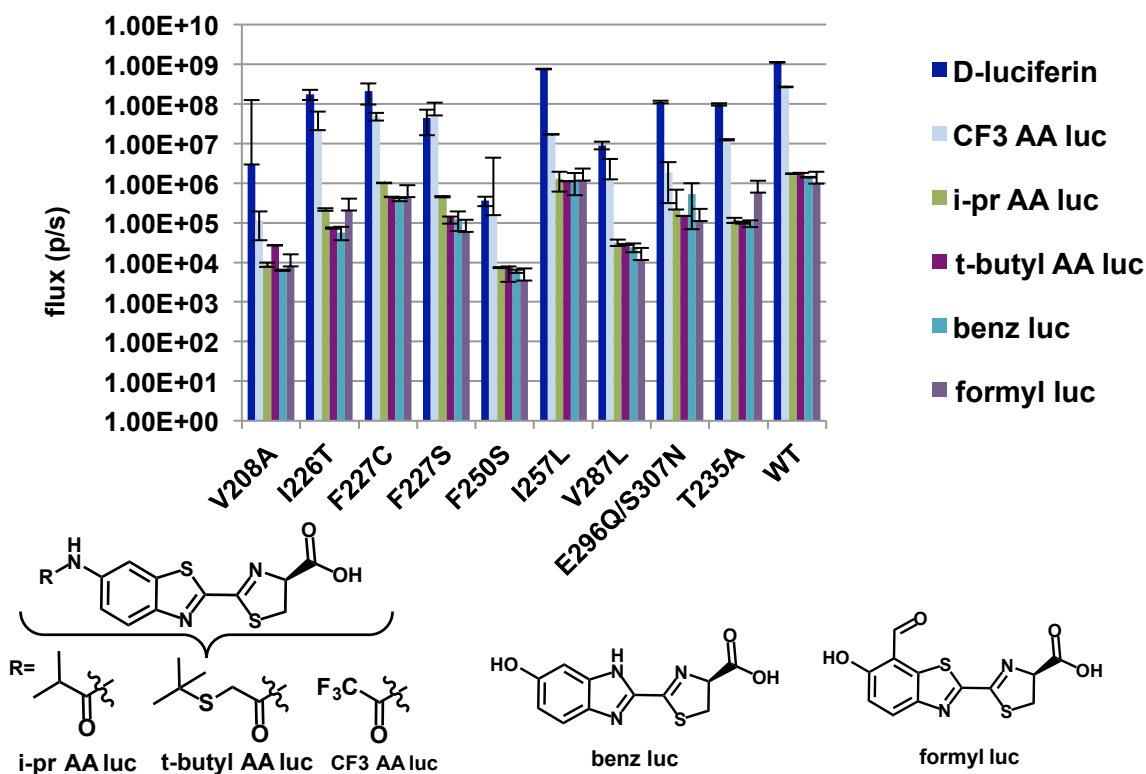
Figure 3-12. Cell lysate re-screening of selected mutants shows different light emission profiles, but not orthogonality. Selected mutant Fluc plasmids were retransformed into BL21 cells, protein expression was induced (500 µM IPTG, 1 hr, 37 °C), and light emission was assayed with luciferin analogs (100 µM) and clarified cell lysate.

3.7 The adoption of a simpler on-plate screen and the analysis of C7 alkyl amino luciferins

In redesigning the screen, I sought a more high-throughput, economical method (with regards to quantities of luciferin). The process should also provide access to pure DNA samples for sequencing. Analyzing the mutant libraries on-plate with the luciferins directly applied to the surface would be the most straightforward. I hadn't pursued an on-plate screen initially, because pipetting substrate onto each colony was work-intensive

and inherently inconsistent. The obvious work-around was to embed the luciferin in the agar itself, but this procedure wasted analog and in early attempts, we needed to keep concentrations of the luciferins low in order to conserve limited supplies of synthetic luciferins.   In later years, better synthetic procedures were developed in the lab to access larger quantities of luciferins for on-plate screening.

Using a similar optimization process to the solution-phase screening, I varied cell lines, IPTG and luciferin concentrations. The best results were obtained with a commercially available, high competency BL21 strain from NEB. This particular cell line was selected to maximize the number of spatially-resolved colonies on a given plate. Colony resolution was essential to clearly demarcate "bright" colonies and avoid mixing DNA with neighboring colonies. Gridded (100 cm^2) agar plates imaged at a short focal plane in four separate quadrants provided the resolution necessary to "see" single colony light emission. I was able to observe light emission first from the more robust light emitters (CF3 AA luc and benz luc) and eventually all luciferins in both the R1 and R1R2 libraries (Figure 3-13). Some luciferin analogs had trouble diffusing through the *E. coli* cell wall. For these substrates, careful application of a 1 mg/mL solution of hen egg white lysozyme on the surface of the plate, followed by a 1 h incubation at 37 °C was sufficient to induce light emission. I found it was necessary to pipet any extra solution off the surface immediately though, or the colonies would degrade entirely. Other means of substrate delivery also appeared viable. Subjecting to the bacteria to a short blast of microwaves, for instance, caused a steep rise in emitted photons. However it was hard to catch the sweet spot between that, and the plastic petri plate and agar melting entirely.

The delicacy of this screening set up was more than made up for by its high-throughput nature and our ability to immediately sequence isolate "hits." In a few days, I could screen 10,000 or more mutants against all the available luciferins in the lab, something that would have taken months with all the transformations and pipetting steps needed for the in-solution screen. Another great benefit was the ability to detect and remove unmutated WT Fluc that was present at low levels in the library. Based on our experience with the solution screen, and not finding true orthogonal pairs off the bat, we expected mutants selected from the plates would go through another round of
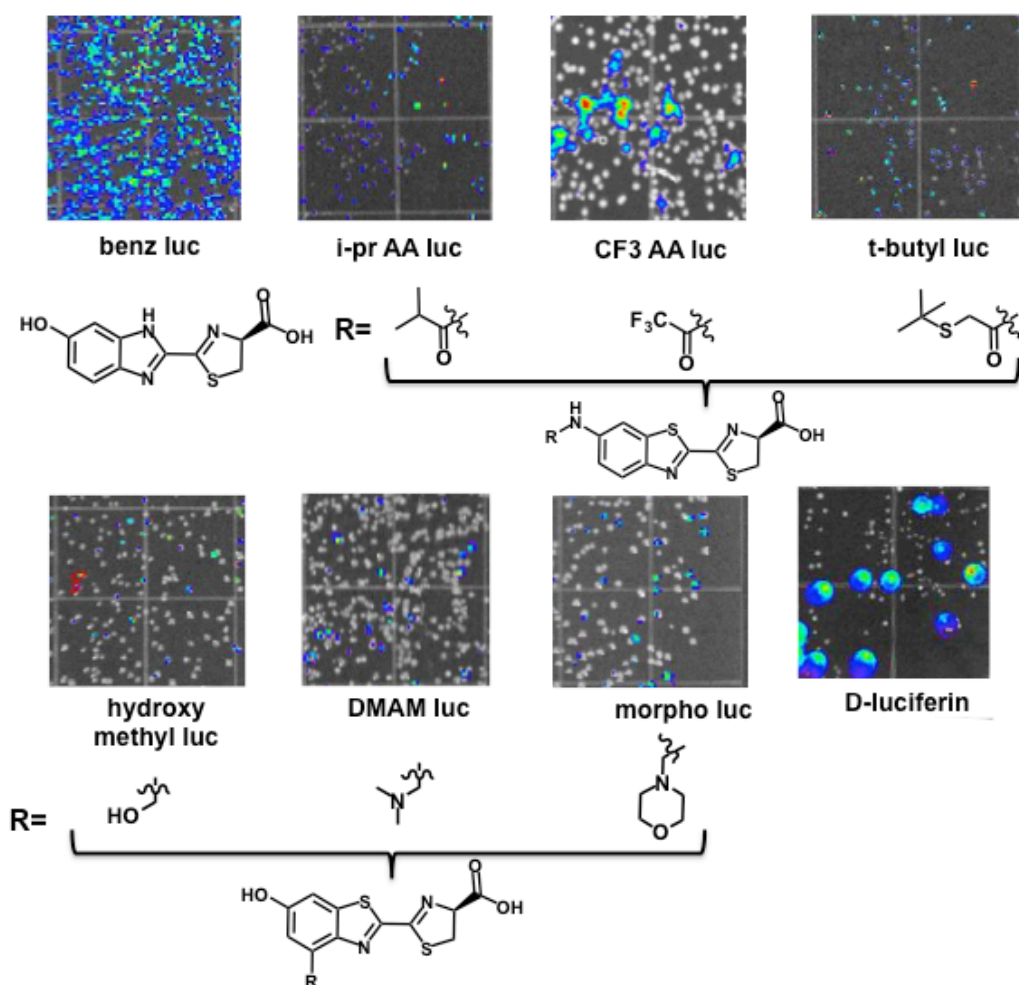
Figure 3-13 Representative images from the compounds evaluated by the on-plate R1R2 screen. Revised R1R2 library DNA was transformed into highly competent BL21 cells and plated on agar containing kanamycin, IPTG and the luciferin of interest (100 μM for analog luciferins, 50 μM D-luciferin) and imaged.

mutagenesis and screening. I therefore reconstructed the library and vaired the mutagenic load slightly (~0.7% of nucleotides, or about one amino acid in the 146 R1R2 region) so that it would be easy to identify what mutation was responsible for unique activity. This new library had ~10^5 members meaning that complete screening could be accomplished using just 5-10 plates. Representative images from screening this library with each analog luciferin plate are presented in Figure 3-13. In screening 10-15% of the new R1R2 library against all available luciferins, I collected approximately thirty mutant Flucs. All the collected mutants are indexed in Table 3-2. To identify potential hotspots and gain insight on how these mutations might influence the binding of luciferins, I mapped their identities along the amino acid sequence, and noted their locations in the 3D crystal structure (Figure 3-14). The locations of mutations clustered along either face (C4′ and C7′ of D-luciferin) show clear remodeling of the active site. It's important to note that while the region submitted to mutagenic PCR included residues that would back up on the adenylation domain, none of these residues appeared mutated in selected sequences, highlighting the mechanistic importance of this region. In addition to the directly substrate-facing plane, a number of mutations clustered around the solvent-exposed cleft. Presumably, these changes eased the entry of the substrate into the binding pocket. One mutation outside the targeted region (meaning it arose from either a non-mutagenic PCR step, or from the *E. coli*'s own DNA replication machinery) was registered in a large number of clones. This S456G mutation lies directly on the other edge of the edge of the entranceway to the active site. This site is highlighted in dark red in the crystal structure in Figure 3-14. As the screening progressed, and we began to rely on larger steric perturbations (see Chapter 4), this mutation appeared more and more frequently. It is

reasonable to assume that with its solvent access, S456G would not affect folding or catalysis, provided better access for larger luciferins.

Collectively, the mutations pulled out of the screen in generation 1, while not sufficient for complete orthogonality, were still capable of perturbing the relative light emission profiles. Additionally, the mutations were distributed throughout the substrate binding domain and so-called second sphere, both of which are known to modulate substrate affinity.
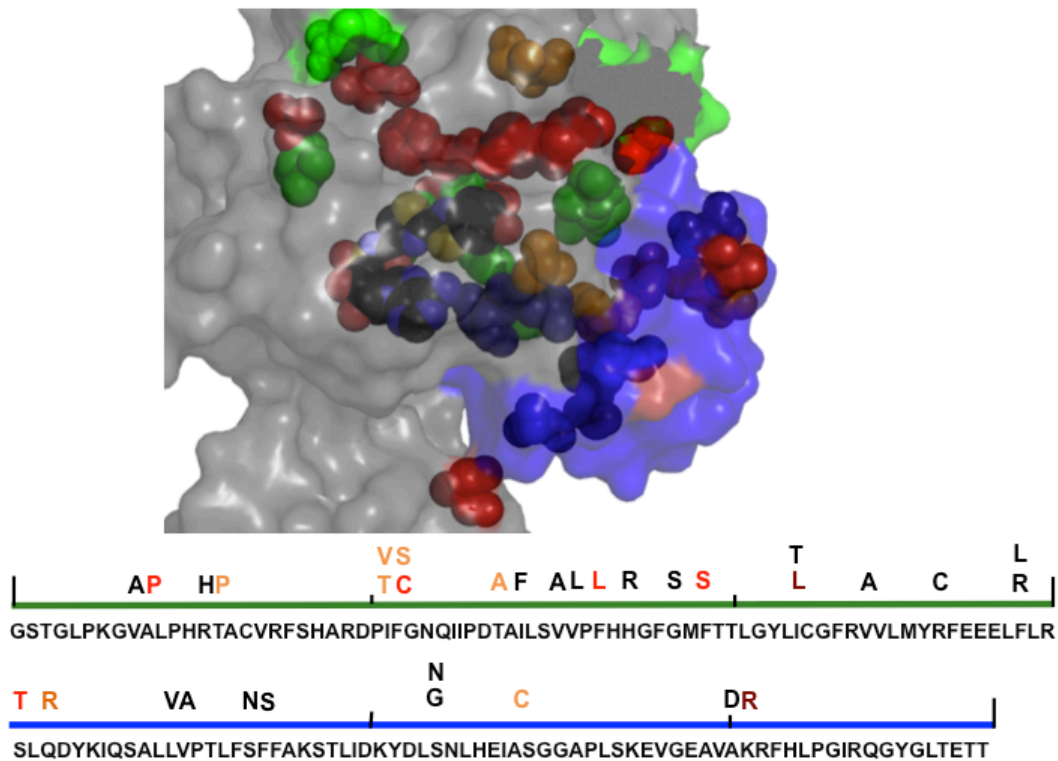
Figure 3-14 Locations of mutations identified from the screen. The identities of the mutations are plotted along the Fluc amino acid sequence. These positions are also highlighted in the crystal structure (PDB:4G36).

Table 3-2 Mutants identified from screening various luciferin analogs.

Analog	Library	Identified mutation(s)
benz luc	R1	T235A, I226V I237F V262A, I257L (*3) I257L, V208A I226V, H246R, G249S F227S
	R1R2	A209P, S276T, A313C, Q278R T214P, V241L, S276T S307G E296Q, S307G F227C
imid luc	R1	A209P
	R212	T214P
CF3AA luc	R1	F250S (*3) I226T (*2)
	R1R2	F243L S307N
t-butyl AA luc	R1R2	R267C, S293N T235A
i-pr AA luc	R1R2	F227C, F227S,
morpho luc	R1R2	S307G, K329R, F273R R213H (*2) V240A F243L F243L/V288A I257T F294S K329R
DMAM luc	R1R2	F273L K329R
hydroxy methyl luc	R1R2	K329R T235A A209P, S276T, A313C, Q278R
D-luciferin	R1R2	L287V

3.8 Conclusions and future directions

In this chapter, I developed constructs for luciferase library generation by designing handles to manipulate the key residues surrounding the active site, and I further demonstrated the viability of these scaffolds. I also identified the optimized conditions to mutagenize Fluc regions and the whole protein without entirely ablating light emission. In addition, we learned some hard-won lessons about liabilities of compounds in our screen. In short: it became apparent that luciferin analogs must be at least as stable as D-luciferin and that the inherent luminescence ability of the molecule, governed, in part, by the electronics of the aromatic core will impact our ability to develop a given probe into an orthogonal pair. While we eventually aim to be restore light-emission to "dark" luciferin oxidation reactions, early efforts will be bolstered by the use of molecules primed for success in the luminescent reaction, particularly those with the proven D-luciferin scaffold and steric perturbations.

Finally, I established that the direct comparison between analogs of an in-solution screen in this first generation library was sufficient to provide differences in the selectivity profiles between various classes of luciferases and to identify some mutants with improved affinity for one or more analog luciferins. That said, the platform was often irreproducible, time-consuming, and in the end, inadequate to provide orthogonal pairs. The move to an on-plate screen provided much more rapid access to interesting and hopefully beneficial mutations, and made it easier to screen-out WT Fluc for later generations of the library. These mutant plasmids were pooled and subjected to additional mutagenesis and new rounds of screening. Eventually, we hope that luciferase mutants

evolved for efficiency with specific luciferin analogs will simultaneously arrive at orthogonal enzymatic activity and will perform better in a head-to-head screen.

3.9 Methods and materials

General methods section

Buffer and media reagents were purchased from Fisher Scientific. BLI buffer (100 mM Tris-HCl, 150 mM NaCl, 5 mM MgCl$_2$, 1.5% (w/v) bovine serum albumin, pH 7.8) was prepared and sterile-filtered; between uses it was kept at 4 ºC. Chemically competent bacteria were either purchased (library efficiency DH5α cells from Life Technologies) prepared according to standard protocols. Restriction enzymes and T4 DNA ligase were purchased from New England Biolabs. Platinum PFX was used for Quikchange mutagenesis, Platinum Taq was used for error-prone PCR (both, Invitrogen) while Dreamtaq (Fermentas) was used for standard PCR applications as well as dNTP analog mutagenesis. All PCR reactions were confirmed by ethidium bromide agarose gel analysis before performing down-stream reactions. Plasmid contstruction was confirmed with sequencing provided by Genewiz, San Diego. For cultures and protein expression, LB and LB agar granulated mixes were purchased from BD Difco. IPTG, PMSF and DTT were purchased from Gold Biosciences.

General bioluminescence imaging protocol

All samples were incubated with D-luciferin or luciferin analog and an excess of ATP and imaged in a light-proof imaging chamber equipped with an IVIS Lumina (Xenogen) CCD camera chilled to -90 ºC. The stage was kept at 37 ºC to promote enzymatic reactions. Photons of light emitted from bioluminescent reactions were collected by the camera, and the captures were controlled by Living Image software. Typical exposure times were 30 s, with data binning levels set to medium. When strong emission saturated the memory on the CCD camera, the exposure time was lowered and binning level was reduced. Conversely, for weak-emitting samples, exposure times were increased to capture more photons. Regions of interest were selected for quantification and total flux data were exported to Microsoft Excel for further analysis.

Construction of restricted library parental vectors

The luciferase gene *luc2*, was amplified from a pcDNA construct, pFluc2-IRES-eGFP provided by J. Prescher. Quikchange mutagenesis (Stratagene, La Jolla) using two sets of primer pairs was used to install two different silent restriction sites in the *luc2* gene for each luciferase library. Primer pairs 1, and then 2, were used sequentially to construct the R1 parental plasmid, pairs 2 and 3 for the R2 parental plasmid and pairs 1 and 3 for the R1R2 plasmid. The mutant plasmids were analyzed by restriction digest with *Hind*III , *Spe*I or *Bam*HI as appropriate. The genes were then then subcloned into pET28 by standard techniques. Colonies were assessed for light emission by application of 5 mM D-luciferin and bioluminescence was captured with an IVIS Lumina (Xenogen) system. Light-emitting colonies were selected for overnight culture, miniprep and sequencing.

Quikchange mutagenic primers

Pair 1: G199 *Bam*HI SS fwd: 5´
 CTGATCATGAACAGTAGTGGATCCACCGGATTGCCC AAGGGCGT-3´
G199 *Bam*HI SS rev: 5´-ACGCCCTTGGGCAATCCGGTGGATCCACTACTGTTCA
TGATCAG-3´

Pair 2: R275 *Hind*III SS fwd: 5´-
GGAGGAGCTATTCTTGCGAAGCTTGCAAGACTATAAG-3´
R275 *Hind*III SS rev: 5´ GAATATCAGAACGAACGAAGCGTTCTTATCGAGGAGG
3´

Pair 3: T346 *Spe*I SS fwd 5´
GGCCTGACAGAAACAACTAGTGCCATTCTGATCACCCC-3´
T346 *Spe*I SS rev: 5´ – GAATATCAGAACGAACGAAAGCGTTCTTATCGAGGAGG
-3´

Synthesis of restricted libraries by dNTP analog mutagenesis

Libraries were prepared essentially according to the method of Gherardi *et al* [14].

Twenty rounds of mutagenic PCR with *luc2* were performed initially in the presence of

200 mM natural dNTPs and 0, 2, 20 or 100 μM each of the unnatural bases dPTP and 8-

oxodGTP (Trilink, San Digeo). The R1 library was amplified with primers MP008 and

MP033, R2 with MP009 and MP010 and R1R2 with MP009 and MP033 (sequences are

listed below). The PCR products from each reaction were used as templates for further

amplifiction, in the absence of dNTP analogs. Further subcloning for introduction into

bacterial expression vector pET28(a)+ was performed with appropriate restriction

enzymes as above.   After initial sequence analysis (Genewiz, San Diego). The

concentration of 10 μM dPTP and 10 μM 8-oxodGTP was determined to provide the

optimal mutagenic load. The synthesis was repeated and scaled up to prepared the other

libraries with other conditions unchanged.

dNTP analog PCR library primers
MP008 R275Rev Analog PCR: 5´ CATATTCGAAGCGTTCTTATCGAGGAGGA 3´

MP009 T346Rev Analog PCR 5′ CGATGCCGGACTGTCTTTGTTGATCAAAA g 3′
MP010 R275Fwd Analog PCR
5′ GGTAAAACGTTGCAAGACTATAAGATTCAATCTGCCC 3′
MP033 G199Fwd Analog PCR: 5′ GTA GTG GAT CCA CCG GAT TGC 3′

Full-length mutant luciferase library synthesis by error-prone PCR

Full length *luc2* was amplified by twenty-five rounds of PCR under error-prone conditions (7 mM MgCl$_2$, 0.1 mM MnCl$_2$, 200 µM dGTP and dATP, 1mM dCTP and dTTP). After the mutagenic rounds, re-amplification was carried out in the presence of 200 µM dNTPs, 1.5 mM MgCl$_2$ and library primers MP022 and MP027 (below) encoding for *Nco*I and *Not*I sites respectively. The PCR product was subcloned as above into pET28a(+).

Luciferase library primers
MP022 *Nco*Ifwd: 5′ TATACCATGGAAGATGCCAAAAACATTAAGAAGGGCCC 3′
MP027 *Not*Irev: 5′ TATAGCGGCCGCCACGGCGATCTTGCCGC 3′

On-plate bioluminescence assays and library analysis

D-Luciferin (5 mM) was spotted onto the surface of colonies of interest. After a five-minute incubation period on the benchtop, BLI images were acquired as above. All light-emitting colonies and several non-emitting colonies were picked off the plate, grown in LB-Kan media overnight and DNA was extracted by miniprep (Qiagen, Germantown MD). Purified DNA was sequenced using appropriate primers for region of interest (T7 forward and reverse, or amplification primers)

Multi-well bioluminescence screening and sequencing

R2 library DNA (75 ng) was transformed into 50 µL BL21DE3 chemically competent cells by heat shock. Next, 100 µL of transformation was plated on an agar plate while the

remaining reaction was diluted ten-fold and distributed over a deep-well plate containing 600 µL LB-Kan (1 µL per well). Upon overnight growth, protein expression was induced using 500 µM IPTG at 37 °C. After a 1 h induction period, the plates were spun down and cell pellets were resuspended in 100 µL cell lysis buffer (100 mM Tris-HCl, 150 mM NaCl, 5 mM MgCl$_2$, 1.5% (w/v) bovine serum albumin, 20 µg/mL hen egg-white lysozyme, pH 7.8) and incubated at 37 °C for 1 h. To measure light emission, the lysates were incubated with 100 µM D-luciferin and imaged in a blackwell plate. Prior to lysis, additional culture (10 µL) was used to inoculate fresh cultures in order to maintain DNA source for sequencing.

Screening of multiple luciferins in duplicate

Library DNA (75 ng) was transformed into 50 µL BL21DE3 chemically competent cells by heat shock. Next, 50 µL of transformation was diluted into 3 mL and distributed over a deep-well plate containing 600 µL LB-Kan (15 µL per well). Additional culture, (15 µL) was also plated onto one agar plate to determine the cfu/well in each well of 19-well deep-well plate. Upon overnight growth, protein expression was induced using 100 µM IPTG at 37 °C. After a 1 h induction period, 200 µL of each culture was transferred to two duplicate black-well plates. The plates were then centrifuged at 3000 rpm for 10 min and 12 °C and cell pellets were resuspended in 100 µL cell lysis buffer (100 mM Tris-HCl, 150 mM NaCl, 5 mM MgCl$_2$, 1.5% (w/v) bovine serum albumin, 20 µg/mL hen egg-white lysozyme, pH 7.8) and incubated at 37 °C for 1 h. To measure light emission, the lysates were incubated with a solution of D-luciferin with equimolar ATP and coenzyme A (50 µM). The plate was imaged according to the general procedure above.

The second plate was screened with 200 µM benz luc in the presence of equimolar ATP and 100 µM coenzyme A. Later, screens were performed as above with 100 µM benz luc, N-met benz luc and CF3 AA luc with ATP (1 mM). When wells were deemed to be of interest, the remaining un-lysed culture was used to inoculate a 3 mL culture suitable for rescreening in triplicate and extracting DNA for sequencing analysis (Genewiz, San Diego). When bacterial growth was poor, 2YT media was substituted for LB. Several methods were used to improve growth and reproducibility involving growing transformations on agar plates and transferring colonies into media for additional growth. The screen was then performed as described above.

On plate screening

Plasmid DNA (10 ng) was transformed into 50 µL NEB high competency BL21 cells. After heat shock, cells were rescued with 950 µL SOC media and shaking 37 °C for 1 h. A portion of the culture (20 µL) was used to seed a 10X10 cm sterile grid plate (VWR) with 1-2 * 10^3 CFU. The remaining transformation was supplemented with 10% sterile glycerol, snap frozen in an isopropanol/dry ice bath and stored at -80 °C in 30-50 µL aliquots. In same cases, these aliquots were used after slow thaw on ice. The transformations were replated for additional screening but required ~50% more transformation solution to achieve the same colony density.   The LB-agar plates themselves were prepared according to manufacturer directions with slight modifications. After autoclaving, the LB-agar was slow-cooled in a 37 °C incubator until just warm to touch. IPTG (100 µM) and luciferin (100-200 µM) were added and the solution was gently mixed and plates cast rapidly before the agar set. Plates were kept tightly sealed at

4 °C and prepared fresh (at least weekly) to ensure that neither IPTG nor the luciferin degraded.

Expression and dose response with F250S Fluc

The mutant Fluc was prepared according to the procedure reported in Chapter 2, using a F250S Fluc pET 28a(+) plasmid.

Cell lysate BLI assays with native and analog luciferases

Plasmids encoding for Fluc mutant of interest (pET28 vector) were transformed into BL21 DE3 cells, and grown on kanamycin plates (40 µg/mL) overnight. One colony was selected to inoculate 5 mL LB broth containing 40 µg/mL kanamycin for 4-6 h until an $OD_{600} \approx 0.4$. Protein expression was then induced with 500 µM IPTG for 1 h. Cells were then harvested by centrifugation, resuspended in BLI reaction buffer and lysed by sonication. Lysate was clarified by centrifugation (13 krpm, 1 min) and 100 µL samples were incubated (in duplicate) with 100 µM of the luciferin of interest as well as 1 mM ATP.

Schrodinger molecular modeling

The F250S Fluc mutant was prepared in Pymol using mutagenesis wizard from the PDB:4G36 Fluc crystal structure. This and WT Fluc were both prepared for docking using the protein prep wizard in Maestro (version 2013-3). The OPLS2005 force field was used for minimization. D-Luciferin, benz luc and CF3 AA luc were all modeled as the AMP conjugate. Glide-grids were generated using the minimized structure and

DSLA was used to provide the coordinates for ligand binding. XP docking was performed with the option for XP descriptor information to be written out in the output file. Settings included flexible ligand sampling, sampling of nitrogen inversions, and ring conformations. Epik state penalities were use to exclude non-physiologically relevant protonation states and non-planar amide bonds were also penalized. The docked ligands were evaluated manually via pose-viewer to choose the most relevant poses as well with XP visualizer to quantify the relative contributions of different ligand interactions to the assessed GlideScore.

References

(1)   Romero, P. A.; Krause, A.; Arnold, F. H. Navigating the Protein Fitness Landscape with Gaussian Processes. *Proc. Natl. Acad. Sci. U.S.A.* **2013**, *110*, E193-201.

(2)   Jackel, C.; Kast, P.; Hilvert, D. Protein Design by Directed Evolution. *Annu. Rev. Biophys.* **2008**, *37*, 153-173.

(3)   Romero, P. A.; Arnold, F. H. Exploring Protein Fitness Landscapes by Directed Evolution. *Nat. Rev. Mol. Cell Biol.* **2009**, *10*, 866-876.

(4)   White, P. J.; Squirrell, D. J.; Arnaud, P.; Lowe, C. R.; Murray, J. A. Improved Thermostability of the North American Firefly Luciferase: Saturation Mutagenesis at Position 354. *Biochem. J.* **1996**, *319*, 343-350.

(5)   Ugarova, N. N. Stabilization of *Luciola mingrelica* Firefly Luciferase by Genetic Engineering Methods. *Moscow Univ. Chem. Bull.* **2010**, *65*, 139-143.

(6)   Hirokawa, K.; Kajiyama, N.; Murakami, S. Improved Practical Usefulness of Firefly Luciferase by Gene Chimerization and Random Mutagenesis. *Biochim. Biophys. Acta* **2002**, *1597*, 271-279.

(7)   Mofford, D. M.; Reddy, G. R.; Miller, S. C. Aminoluciferins Extend Firefly Luciferase Bioluminescence into the Near-Infrared and can be Preferred Substrates Over D-Luciferin. *J. Am. Chem. Soc.* **2014**, *136*, 13277-13282.

(8)   Mofford, D. M.; Reddy, G. R.; Miller, S. C. Latent Luciferase Activity in the Fruit Fly Revealed by a Synthetic Luciferin. *Proc. Natl. Acad. Sci. U.S.A.* **2014**, *111*, 4443-4448.

(9)   Viviani, V. R.; Prado, R. A.; Arnoldi, F. C. G.; Abdalla, F. C. An Ancestral Luciferase in the Malpighi Tubules of a Non-Bioluminescent Beetle! *Photochem. Photobiol. Sci*. **2009**, *8*, 57-61.

(10)   Branchini, B. R.; Rosenberg, J. C.; Fontaine, D. M.; Southworth, T. L.; Behney, C. E.; Uzasci, L. Bioluminescence is Produced From a Trapped Firefly Luciferase Conformation Predicted by the Domain Alternation Mechanism. *J. Am. Chem. Soc*. **2011**, *133*, 11088-11091.

(11)   Fraga, H. Firefly Luminescence: a Historical Perspective and Recent Developments. *Photochem. Photobiol. Sci.* **2008**, *7*, 146-158.

(12)   Hastings, J. W.: Chemistries and Colors of Bioluminescent Reactions: a Review. *Gene* **1996**, *173*, 5-11.

(13)   Cirino, P. C. M., K. M; & Umeno, D.: Generating Mutant Libraries Using Error-Prone PCR. *Methods in Molecular Biology: Directed Evolution Library Creation: Methods and Protocols*; Arnold, F. H., Georgiou, G., Ed. *231*, 3-9.

(14)   Zaccolo, M.; Williams, D. M.; Brown, D. M.; Gherardi, E.: an Approach to Random Mutagenesis of DNA Using Mixtures of Triphosphate Derivatives of Nucleoside Analogs. *J. Mol. Biol*. **1996**, *255*, 589-603.

(15)   Koksharov, M. I.; Ugarova, N. N. Random Mutagenesis of Luciola Mingrelica Firefly Luciferase. Mutant Enzymes tith Bioluminescence Spectra Showing Low pH Sensitivity. *Biochemistry Mosc.* **2008**, *73*, 862-869.

(16)   Branchini, B. R.; Ablamsky, D. M.; Rosenman, J. M.; Uzasci, L.; Southworth, T. L.; Zimmer, M.: Synergistic Mutations Produce Blue-Shifted Bioluminescence in Firefly Luciferase. *Biochemistry*, **2007**, *46*, 13847-13855.

(17)   McCullum, E. O.; Williams, B. A.; Zhang, J.; Chaput, J. C. Random Mutagenesis by Error-Prone PCR. *Methods Mol. Biol.* **2010**, *634*, 103-109.

CHAPTER 4: Sterically modified luciferins

for orthogonal probe development

4.1 Introduction

To expand the bioluminescence toolkit, we were aiming to identify new luciferases that were responsive to unique luciferins. Such orthogonal luciferase-luciferin pairs would enable multi-component imaging in a variety of settings. Our approach involved modifying the enzyme and luciferin concurrently; sequential administration of substrates will enable unique luciferases to be illuminated (and thus resolved) within a complex mixture, even living animals.

In the preceding chapters, I evaluated and analyzed both luciferin analogs and luciferase mutants for their suitability for screening for orthogonal pairs. Our evidence pointed to the need for probes with an equal propensity to emit light (ideally as well as D-luciferin), but with bulky moieties off the luciferin core. My work suggested these molecules would be most easily distinguished by the Fluc active site and developed into orthogonal systems. However, until recently, a palette of luciferins with steric modifications and "matched" electronics was not synthetically available.

Generating mutant enzymes that utilize modified substrates with increased steric bulk is a well-known strategy for deciphering the roles of individual members within a large family of related structures [1-5]. Among the best examples of this approach is work from the Shokat lab aimed at discriminating among protein kinases [1,5]. These researchers demonstrated that ATP analogs with appended functional groups (or

"bumps") are preferentially utilized by kinases possessing complementary voids (or "holes") generated by amino substitutions that accommodate the additional steric bulk. Thus, altering the firefly luciferase enzyme-substrate interface, creating luciferase variants with "holes" to accept distinct, chemically modified versions of luciferin (with "bumps") appeared to be a promising scheme to provide orthogonal luciferin-luciferase pairs. Simultaneous manipulation of firefly luciferase and D-luciferin is also supported by a key literature precedent: Miller and coworkers recently prepared a class of unnatural aminoluciferin analogs that were found to be robust light emitters with luciferase, but the products inhibited the enzymatic reaction. Product inhibition was partially relieved using mutated versions of the enzyme (including a Phe 247 deletion to create additional "space" in the binding pocket) [6]. These results imply that altered bioluminescent activities can be achieved by simultaneous modification of the enzyme and substrate.

Screening of a second-generation Fluc library based on Chapter 3 "hits" against 7′′ DMAM luc, morpho luc and mor-pip luc afforded a series of Fluc mutants with increased specificity for one or more amino alkyl luciferins over D-luciferin. These mutant Flucs were recombinantly expressed, purified and analyzed biochemically.

4.2 Selection of luciferin ring positions for steric manipulation

While a number of luciferin analogs were originally designed for orthogonal probe development, we ultimately focused on the sterically modified probes due to some of the limitations discussed in Chapters 2 and 3. As I established in Chapter 2, steric perturbations at the 5′ and 6′-positions are accepted surprisingly well as evidenced by their light emission [6-8]. I also established that "mis-matched" electronics can

complicate the analysis of analog utilization by Fluc mutants. We felt that incorporating appendages at either the 4′ or 7′ position of D-luciferin would preserve the structural elements required for the most productive light emission while simultaneously disrupting utilization by Fluc. We hoped that this deficit could be repaired with an appropriate mutant enzyme. The 7′ position was an ideal target for several reasons. Electronically, it's the most nucleophilic position on the ring, which allowed us to access the modified scaffolds shown in Figure 4-2 via Mannich chemistry [9]. We envisioned installing a functional handle at the 7′ position that could be used to assemble a variety of structurally modified scaffolds. In order to generate the collection of related probes through a rapid, late-stage diversification, we thought the aldehyde was a reasonable choice. This group is easily diversified under mild conditions (e.g., reductive amination) and compatibile with a broad range of functional groups. Installation of the aldehyde itself, though, presented some challenges. Fortunately, the modified luciferins can be derived from a common synthetic route developed in our lab [10]. This method is expedient and high-yielding making it suitable for the on-plate screening method introduced in Chapter 3. In addition, we felt the native enzyme likely would not tolerate steric bulk at the 7′ position nearly as well as with the 5′ and 6′ positions.

Docking analyses revealed that the 7′ position lies in close proximity to the Fluc backbone. I built the 7′ series of luciferins (formyl luc, methyl alcohol luc, DMAM luc, morpho luc and mor-pip luc) off D-luciferin in the 4G36 crystal structure. Even prior to docking, it was clear that as steric bulk and flexibility increased, clashes with active site residues also increased in number and severity (Figure 4-2). When these luciferins were included in a larger panel of candidate orthogonal luciferins, only the precursor, 7′ formyl luc and the related 7′ methyl alcohol luc docked in the presumed light emitting conformation. (Table 4-1). 7′ DMAM luc, morpho luc and mor-pip luc all failed to dock entirely, as did their 4′ regioisomers. Interestingly, using a more forgiving, lower level calculation, we did obtain poses for both the 4′ and 7′ DMAM lucs (but not the other 4′ and 7′ alkyl amino appendages) (Figure 4-3 A). The two DMAM lucs maintain essentially the same footprint with the exception of a rotation in the C2-C2' bond resulting in an "s-cis" conformation for 7′ DMAM luc (Figure 4-3 B). The electron clouds on the sulfurs are large and would prefer to sit further apart, in an "s-trans" conformation [11]. We must therefore conclude that the space around the 4′ position is
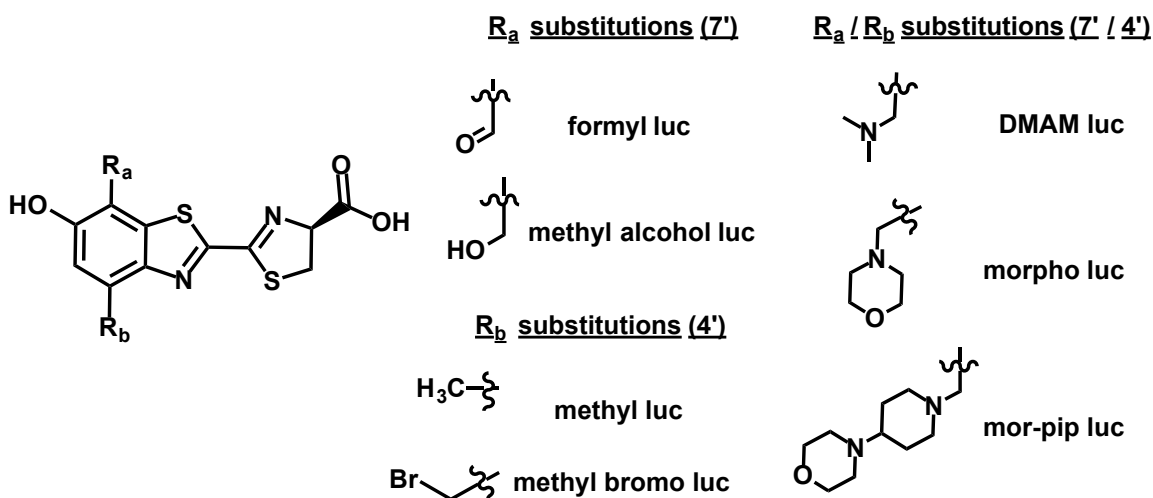
Figure 4-1 Sterically modified luciferins under investigation.

more favorable for a "bump" to get over the ~7 kcal/mol predicted barrier to trans-cis transitions [11]. Several other 4′, 5′ and 7′ substituted luciferins also initially docked in "s-cis" conformations ("Notes" column, Table 4-1). In these cases, I performed the calculation again with a SMARTS pattern constraining The N=C-C=N bonds in the desired "s-trans" configuration. Most substitutions demonstrated improved scoring (typically by ~3 kcal/mol) with use of this constraint, validating its use and our assumption that the "s-trans" is the valid conformation. However, the 4′ and 7′ DMAM luc, morpho luc and mor-pip luc still failed to produce poses; we are looking into flexible docking to further investigate these luciferins because the observed light emission suggests that these probes should be able to bind the active site to some degree.
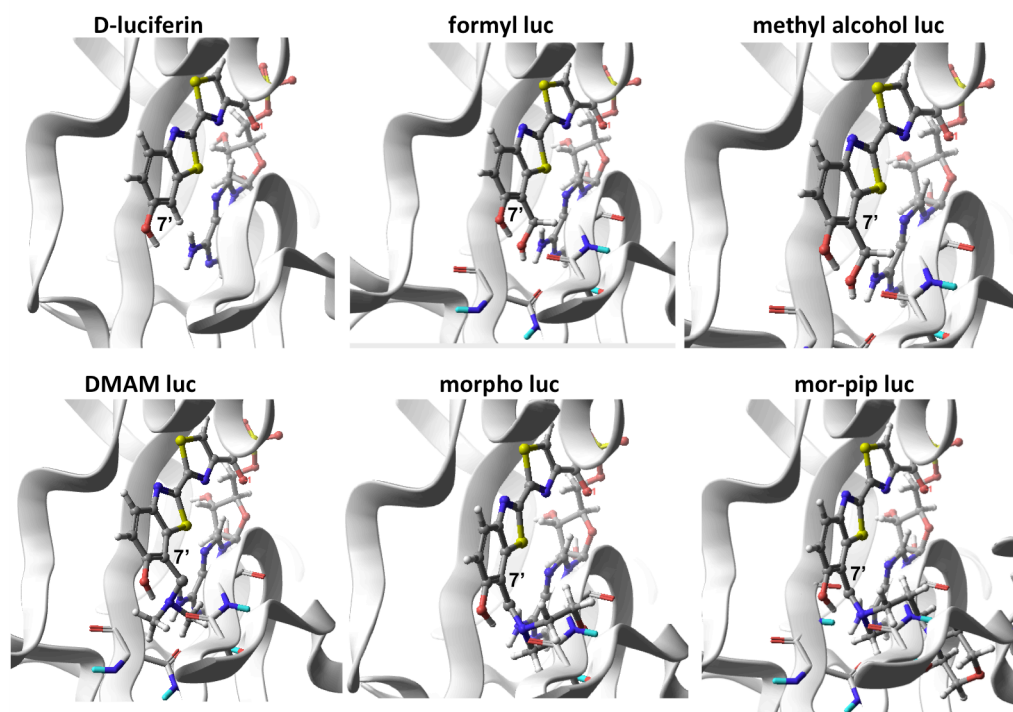
Figure 4-2 The 7′ position of D-luciferin abuts the Fluc secondary structure. The Fluc-DSLA crystal structure (PDB: 4G36) was modified to contain a 7′ aldehyde (formyl luc), methyl alcohol, dimethyl amino methyl (DMAM luc), methyl morpholino (morpho luc) or methyl morpholino-piperidyl (mor-pip luc). As the steric bulk increased, more steric clashes with β=please architecture were apparent. The latter three luciferins (DMAM luc, morpho luc and morpho-pip luc) failed to dock in any conformation under various Glide conditions: (SP, XP, or with SMARTS constraints).
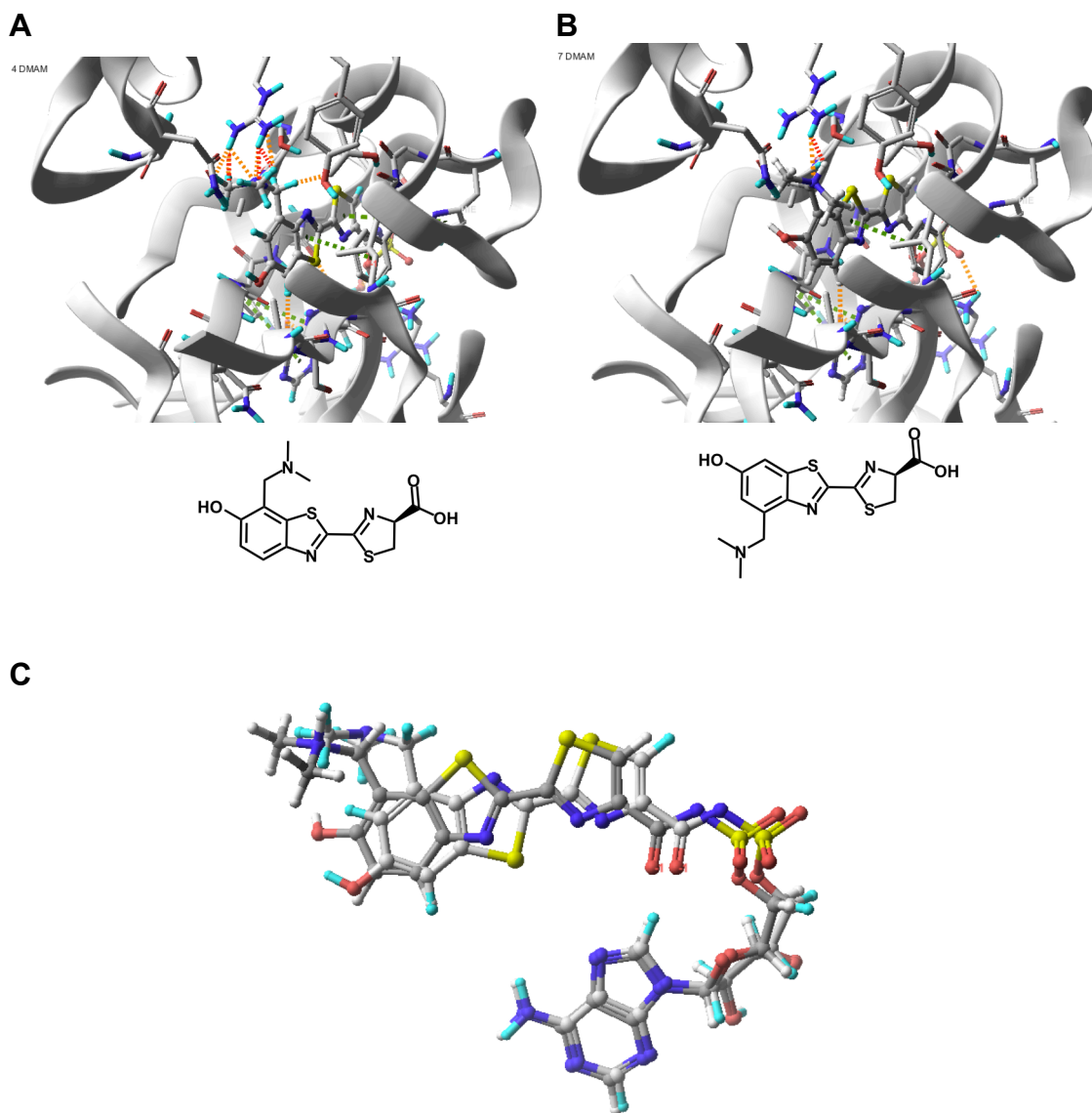
Figure 4-3 Docking studies indicate space around the 4′ of D-luciferin. 4′ DMAM luc (A) docks in the same "s-trans" configuration as D-luciferin while 7′ DMAM luc (B) adopts an "s-cis" conformation. (C) Overlay of the two DMAM luc footprints within the Fluc binding pocket in the absence of the enzyme highlights the relative positions of the heteroatoms in the rings and the incorrect position of the sulfurs (yellow) in 7′ DMAM luc.

Table 4-1 Docking data for a variety of modified luciferins.

ligand	Notes	GScore	DockScore	LipophilicEvdW	HBond	Contraints?
DSLA	s-trans	-11.74	-11.74	-6.22	-2.76	Y
DSLA	s-trans	-10.57	-10.57	-5.45	-1.52	N
4 bromo luc	s-trans	-10.97	-10.77	-5.79	-1.7	N
4 bromo luc	s-trans	-10.31	-10.31	-5.97	-2.02	Y
4 DMAMn luc	linear	-9.42	-8.63	-4.95	-2.63	N
4 fluoro luc	s-trans	-10.83	-10.66	-5.7	-1.54	N
4 methyl amino benzyl	outside pocket	-8.42	-7.38	-3.21	-3.72	N
4 methyl bromo luc	s-trans	-12.11	-12.11	-5.8	-2.29	Y
4 methyl bromo luc-2	s-cis	-9.06	-9	-5.53	-1.52	N
4 methyl luc	s-trans	-12.58	-12.58	-6.1	-2.3	Y
4 methyl luc	s-trans	-9.78	-9.75	-6.04	-1.76	N
4 methyl luc-2	s-trans	-12.11	-12.11	-6.26	-2.7	Y
4 Nitro luc	s-trans	-10.88	-10.34	-5.7	-1.75	N
4 vinyl luc	s-trans	-12.19	-12.19	-5.62	-2.49	Y
4 vinyl luc	s-trans	-10.64	-10.59	-5.82	-2.22	N
5 alkynyl luc	s-trans	-11.6	-11.6	-5.66	-2.26	Y
5 bromo luc	s-trans	-12.05	-12.05	-5.5	-2.57	Y
5 bromo luc	s-cis	-9.67	-9.42	-5.71	-2.54	N
5 bromo luc-2	s-trans	-11.12	-11.12	-5.37	-2.05	Y
5 fluoro luc	s-trans	-12.33	-11.8	-5.55	-2.44	N
5 methyl luc	s-trans	-11.31	-11.31	-5.34	-1.93	Y
5 methyl luc	s-cis	-9.98	-9.97	-5.66	-2.02	N
5 N methyl pyridone	s-trans	-11.14	-11.14	-5.65	-2.96	Y
5 N-ethyl pyridone	s-trans	-11.3	-11.3	-5.44	-2.17	Y
5 N-iPr pyridone	s-trans	-11.61	-11.61	-5.51	-2.31	Y
5 N-propyl pyridone	s-trans	-11.22	-11.22	-5.42	-1.82	Y
5 Nitro luc	s-trans	-11.18	-11.17	-5.22	-2.18	N
5 Nitro luc-2	s-cis	-10.11	-10.1	-5.41	-2.4	N
5 pyridone	s-trans	-11.09	-11.09	-5.94	-2.86	Y
6 amino luc	s-trans	-10.87	-10.87	-5.49	-1.54	N
6 amino luc-2	s-cis	-7.48	-7.48	-5.71	-2.08	N
6 azido luc	s-trans	-11.57	-11.57	-5.51	-2.27	N
6 benzyl click luc	s-trans	-11.69	-11.69	-6.18	-1.73	N
6 deoxy luc	s-trans	-10.76	-10.76	-5.72	-1.55	N
6 di methyl amino luc	s-trans	-11.17	-11.17	-5.68	-1.74	N
6 EtOH click luc	s-trans	-11.65	-11.65	-5.92	-1.8	N
6 methyl amino luc	s-trans	-10.99	-10.99	-5.88	-1.55	N
6 methyl ether luc	s-trans	-10.92	-10.92	-5.88	-1.53	N
6-OH 5 aza pyridine luc	s-trans	-11.09	-11.09	-5.94	-2.86	Y
6-OH 7-pyridine	s-trans	-10.94	-10.94	-5.42	-1.73	Y
7 formyl luc	s-trans	-9.97	-9.86	-6.04	-2.09	N
7 formyl luc	s-cis	-9.92	-9.81	-6.11	-1.63	N
7 bromo luc	s-trans	-8.36	-8.11	-6.11	-1.75	N
7 DMAM	outside pocket	-10.45	-10.14	-2.67	-4.04	N
7 fluoro luc	s-trans	-11.44	-11.13	-6.26	-2.89	N
7 methyl alcohol luc	s-trans	-12.42	-12.42	-6.29	-3.43	Y
7 methyl alcohol luc	s-trans	-12.34	-12.32	-6.17	-3.35	N
7 methyl luc	s-trans	-11.19	-11.19	-5.77	-3.13	Y
7 methyl luc	s-cis	-9.84	-9.83	-5.81	-1.8	N
7 N-ethyl pyridone luc	s-trans	-10.47	-10.47	-5.95	-2.49	Y
7 N-methyl pyridone luc	s-trans	-11.64	-11.64	-5.52	-3.68	Y
7 Nitro luc	s-cis	-8.24	-8.23	-5.96	-1.6	N
7 Nitro luc-2	s-trans	-5.69	-5.68	-5.96	-1.78	N
7 pyridone luc	s-trans	-12.9	-12.9	-5.86	-2.97	Y
CycLuc1 luc	s-trans	-10.92	-10.92	-5.46	-1.74	Y
CycLuc2 luc	s-trans	-11	-11	-5.44	-1.55	Y
Indoleluc	s-trans	-10.91	-10.91	-5.43	-1.67	Y

4.3 Evaluation of 7′ luciferin derivatives *in vitro*

We first evaluated the light emitting properties of the 7′ series of analogs with Fluc. As expected, when Fluc was incubated with hydroxy methyl luc, formyl luc, DMAM luc, morpho luc and mor-pip luc at 100 μM, weaker bioluminescence was observed compared to D-luciferin. In particular, morpho luc, and morpho-pip luc were
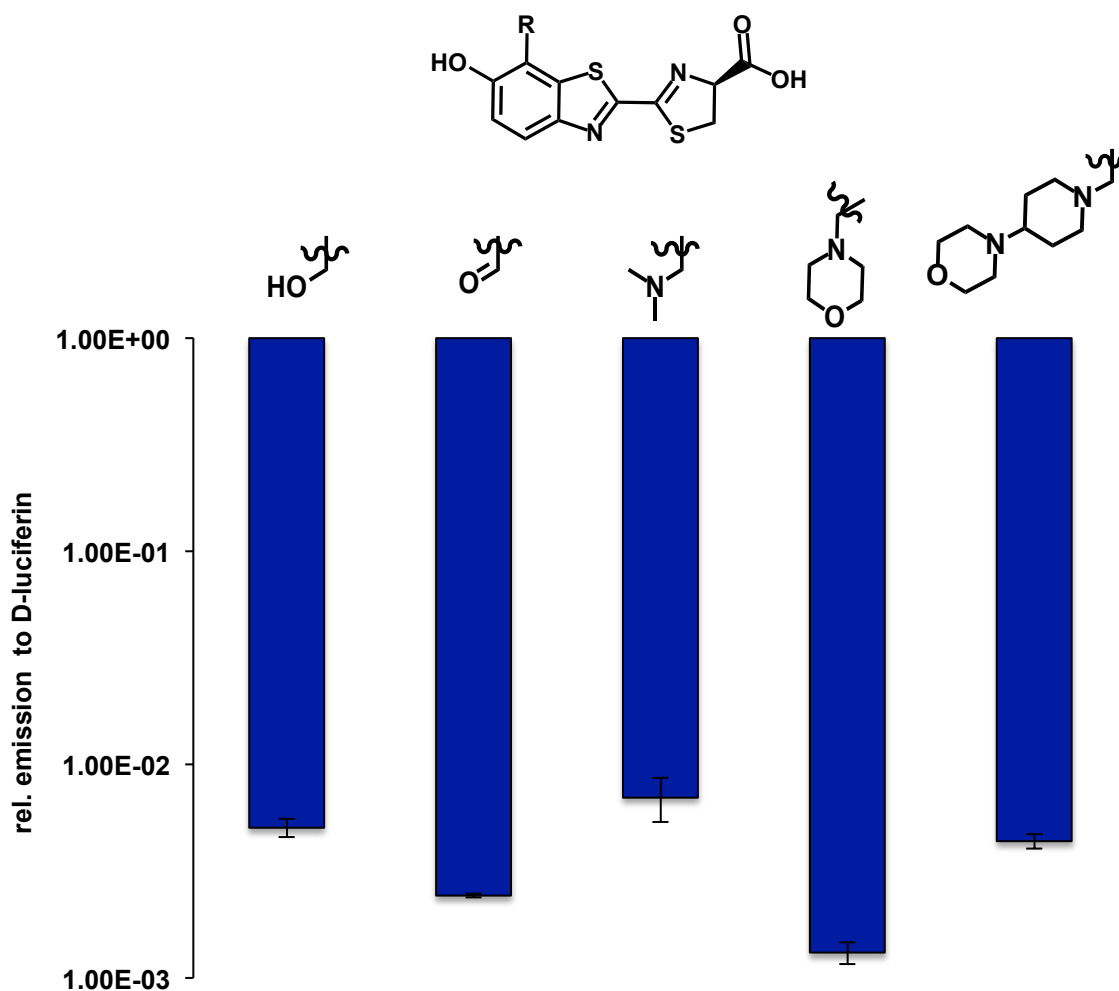
Figure 4-4 7′ Modified luciferins are poor light emitters compared to D-luciferin. Quantification of bioluminescence from hydroxy methyl luc, formyl luc, DMAM luc, morpho luc and mor-pip luc at 100 μM when incubated with Fluc and ATP is shown relative to the emission observed with D-luciferin. Error bars represent the standard error of the mean from three independent replicates.

more than three orders of magnitude poorer emitters than D-luciferin (Figure 4-4). Even though mor-pip luc is larger than morpho luc, mor-pip luc emitted more light with Fluc than the smaller analog. This result suggests that mor-pip luc is flexible and can adopt a better light-emitting conformation in the active site. Like with other analogs in Chapters 2 and 3, additional Fluc mutations should improve light emission for the 7′ amino alkyl luciferins.

The weak emission of these luciferins may be attributed to interference from the tertiary amine with the phenolate. Studies by Branchini have previously shown active site deprotonation of the 6′-OH substituent is critical for successful expulsion of CO_2. In the case of DMAM luc, the basic nitrogen atoms would likely be protonated at physiologically relevant pH, and as they sit near the phenol group, a zwitterionic state may be unfavorable. When I titrated the BLI buffer from pH 5 to 9, as expected, the emission from DMAM luc became ten times brighter from pH 7 to pH 9. The pH emission curve for morpho-luc was similar to that of hydroxyl methyl luc, although the global emission was lower (Figure 4-5). We can explain the discrepancy via the relative pKas of the two luciferins, although they're both tertiary amines, the pKa of the morpholino group (8.36) is low enough to limit its liability for *in vivo* imaging.

It is possible, though, that the luciferins themselves are not efficient photo producers. If the analogs are incapable of efficiently reaching the excited state, reduced light emission with Fluc would be expected. These molecules would also be poor candidates for orthogonal probe development. To ensure that the analogs were intrinsically capable of light emission, we turned to a non-enzymatic assay that mimics the luciferase-luciferin reaction. The chemiluminescent process invokes a similar

mechanism as the bioluminescent one: formation of an activated ester intermediate, followed by H-atom abstraction and subsequent reaction with molecular oxygen and ejection of CO_2. When the three 7′ alkyl amino analogs were subjected to the assay, robust light emission was observed, with the photon output on par with D-luciferin for morpho luc and mor-pip luc. Mor-pip was the brightest of the analogs (Figure 4-6). Surprisingly, DMAM luc the strongest bioluminescent light emitter, (Figure 4-4), exhibited a >10-fold reduction in chemiluminescence compared to the other alkyl amino luciferins (Figure 4-6). As a negative control, 6′-deoxy and 6′-OMe luc were subjected to the chemiluminescence assay. These molecules lack a strongly electron-donating group on the ring (a key feature of luciferins). As expected, these molecules displayed minimal luminescence. These results provided assurance that while the luciferin scaffolds for DMAM luc, morpho luc and mor-pip luc may be poor substrates for Fluc, they are still capable of emission from an electronic excited state.
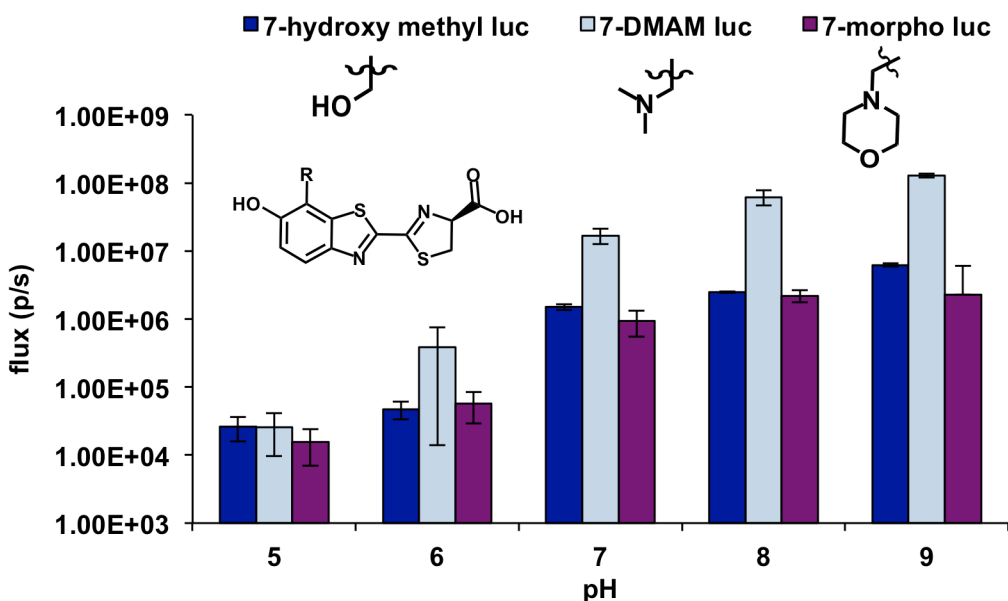
Figure 4-5 Effect of pH on 7′ alkyl modified luciferins. BLI buffer was titrated from pH 5 to pH 9 and luminescence was assayed with Fluc in the presence of 7′ modified luciferin hydroxy methyl luc (dark blue). DMAM luc (light blue), or morpho luc (raspberry). Error bars represent the standard error of the mean for three replicate samples.

When paired with the bioluminescent data sets, the chemiluminescence data suggested that the 7′ series of alkyl amino luciferins, and morpho-luc in particular, were ideal for orthogonal probe development.
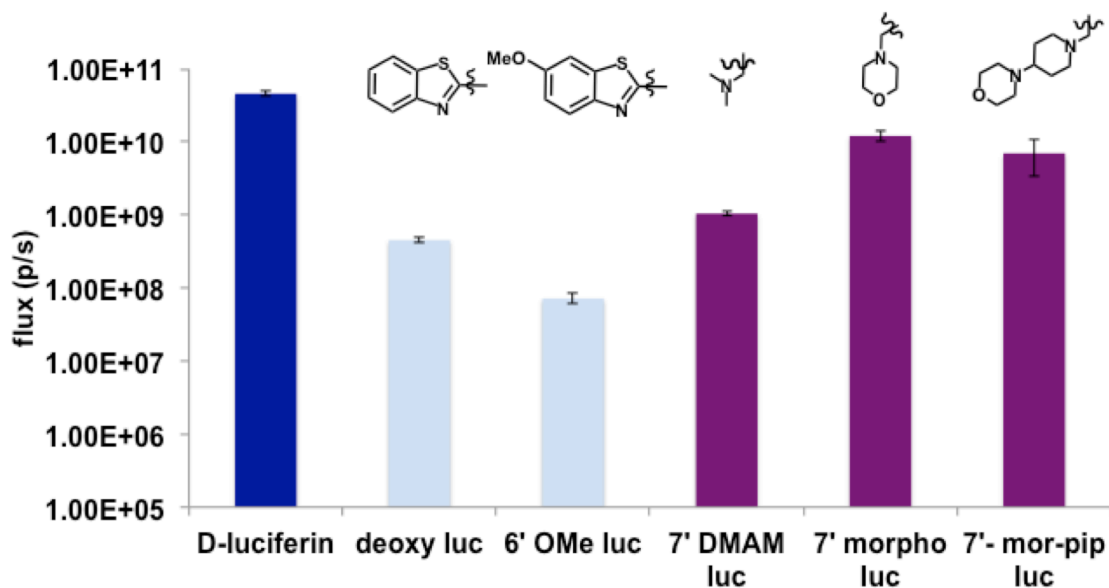
Figure 4-6 Chemiluminescence reveals intrinsic ability of 7′ amino acyl luciferins to produce light. D-luciferin (dark blue), DMAM luc, morpho luc, mor-pip luc (raspberry), and 6′ deoxy luc and 6′ OMe luc (light blue) were activated as phenyl esters, and oxidized with phenoxide. The emitting photons were captured with a Tecan luminometer and integrated over a BLANK min run. Error bars represent the standard error of the mean for three independent experiments.

4.4 Mutant luciferases can be identified/evolved to provide improved and orthogonal bioluminescent systems

Having identified DMAM luc, morpho luc and mor-pip luc as potential orthogonal luciferins, we set out to identify mutant luciferases that could efficiently andselectively process the structures. We decided to use the generation 1 library as a starting point because these mutants had already been shown to have unique light emission profiles (Chapter 3), and a number of them had already been selected for the 7′ amino alkyl luciferins (Table 3-2). In case all the mutations that had previously been selected were deleterious for this class of luciferins, I also doped in a small amount of WT Fluc that, once randomized, would serve as a naïve-library control. Because previous studies have demonstrated that distant mutations can profoundly influence the architecture of the luciferase active site, we decided at this point to scatter mutations throughout the length of the Fluc gene.

I generated a second generation library of luciferases using analog mutagenesis. This "G2" library had a ~$1.4*10^7$ member theoretical diversity. Sequencing revealed a ~0.6% amino acid substitution rate, meaning that about ~3-4 mutations would be incorporated in the gene, or one additional mutation in the luciferin binding site plus 1-2 others scattered throughout the rest of the structure. This new library was introduced into bacteria and the transformants were arrayed across agar plates containing embedded 7′ DMAM luc and morpho luc (See Figure 3-7 for example plates). Light emission was measured using a cooled CCD camera. Differential light emission was observed from each analog, suggesting that mutant luciferases can catalyze light emission with a range of efficiencies. Plasmid DNA was recovered from wells exhibiting the most robustly

emitting colonies (the top 10% were selected using IVIS illumina's Living Image software to auto-pick colonies by their light emission).

At this point, we had only screened the Fluc mutants for affinity for a particular luciferin, not the specificity or preference for one luciferin over another. To address the latter point, we picked colonies from the plates, grew them up, induced expression, lysed and distributed the lysate across several black-well plates, much like the solution screen in Chapter 2. We then imaged the analog of interest against the other compounds in a head-to-head screen. Sequencing analysis revealed mutations for the "hits" that correlated with each structure. Some of these mutations were observed for multiple analogs, suggesting that they might be selective for 7′-modified luciferins. Other mutations were unique to each compound, notable, given the subtle structural differences between the analogs.

We used the emission from WT Fluc with the analogs and D-luciferin as a control. The ratio of emission observed from DMAM luc, morpho luc and mor-pip compared to D-luciferin was calculated for each mutant. This value was then further compared to the same ratio in WT Fluc to demonstrate increased specificity for bulky luciferins (Figure 4-7 A). Some mutants (e.g., WP03) showed improvement across the panel of analogs, while others (e.g., WP04) only had a preference for DMAM luc. We also analyzed the mutants for their specificity for one analog over another using the same calculation described above. Here, nearly all mutants showed improvement in distinguishing between the DMAM, morpho and mor-pip groups compared to WT (Figure 4-7 B). While the emission intensities remained weak, the feasibility of our approach to generating new bioluminescent tools was established.
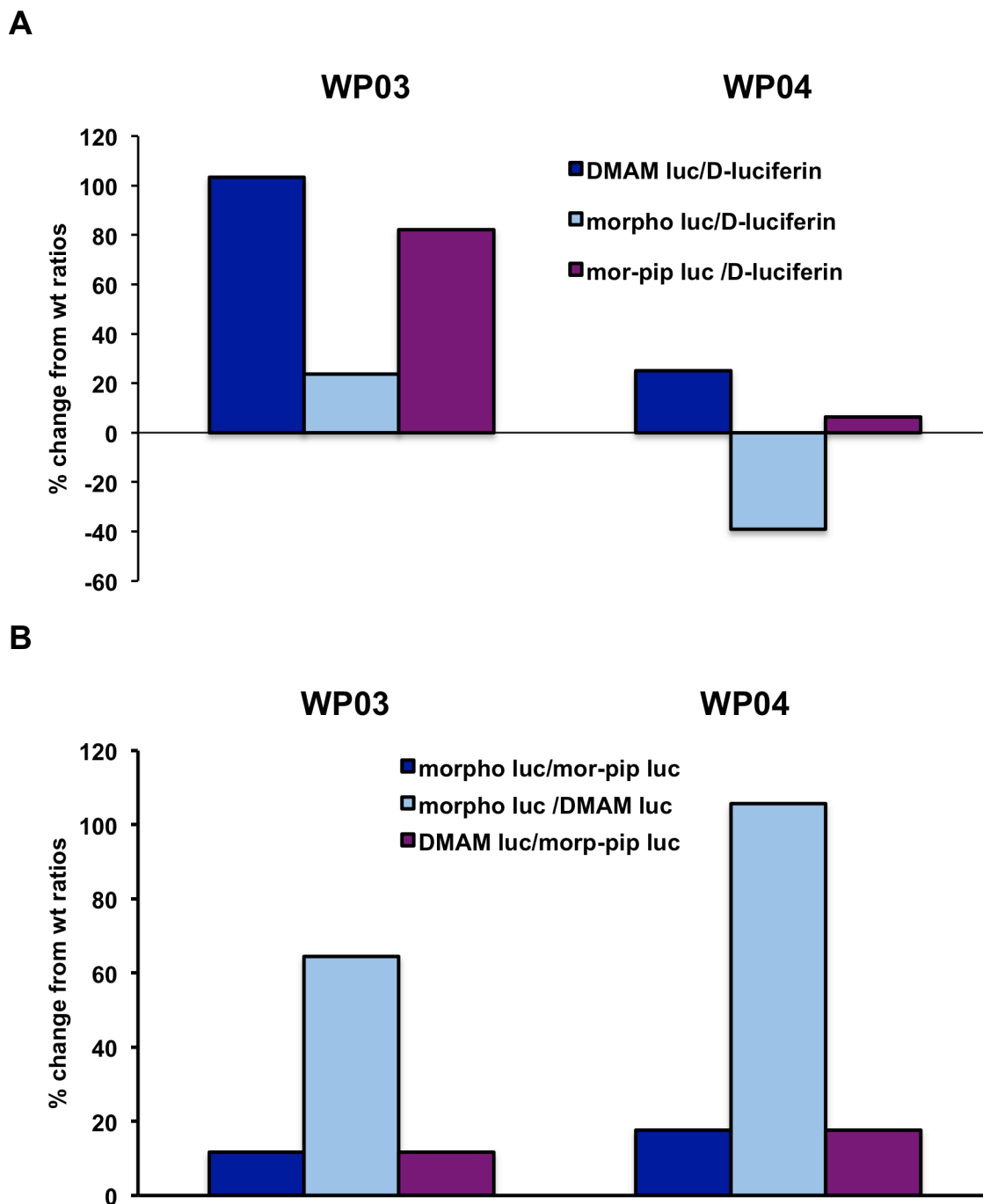
Figure 4-7 Mutants from generation 2 Fluc library prefentially catalyze light emission with 7′ alkyl aminoluciferins. *E. coli* cell lysate expressing WP03, WP04 and a WT Fluc control were assayed with 1 mM ATP and 100 µM D-luciferin, DMAM luc, mor-pip luc or morpho luc and the ratios between the analogs were compared. (A) The emission observed with alkyl amino luciferins DMAM luc (dark blue), morpho luc (light blue), and mor-pip luc (raspberry) was divided by that observed with D-luciferin. This ratio was in turn compared to the same ratio for WT Fluc and expressed as percent change. (B) The same analysis as (A) with morpho luc/ mor-pip luc (dark blue) morpho luc/ DMAM luc (light blue) and DMAM luc (mor-pip luc) is presented to demonstrate these mutants can distinguish between similarly shaped luciferins. This assay was not replicated and thus error is not reported.

The enzyme-substrate partners that emitted the most light (Table 4-2) were further characterized using standard biochemical assays (in terms of binding affinity, turnover efficiency, and selectivity). Clones 1-8 were isolated using standard protein expression and affinity chromatography techniques. No mutant Fluc out-performed WT Fluc in global light emission (Figure 4-8 A), but many demonstrated an increased tolerance for morpho luc and mor-pip luc (Figure 4-8 B). Most importantly, there was agreement between the initial cell lysate experiments and the refined assays in purified Fluc, suggesting that the screening procedure provides a fruitful readout on viable Fluc-luciferin analog pairs

The mutations identified corroborate previous crystal structure and biochemical analyses. Amino acids likely to interact with D-luciferin were found. These mutations included S456G, a carry-over from the first generation library. Because it lies outside the targeted R1R2 region, this mutation appeared to arise from the *E. coli*'s plasmid replication machinery, rather than our analog PCR reactions. When we studied the old sequencing data from that library more closely, I observed S456G appear with increasing frequency as I screened larger luciferins on plate in the G1 R1R2 library. Its location along the substrate entry pathway could enable the 7′ series access to the active site (Figure 3-14) more efficiently. Importantly Ser456 has previously been subject to saturation mutagenesis in order to increase specificity, and to improve the reaction performance with a dATP cofactor [12]. Several other mutations within our "hit" list have been investigated for their effects on the active site. For example, S307 [13] and E389 [14] have been shown to perturb D-luciferin binding with firefly luciferase (and thus light emission with the natural substrate), while preserving the overall structural

integrity of the enzyme. Changing aliphatic residues like V288 (specifically, mutating valine 288 to either isoleucine or alanine) has been used to red-shift emission [15]. Since longer wavelength of light can signal looser binding of the excited state product, this change and others may be responsible for improved accommodation of bulky substrates [16]. Taken together, we might hypothesize that the improvements shown in Figures 4-7 (A) and 4-8 (B) arise from loosening the active site and providing better access universally to larger luciferins. The specificity of some mutant Flucs for different 7′ amino alkyl luciferins (Figure 4-7 B), though, suggests that the active site architecture could be more discerning than that.

Table 4-2. Selected mutants from the generation 2 screening of 7′ amino alkyl luciferins.

clone	mutations
WP01	V240A, S456G, G545S
WP02	M59R, F243L, V288A, S307N, N409S, S456G
WP03	K329R, Q505R
WP04	F294S, H419R, S456G
WP05	K380R, E389K, N403T
WP06	K329R
WP07	S456G
WP08	G256S, S456G E537G, G545S
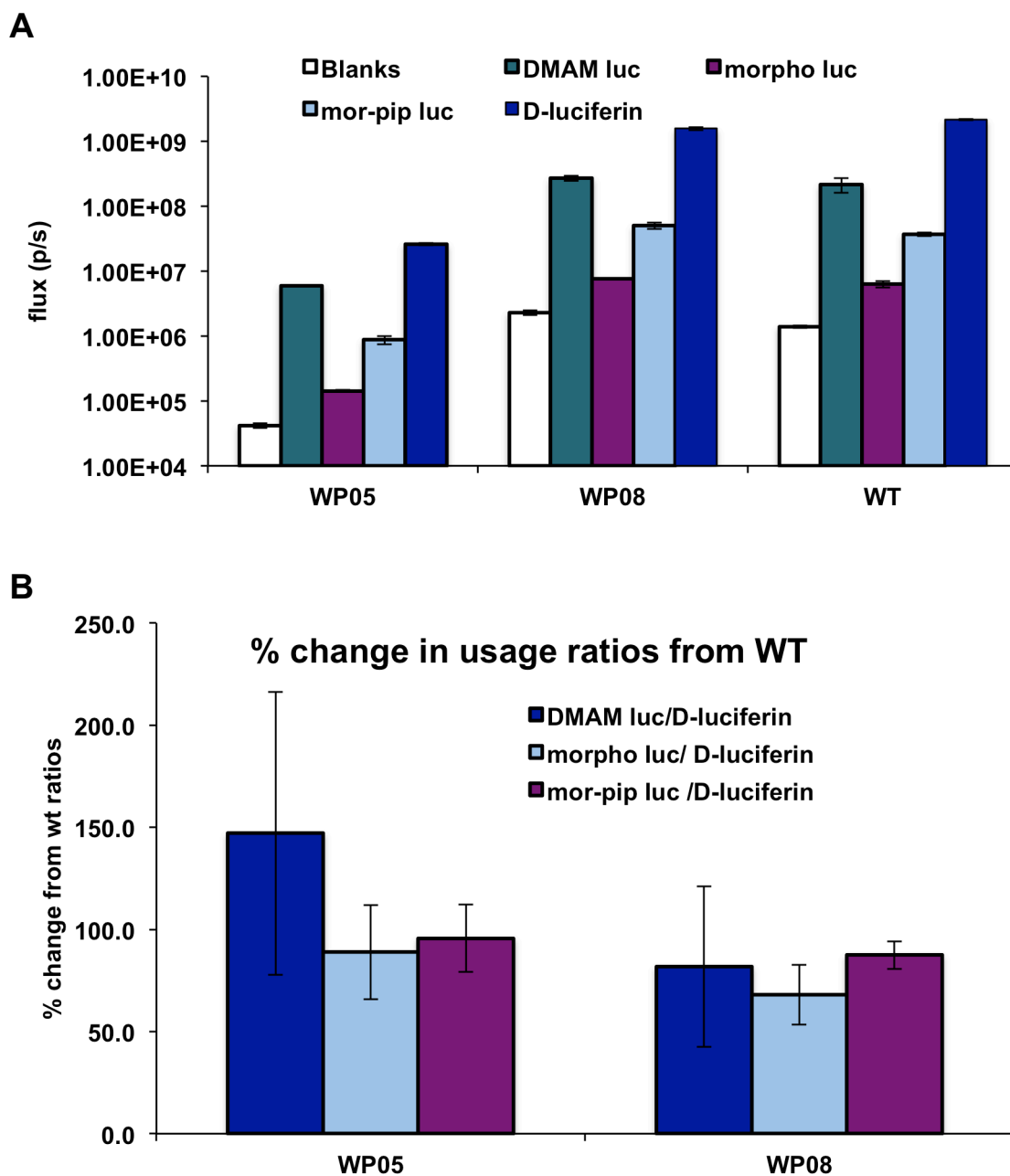
Figure 4-8 Mutant Flucs from the generation 2 screen show improved affinity for 7′ amino alkyl series luciferins. (A) Bioluminescence from purified WP05 and WP08 in the presence of DMAM luc, morpho luc, mor-pip luc or D-luciferin (100 μM) and ATP (1 mM) was observed and quantified. (B) The emission observed with alkyl amino luciferins DMAM luc (dark blue), morpho luc (light blue), and mor-pip luc (raspberry) was divided by that observed with D-luciferin. This ratio was in turn compared to the same ratio for WT Fluc and expressed as percent change. Error bars for (A) and (B) represent the standard error of the mean from three independent replicates.

For eventual orthogonal imaging applications, it will not be sufficient to simply use luciferases with "carved-out" active sites. Wide-open active sites accept a host of luciferins, making them difficult to distinguish. Each mutant Fluc will eventually need to be exquisitely specific for its orthogonal luciferin. In order to test whether we had engendered any substrate selectivity in the generation 2 library hits for 7′ analogs, we needed an analogous set of luciferins. Dave McCutcheon synthesized a sterically "matched" 4′ morpho luc (Figure 4-1). He then assayed the bioluminescence from WP01, WP02, WP05, WP08 and WT Fluc with D-luciferin, 4′ and 7′ morpho luc in order to compare the light emission from the best mutant Flucs. 4′ Morpho luc appears to be a more robust emitter across all luciferases than 7′ morpho luc (data not shown). More exciting, though, is the increased preference of the mutants of WP01 WP05 WP08 to 4′ morpho luc. With WT Fluc, 4′ morpho luc still only emits 2.5% of the photons that D-luciferin does. For WP01, WP05 and WP08, that percentage is over 5.0% (Figure 4-9 A) The trends are exactly the same with 7′ morpho luc, albeit nearly two orders of lower (Figure 4-9 B). The percent changes from the ratio observed in WT Fluc are inconsistent (Figure 4-9 C). All mutants tested have improved specificity for 4′ morpho luc compared to D-luciferin, but WP02 is poorer than WT Fluc at accepting 7′ morpho luc compared to D-luciferin. Furthermore, WP01 and WP02 have increased ability to distinguish between the 4′ and 7′ morpho groups, while WP05 and WP08 show the exact opposite trend. Previously, WP02 had demonstrated a significant (200%) improvement over WT in selecting 7′ morpho luc, so these assays will require repetition before anything can be said conclusively. It is disappointing that we have not yet achieved complete substrate

selectivity among the, but luciferase-luciferin pairs, we have definitively demonstrated that we can improve mutant luciferases' abilities to accept novel substrates.
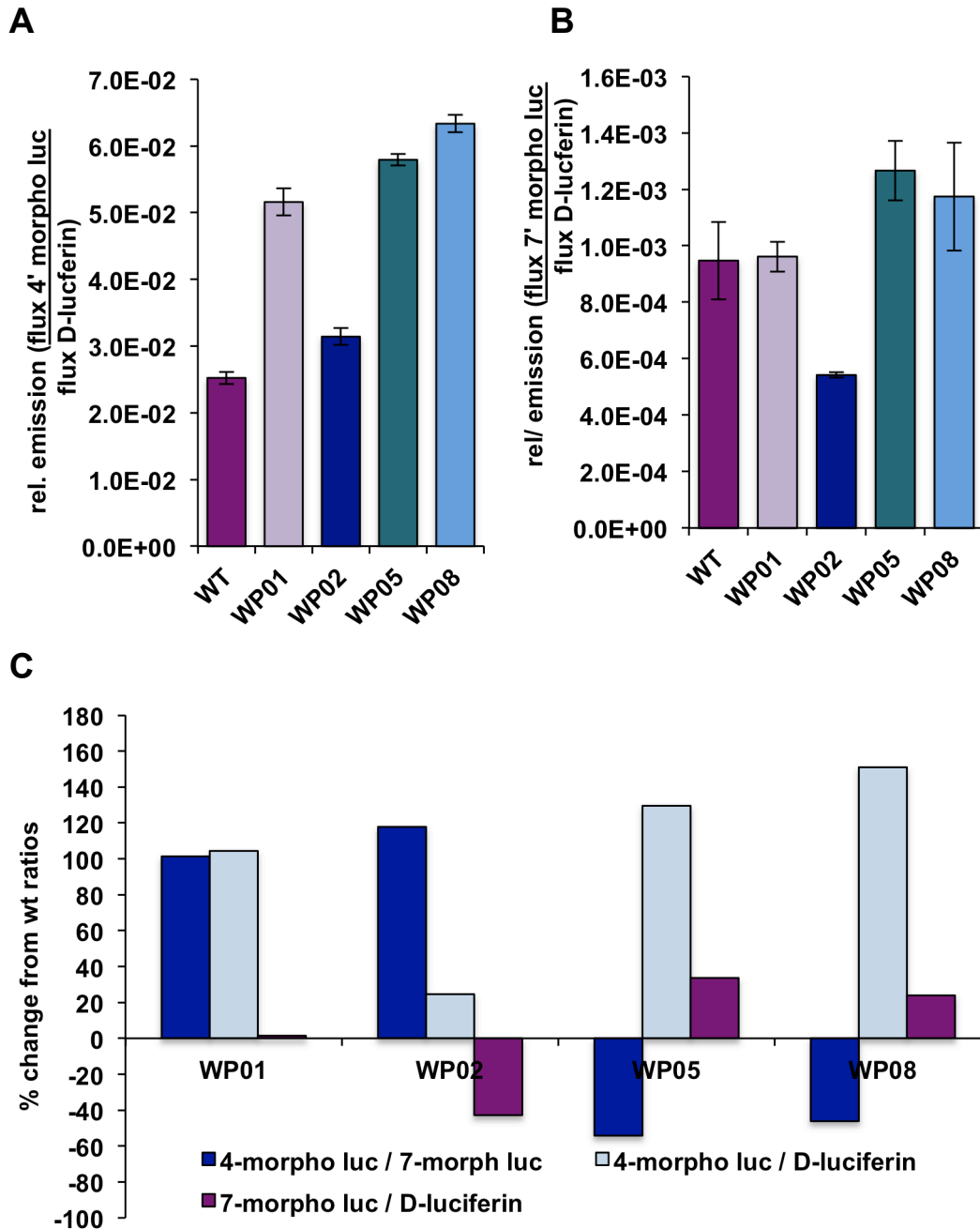
Figure 4-9 Mutant Flucs from the generation 2 screen show increased affinity for 4′ morpho luciferin. (A) The emission observed with 7′ morpho luc (A) and 4′ morpho luc (B) was compared to that of D-luciferin in WT Fluc, and WP01, WP02, WP05 and WP08. (C) The ratio of emission between the 4′ and 7′ morpho luc (dark blue) 4′ morpho luc and D-luciferin (light blue) and 7′ morpho luc and D-luciferin (raspberry) were calculated. This ratio was in turn compared to the same ratio for WT Fluc and expressed as percent change. This assay has not been replicated yet and thus error is not reported.

4.5 Conclusions and future directions

Bioluminescence has been largely limited to visualizing one biological feature at a time, as the most advantageous luciferases and luciferins for whole animal imaging utilize the same substrate and cannot be spectrally distinguished *in vivo*. We are expanding the bioluminescent toolkit by creating mutant versions of firefly luciferase that accept distinct, chemically modified luciferins.

In this chapter, I investigated a new class of sterically modified luciferins. Through docking studies, the analogs were predicted to bind exceedingly poorly to WT Fluc due to clashes with both active site side chains, and even the amino acid backbone. As predicted, the 7′ series of luciferin analogs were poor substrates for firefly luciferase, but by playing with pH and using chemiluminescence, we were able to demonstrate that they are inherently capable of producing light. Using an on-plate screening method, mutant versions of luciferase were identified that could also catalyze light emission with the analogs. Many of these mutants showed a preference for morpho luc, mor-pip luc, or both analogs as compared to the ratio with which WT Fluc used them. Interestingly, the mutations enabling productive light emission were positioned throughout the enzyme and several have previously been identified as mutations capable of generating space near the bound luciferin. Based on these data, we evaluated the mutants with a regioisomer of 7′ morpho luc, moving the steric bulk to a position predicted to be more tolerated by the enzyme. Not surprisingly, the "hit" mutant Flucs were also capable of emitting light with this luciferin. In fact, they were more specific for the 4′ probe than the 7′ morpho luc for which they were initially selected. These data are consistent with the idea that, thus far, our mutations have opened up the active site. Further, docking studies suggest that steric

clash with WT Fluc may enforce an energetically disfavorable (and potentially "dark") s-cis conformation [9]. At this point, it is hard to deconvolute whether emission from the 7′ probes involves a diminished quantum yield coming from a "dark" reaction in the cis conformation, or whether only a small proportion of the population adopts the proper trans conformation and that is the true light-emitter. Performing the chemiluminescence assay should help determine the source of decreased 7′ amino alkyl luminescence. Either the difference is inherent to the electronics of the two regioisomers (visible by chemiluminescence), or it is a function of the interactions of the enzyme. In the latter case, the bioluminescence spectra of these compounds with the different mutants should provide insight. s-Cis configurations in related fluorophores are associated with significant red-shifted emission [17]. I would expect the un-bound fluorescence of the 4′ and 7′ series to be very similar, so large differences in the bioluminescent spectra would indicate a difference in the active-site environment for each set of probes.

Collectively, these data suggest that "orthogonal" luciferase/luciferin pairs can be efficiently identified. Our data also suggest that the initial enzyme-substrate "hits", while orthogonal, are weak light emitters. Thus, the "hits" will be subjected to further rounds of mutagenesis and screening for improved light output with their respective luciferins. . It is reasonable to presume that targeting the amino acids directly in contact with the 7′ face of the molecule (in WT Fluc) should help "turn-on" emission with the 7′ series. This would further help us develop the first pairs of truly orthogonal luciferin-luciferases. In fact, if the cis conformation were indeed incapable of emitting light, this would provide a great mechanism for "turning off" emission in the mismatched case. Future studies will

also address the cellular compatibility and bioavailability of the probes in relevant models.

Orthogonal luciferin-luciferase tools will address a long-standing void in imaging capabilities. A collection of bioluminescent probes suitable for visualizing multiple cell populations at a macroscopic level could revolutionize our understanding of many disease states involving the interactions of diverse cell populations. Our long-term goal is to utilize these tools to probe complex cellular networks involved in tumor progression and immune function, although they will likely inspire new discoveries in a variety of disciplines, similar to how fluorescent protein technology enabled seminal advancements in numerous fields.

4.6 Methods and materials

General methods section

Buffer reagents purchased from Fisher Scientific. BLI buffer (100 mM Tris-HCl, 150 mM NaCl, 5 mM MgCl$_2$, 1.5% (w/v) bovine serum albumin, pH 7.8) was prepared and sterile-filtered for various assays. Unnatural dNTPs were synthesized on demand by Tri-link, San Diego; natural dNTPs were purchased from Fisher. Chemically competent bacteria were either purchased (Invitrogen/NEB) or prepared according to standard protocols (Sambrook and Russell, 2002). Restriction enzymes and T4 DNA ligase were purchased from New England Biolabs. DNA polymerases were purchased from a variety of suppliers. Platinum PFX was used for Quikchange mutagenesis while Platinum Taq was used for error-prone PCR (Invitrogen). Dreamtaq (Fermentas) was used for analog mutagenesis and standard PCR applications. All PCR reactions were confirmed by

ethidium bromide agarose gel analysis before performing down-stream reactions (sequencing was provided by Genewiz, San Diego). For cultures and protein expression, LB and LB agar granulated mixes were purchased from BD Difco. IPTG, PMSF and DTT were purchased from Gold Biosciences.

Synthesis of a generation 2 library by dNTP analog mutagenesis

Libraries were prepared essentially according to the method of Gherardi *et al* [18]. Twenty rounds of mutagenic PCR with *luc2* were performed initially in the presence of 200 mM natural dNTPs and 1 μM each of the unnatural bases dPTP and 8-oxodGTP (Trilink, San Digeo). The G2 library was amplified with primers MP022 and MP027 (sequences are listed below). The PCR products from each reaction were used as templates for further amplifiction, in the absence of dNTP analogs. Further subcloning for introduction into bacterial expression vector pET28 was performed with appropriate restriction enzymes as above. After initial sequence analysis (Genewiz, San Diego). The concentration of 1 μM dPTP and 1 μM 8-oxodGTP was determined to provide the optimal mutagenic load. The synthesis was repeated and scaled up for electroporation into XL1 ecomp cells and DNA extraction through midiprep (Zymo, San Diego).

Luciferase library primers
MP022 *Nco*Ifwd: 5′ TATACCATGGAAGATGCCAAAAACATTAAGAAGGGCCC 3′
MP027 *Not*Irev: 5′ TATAGCGGCCGCCACGGCGATCTTGCCGC 3′

General bioluminescence imaging protocol

All sampled were incubated with D-luciferin or luciferin analog and an excess of ATP on the stage with in a light-proof imaging chamber and imaged with IVIS Lumina (Xenogen) CCD camera chilled to -90 ºC. The stage was kept at 37 ºC to promote enzymatic reactions. Photons of light emitted from bioluminescent reactions were collected by the camera, and the captures were controlled by Living Image software. Typical exposure times were 30 s, with data binning levels set to medium. When strong emission saturated the memory on the CCD camera, the exposure time was lowered and binning was made smaller. Conversely, in low emitting samples, exposure was increased to capture more photons. Regions of interest were selected for quantification and total flux data were exported to Microsoft Excel for further analysis.

On-plate bioluminescence assays and library analysis

D-Luciferin (5 mM) was spotted onto the surface of colonies of interest. After a five-minute incubation period on the benchtop, BLI images were acquired as above. All light-emitting colonies and several non-emitting colonies were picked off the plate, grown in LB media overnight and DNA was extracted by miniprep (Qiagen, Germantown MD). Purified DNA was sequenced using appropriate primers for region of interest (T7 forward and reverse, or internal primer MP049)

MP049 Internal Fluc sequencing primer 5′ AGGGCTTCCAAAGCATGTAC3 3′

On plate screening

Plasmid DNA (10 ng) was transformed into 50 µL NEB high competency BL21 cells. After heat shock, cells were rescued with 950 µL SOC media and shaking at 37 °C for 1 h.   A portion of the culture (20 µL) was used to seed a 10X10 cm sterile grid plate (VWR) with 1-2 * 10^3 CFU. The remaining transformation was supplemented with 10% sterile glycerol, snap frozen in an isopropanol/dry ice bath and stored at -80 °C in 30-50 µL aliquots.   In some cases, these aliquots were used after slow thaw on ice. The transformations were replated for additional screening but required ~50% more transformation solution to achieve the same colony density.   The LB-agar plates themselves were prepared according to manufacturer directions with slight modifications. After autoclaving, the LB-agar was slow-cooled in a 37 °C incubator until just warm to touch. IPTG (100 µM) and luciferin (100-200 µM) were added and the solution was gently mixed and plates cast rapidly before the agar set. Plates were kept tightly sealed at 4 °C and prepared fresh (at least weekly) to ensure that neither IPTG nor the luciferin degraded.

Cell lysate BLI assays with native and analog luciferases

Plasmids encoding for Fluc of interest (pET28 vector) were transformed into BL21 DE3 cells, and grown on kanamycin plates (40 µg/mL) overnight. One colony was selected to inoculate 5 mL LB broth containing 40 µg/mL kanamycin nfor 4-6 h until an OD_{600}≈ 0.4 at which point protein expression was induced with 500 µM IPTG for 1 h. Cells were then harvested by centrifugation, resuspended in BLI reaction buffer and lysed by sonication. Lysate was clarified by centrifugation (13 krpm, 1 min) and 100 µL samples were incubated (in duplicate) with 100 µM of the luciferin of interest as well as 1 mM

ATP.

Expression of mutant Flucs WP01-06, and WP08

The mutants WP01-WP04 were prepared according to the procedure reported in Chapter 2, using WP01-WP04 Fluc pET 28a(+) plasmid. WP05 and WP08 were expressed under milder induction conditions (100μM IPTG, 20 °C) to maintain soluble expression. WP06 was expressed for 6 h, at 500 μM IPTG, 25 °C. WP08 was not purified with affinity purification as it was discovered that a frame-shift mutation at position 1638 pushed the His$_6$ tag out of frame.

Schrödinger molecular modeling

WT Fluc was prepared for docking using the protein prep wizard in Maestro (version 2014-3). The OPLS2005 force field was used for minimization. A Glide-grid wwas generated using this minimized structure and DSLA was used to provide the coordinates for ligand binding. The luciferins listed in table 4-1 were prepared by as the AMP conjugate; their geometries were cleaned and prepared through the LigPrep modeule prior to docking. SP docking was used to obtain the input poses for high-level calculations. XP docking was then performed using flexible ligand sampling, sampling of nitrogen inversions and ring conformations. Epik state penalities were use to exclude non-physiologically relevant protonation states and non-planar amide bonds were also penalized. An XP descriptor file was written in order to facilitate post-docking analysis. The docked ligands were evaluated manually via pose-viewer to choose the most relevant poses as well with XP visualizer to quantify the relative contributions of different ligand

interactions to the assessed GlideScore. For the molecules listed as s-cis, the XP docking was rerun with a SMARTS file used to constrain the rotation around the C2-C2' bond. When available, both docking scores are reported.

References

(1)   Bishop, A. C.; Buzko, O.; Shokat, K. M. Magic Bullets for Protein Kinases. *Trends Cell Biol.* **2001**, *11*, 167-172.

(2)   Boyle, S. N.; Koleske, A. J. Use of a Chemical Genetic Technique to Identify Myosin Iib as a Substrate of the Abl-Related Gene (Arg) Tyrosine Kinase. *Biochemistry* **2007**, *46*, 11614-11620.

(3)   Clemons, P. A.; Gladstone, B. G.; Seth, A.; Chao, E. D.; Foley, M. A.; Schreiber, S. L. Synthesis of Calcineurin-Resistant Derivatives af FK506 And Selection of Compensatory Receptors. *Chem. Biol.* **2002**, *9*, 49-61.

(4)   Islam, K.; Chen, Y.; Wu, H.; Bothwell, I. R.; Blum, G. J.; Zeng, H.; Dong, A.; Zheng, W.; Min, J.; Deng, H.; Luo, M. Defining Efficient Enzyme-Cofactor Pairs for Bioorthogonal Profiling of Protein Methylation. *Proc. Natl. Acad. Sci. U.S.A.* **2013**, *110*, 16778-1678.

(5)   Lopez, M. S.; Kliegman, J. I.; Shokat, K. M. The Logic and Design of Analog-Sensitive Kinases and Their Small Molecule Inhibitors. *Method. Enzymol.* **2014**, *548*, 189-213.

(6)   Mofford, D. M.; Reddy, G. R.; Miller, S. C. Aminoluciferins Extend Firefly Luciferase Bioluminescence into the Near-Infrared and can be Preferred Substrates over D-Luciferin. *J. Am. Chem. Soc.* **2014**, *136*, 13277-13282.

(7)   Reddy, G. R.; Thompson, W. C.; Miller, S. C. Robust Light Emission from Cyclic Alkylaminoluciferin Substrates for Firefly Luciferase. *J. Am. Chem. Soc.* **2010**, *132*, 13586-13587.

(8)   Woodroofe, C. C.; Shultz, J. W.; Wood, M. G.; Osterman, J.; Cali, J. J.; Daily, W. J.; Meisenheimer, P. L.; Klaubert, D. H. N-Alkylated 6′-Aminoluciferins are Bioluminescent Substrates for Ultra-Glo and QuantiLum Luciferase: New Potential Scaffolds for Bioluminescent Assays. *Biochemistry* **2008**, *47*, 10383-10393.

(9)   Roman, G. Mannich Bases in Medicinal Chemistry and Drug Design. *Eur. J. Med. Chem.* **2014**, *89C*, 743-816.

(10) McCutcheon, D. C.; Paley, M. A.; Steinhardt, R. C.; Prescher, J. A. Expedient Synthesis of Electronically Modified Luciferins for Bioluminescence Imaging. *J. Am. Chem. Soc.* **2012**, *134*, 7604-7607.

(11) YaJun, L.; Fang, W. H. *Ab initio* Investigation on the Structures and Spectra of the Firefly Luciferin. *Sci. China Ser. B.* **2007**, *50*, 725-730.

(12) Fushimi, T.; Miura, N.; Shintani, H.; Tsunoda, H.; Kuroda, K.; Ueda, M. Mutant firefly luciferases with improved specific activity and dATP discrimination constructed by yeast cell surface engineering. *Appl. Microbiol. Biotech.* **2013**, *97*, 4003-4011.

(13) Branchini, B. R. 01-12-2007 to 28-02-2010. Final grant report. **2010**.

(14) Conti, E.; Franks, N. P.; Brick, P.: Crystal Structure of Firefly Luciferase Throws Light on a Superfamily of Adenylate-Forming Enzymes. *Structure* **1996**, *4*, 287-298.

(15) Nakatsu, T.; Ichiyama, S.; Hiratake, J.; Saldanha, A.; Kobashi, N.; Sakata, K.; Kato, H. Structural Basis for the Spectral Difference in Luciferase Bioluminescence. *Nature* **2006**, *440*, 372-376.

(16) Fraga, H. Firefly Luminescence: a Historical Perspective and Recent Developments. *Photochem. Photobiol. Sci.* **2008**, *7*, 146-158.

(17) Knudtson, J. T.; Etring, E. M. Photophysical Effects of Sterolsomers in Thlacarbocynaine Dyes. *J. Phys. Chem.* **1974**, *78*, 2355-2363.

(18) Zaccolo, M.; Williams, D. M.; Brown, D. M.; Gherardi, E. An Approach oo Random Mutagenesis Of DNA Using Mixtures of Triphosphate Derivatives of Nucleoside Analogues. *J. Mol. Biol.* **1996**, *255*, 589-603.

CHAPTER 5: Summary and future directions

The development of orthogonal luciferase-luciferin tools promises to expand the breadth and depth of experimental questions regarding multi-cellular interactions that may be investigated in live animals. In this thesis, significant progress toward a novel imaging platform was demonstrated through the generation and screening of multiple generations of mutant Fluc libraries. For the orthogonal luciferins, baseline emissions in the presence of Fluc have been quantified. The cell-permeability of some analogs has been assessed in tissue culture models.

Both generation 1 and generation 2 Fluc libraries produced mutants that exhibited differential light emission with luciferin analogs. The analogs investigated include electronic, steric and altered aromatic core derivatives. Screening nitrogenous luciferins and 6′ acylated luciferins afforded mutant Flucs with improved $K_m$app and unique light emission profiles. In the end, however, it was discovered that steric bulk without significant perturbations to the electronics of the core most efficiently yielded orthogonal luciferase "hits" in the screen. The best mutants from the generation 2 screen several-fold times better at utilizing 4′ or 7′ amino alkyl luciferins compared to WT Fluc. While many of these mutants likely harbor more-opened active sites, some appeared to be specific for one regioisomer over another. Docking studies more severe active site remodeling is necessary to the 7′ luciferins while maintaining the more-favorable s-trans configuration. Initial light emission assays from 4′ morpho luc in the presence of the 7′ amino alkyl luc "hits" appear to supportthis assertion. Chemiluminescence studies, bioluminescent spectra and docking of the mutant Flucs with the two regioisomers will

begin to answer these questions. In addition, classic dye-binding studies could provide readouts on the relative polarity of the different mutant active sites.

We are also excited by the prospect of modeling the entire Fluc reaction coordinate with molecular dynamics. Such studies would capture the approach of the substrate towards the active site, and potentially reveal additional residues (like S456) to target for improved substrate accessibility. We have also initiated further studies involving rational design of luciferases. The targeted residues are based on literature precedent and the ability to perform *in silico* saturation mutagenesis. We are pursuing these and other computational studies in collaboration with the Mobley lab at UCI.

While the Prescher lab will continue screening libraries and compounds in house for many years, potential collaborations with NIH screening facilities could accelerate these studies, particularly by moving the screen into mammalian cells from the onset. These screening centers also have efficient compound-delivery technologies, that would address a current limitation of our on-plate screen. There is also the potential to design a streamlined screen or a selection. For the former, we envision coupling the bioluminescent light emission to a fluorescent protein like Kindling, enabling fluorescence-activated cell sorting (FACS). Woe could also couple bioluminescent light emission to drive the expression of cell survival markers. In this scenario, only transformants expressing a functional Fluc in the presence of analog would survive.

Upon discovery, the orthogonal luciferase/luciferin pairs will be analyzed for their suitability *in vivo*, including toxicity, bioavailability and clearance rates. From there, we intend to utilize the tools for multi-component imaging *in vivo*. We are particularly

interested in monitoring the interactions of tumor cells with those of the immune system in metastatic cancer models.

Finally, as a molecular biologist, I hope that once a family of related orthogonal luciferase-luciferin pairs has been discovered, structural biology studies will be performed. Most structure/function studies look at point mutants and gain or loss-of-function. Thus, they model the climb up and down the fitness landscape for a given enzymatic function. By contrast, our work will provide a series of enzymes that work on different substrates, which would be a wonderful model for divergent evolution. To perform these experiments, we would likely need crystal structures; thankfully UCI is home to wonderful molecular and structural biologists with whom to collaborate. From there, many opportunities for modeling and structure-function relationship work naturally arise. Potentially these insights could lead to new rationally-designed, task-specific luciferase-luciferin pairs.

APPENDIX A Sequencing data

<u>WT Fluc DNA sequence:</u>

5'ATGGAAGATGCCAAAAACATTAAGAAGGGCCCAGCGCCATTCTACCCACTC
GAAGACGGGACCGCCGGCGAGCAGCTGCACAAAGCCATGAAGCGCTACGCC
CTGGTGCCCGGCACCATCGCCTTTACCGACGCACATATCGAGGTGGACATTA
CCTACGCCGAGTACTTCGAGATGAGCGTTCGGCTGGCAGAAGCTATGAAGCG
CTATGGGCTGAATACAAACCATCGGATCGTGGTGTGCAGCGAGAATAGCTTG
CAGTTCTTCATGCCCGTGTTGGGTGCCCTGTTCATCGGTGTGGCTGTGGCCCC
AGCTAACGACATCTACAACGAGCGCGAGCTGCTGAACAGCATGGGCATCAGC
CAGCCCACCGTCGTATTCGTGAGCAAGAAAGGGCTGCAAAAGATCCTCAACG
TGCAAAAGAAGCTACCGATCATACAAAAGATCATCATCATGGATAGCAAGAC
CGACTACCAGGGCTTCCAAAGCATGTACACCTTCGTGACTTCCCATTTGCCAC
CCGGCTTCAACGAGTACGACTTCGTGCCCGAGAGCTTCGACCGGGACAAAAC
CATCGCCCTGATCATGAACAGTAGTGGCAGTACCGGATTGCCCAAGGGCGTA
GCCCTACCGCACCGCACCGCTTGTGTCCGATTCAGTCATGCCCGCGACCCCAT
CTTCGGCAACCAGATCATCCCCGACACCGCTATCCTCAGCGTGGTGCCATTTC
ACCACGGCTTCGGCATGTTCACCACGCTGGGCTACTTGATCTGCGGCTTTCGG
GTCGTGCTCATGTACCGCTTCGAGGAGGAGCTATTCTTGCGCAGCTTGCAAGA
CTATAAGATTCAATCTGCCCTGCTGGTGCCCACACTATTTAGCTTCTTCGCTA
AGAGCACTCTCATCGACAAGTACGACCTAAGCAACTTGCACGAGATCGCCAG
CGGCGGGGCGCCGCTCAGCAAGGAGGTAGGTGAGGCCGTGGCCAAACGCTT
CCACCTACCAGGCATCCGCCAGGGCTACGGCCTGACAGAAACAACCAGCGCC
ATTCTGATCACCCCCGAAGGGGACGACAAGCCTGGCGCAGTAGGCAAGGTG
GTGCCCTTCTTCGAGGCTAAGGTGGTGGACTTGGACACCGGTAAGACACTGG
GTGTGAACCAGCGCGGCGAGCTGTGCGTCCGTGGCCCCATGATCATGAGCGG
CTACGTTAACAACCCCGAGGCTACAAACGCTCTCATCGACAAGGACGGCTGG
CTGCACAGCGGCGACATCGCCTACTGGGACGAGGACGAGCACTTCTTCATCG
TGGACCGGCTGAAGAGCCTGATCAAATACAAGGGCTACCAGGTAGCCCCAGC
CGAACTGGAGAGCATCCTGCTGCAACACCCCAACATCTTCGACGCCGGGGTC
GCCGGCCTGCCCGACGACGATGCCGGCGAGCTGCCCGCCGCAGTCGTCGTGC
TGGAACACGGTAAAACCATGACCGAGAAGGAGATCGTGGACTATGTGGCCA
GCCAGGTTACAACCGCCAAGAAGCTGCGCGGTGGTGTTGTGTTCGTGGACGA
GGTGCCTAAAGGACTGACCGGCAAGTTGGACGCCCGCAAGATCCGCGAGATT
CTCATTAAGGCCAAGAAGGGCGGCAAGATCGCCGTGTAA 3'

Total number of bases : 1653
% A = 23.71   [392]   % G = 27.95   [462]
% T = 18.21   [301]   % C = 30.13   [498]
% A+T = 41.92   [693]   % C+G = 58.08   [960]

WT Fluc amino acid sequence

H2N-
MEDAKNIKKGPAPFYPLEDGTAGEQLHKAMKRYALVPGTIAFTDAHIEVDITYA
EY
FEMSVRLAEAMKRYGLNTNHRIVVCSENSLQFFMPVLGALFIGVAVAPANDIYN
ERELLNSMGISQPTVVFVSKKGLQKILNVQKKLPIIQKIIIMDSKTDYQGFQSMYT
FVTSHLPPGFNEYDFVPESFDRDKTIALIMNSSGSTGLPKGVALPHRTACVRFSHA
RDPIFGNQIIPDTAILSVVPFHHGFGMFTTLGYLICGFRVVLMYRFEEELFLRSLQD
YKIQSALLVPTLFSFFAKSTLIDKYDLSNLHEIASGGAPLSKEVGEAVAKRFHLPGI
RQGYGLTETTSAILITPEGDDKPGAVGKVVPFFEAKVVDLDTGKTLGVNQRGEL
CVRGPMIMSGYVNNPEATNALIDKDGWLHSGDIAYWDEDEHFFIVDRLKSLIKY
KGYQVAPAELESILLQHPNIFDAGVAGLPDDDAGELPAAVVVLEHGKTMTEKEI
VDYVASQVTTAKKLRGGVVFVDEVPKGLTGKLDARKIREILIKAKKGGKIAV-
CO₂H

Molecular Weight 60644.15 Daltons   550 Amino Acids   59 Strongly Basic(+)
Amino Acids (K,R)   65 Strongly Acidic(-) Amino Acids (D,E)   210
Hydrophobic Amino Acids (A,I,L,F,W,V)   113 Polar Amino Acids (N,C,Q,S,T,Y)
6.460 Isolectric Point   -3.836 Charge at PH 7.0

Sample Screening Alignments

Screening alignments and the identification of S456G outside cloning region

Early screening alignment: no S456G present (1.20.2014)

```
Sequence Name                          < Pos = 399
Consensus        SGYVNNPEATNAL IDKDGWLHSGD IAYWDEDEHFF IVDRLKSL IKYKGYQVAPAELES ILLQHPN IFDAG
12 Sequences     400      410      420      430      440      450      460
1_30_CF3_3-MP049_E06.ab1     SGYVNNPEATNAL IDKDGWLHSGD IAYWDEDEHFF IVDRLKSL IKYKGYQVAPAELES ILLQHPN IFDAG
1_30_CF3_17-MP049_C07.ab1    SGYVNNPEATNAL IDKDGWLHSGD IAYWDEDEHFF IVDRLKSL IKYKGYQVAPAELES ILLQHPN IFDAG
1_30_CF3_18-MP049_D07.ab1    SGYVNNPEATNAL IDKDGWLHSGD IAYXDEDEHFF IVDRLKSL IKYKGYQVAPAELES ILLQHPN IFXAG
1_30_CF3_19-MP049_E07.ab1    SGYVNNPEATNAL IDKDGWLHSGD IAYXDEDEHFF IVDRLKSL IKYKGYQVAPAELES ILLQHPN IFDAG
1_30_Dluc_20-MP049_F07.ab1   SGYVNNPEATNAL IDKDGWLHSGD IAYXDEDEHFF IVDRLKSL IKYKGYQVAPAELES ILLQHPN IFDAG
1_30_Dluc_21-MP049_G07.ab1   SGYVNNPEATNAL IDKDGWLHSGD IAYWDEDEHFF IVDRLKSL IKYKGYQVAPAELES ILLQHPN IFDAG
1_30_Dluc_22-MP049_H07.ab1   SGYVNNPEATNAL IDKDGWLHSGD IAYXXDEHFF IVDRLKSL IKYKGYQVAPAELES ILLQHPN IFDAG
1_30_Tbutylthio_5-MP049_F06.ab1   SGYVNNPEATNAL IDKDGWLHSGD IAYXDEDEHFF IVDRLKSL IKYKGYQVAPAELES ILLQHPN IFDAG
1_30_Tbutylthio_6-MP049_G06.ab1   SGYVNNPEATNAL IDKDGWLHSGD IAYWDEDEHFF IVDRLKSL IKYKGYQVAXAELES ILLQHPN IFDAG
1_30_Tbutylthio_13-MP049_B07.ab1  SGYVNNPEATNAL IDKDGWLHSGD IAYWDEDEHFF IVDRLKSL IKYKGYQVAPAELES ILLQHPN IFDAG
1_30_Benzimidluc_8-MP049_A07.ab1  SGYVNNPEATNAL IDKDGWLHSGD IAYWDEDEHFF IVDRLKSL IKYKGYQVAPAELES ILLQHPN IFDAG
Luc2WT           SGYVNNPEATNAL IDKDGWLHSGD IAYWDEDEHFF IVDRLKSL IKYKGYQVAPAELES ILLQHPN IFDAG
```

First appearance of S456G with t-butyl AA luc screening: (2.14.2014)

```
Sequence Name
Consensus          YWDEDEHFF IVDRLKSL IKYKGYQVAPAELES IL
13 Sequences       430      440      450
MP_Blucrescreen-2-YWDEDEHFF IVDRLKSL IKYKGYQVAPAELES IL
MP_Blucrescreen-3-YWDEDEHFF IVDRLKSL IKYKGYQVAPAELES IL
MP_Blucrescreen-4-YWDEDEHFF IVDRLKSL IKYKGYQVAPAELES IL
MP_Blucrescreen-5-YWDEDEHFF IVDRLKSL IKYKGYQVAPAELES IL
MP_Dlucrescreen-6-YWDEDEHFF IVDRLKSL IKYKGYQVAPAELES IL
MP_Dlucrescreen-7-YWDEDEHFF IVDRLKSL IKYKGYQVAPAELES IL
MP_thioetherAA-15-YWDEDEHFF IVDRLKSL IKYKGYQVAPAELEG IL
MP_thioetherAA-16-YWDEDEHFF IVDRLKSL IKYKGYQVAPAELES IL
MP_thioetherAA-17-YWDEDEHFF IVDRLKSL IKYKGYQVAPAELES IL
MP_thioetherAA-18-YWDEDEHFF IVDRLKSL IKYKGYQVAPAELES IL
MP_thioetherAA-22-YWDEDEHFF IVDRLKSL IKYKGYQVAPAELES IL
MP_Blucrescreen-1-YWDEDEHFF IVDRLKSL IKYKGYQVAPAELES IL
Luc2WT            YWDEDEHFF IVDRLKSL IKYKGYQVAPAELES IL
```

T-butyl thioether "hits." S456G begins to appears in R1R2 library regularly (1.30.2014)

```
Sequence Name
Consensus        IFGNQI IPDTAILSVVPFHHGFGMFTTLGVL ICGFRVVLMVRFEEEELFLRSLQDYK IQSALLVPTLFSFFF
5 Sequences      230      240      250      260      270      280      290
MP_R1R1_tbutylthioether-02-MP049.ab1  IFGNQI IPDTAILSVVPFHHGFGMFTTLGVL ICGFRVVLMVRFEEEELFLRSLQDYK IQSALLVPTLFSFFF
MP_R1R1_tbutylthioether-03-MP049.ab1  IFGNQI IPDTAILSVVPFHHGFGMFTTLGVL ICGFRVVLMVRFEEEELFLRSLQDYK IQSALLVPTLFSFFF
MP_R1R1_tbutylthioether-04-MP049.ab1  IFGNQI IPDTAILSVVPFHHGFGMFTTLGVL ICGFRVVLMVRFEEEELFLRSLQDYK IQSALLVPTLFSFFF
MP_R1R1_tbutylthioether-05-MP049.ab1  IFGNQI IPDTAILSVVPFHHGFGMFTTLGVL ICGFRVVLMVCFEEEELFLRSLQDYK IQSALLVPTLFNFFF
Luc2WT                                IFGNQI IPDTAILSVVPFHHGFGMFTTLGVL ICGFRVVLMVRFEEEELFLRSLQDYK IQSALLVPTLFSFFF
```

...

```
Sequence Name                          < Pos = 406
Consensus        EATNAL IDKDGWLHSGD IAYWDEDEHFF IVDRLKSL IKYKGYQVAPAELEG ILLQHPN IFDAGVAG
5 Sequences      410      420      430      440      450      460      470
MP_R1R1_tbutylthioether-02-MP049.ab1  EATNAL IDKDGWLHSGD IAYWDEDEHFF IVDRLKSL IKYKGYQVAPAELEG ILLQHPN IFDAGVAG
MP_R1R1_tbutylthioether-03-MP049.ab1  EATNAL IDKDGWLHSGD IAYXDEDEHFF IVDRLKSL IKYKGYQVAPAELEG ILLQHPN IFDAGVAG
MP_R1R1_tbutylthioether-04-MP049.ab1  EATNAL IDKDGWLHSGD IAYWDEDEHFF IVDRLKSL IKYKGYQVAPAELEG ILLQHPN IFDAGVAG
MP_R1R1_tbutylthioether-05-MP049.ab1  EATNAL IDKDGWLHSGD IAYXDEDEHFF IVDRLKSL IKYKGYQVAPAELEG ILLQHPN IFDAGVAG
Luc2WT                                EATNAL IDKDGWLHSGD IAYWDEDEHFF IVDRLKSL IKYKGYQVAPAELES ILLQHPN IFDAGVAG
```

Revised R1R2 library hits for morpholino luc (4.30.2014)

On-plate generation 1 screening with 7' alkyl series lucs. Every hit now has S456G (5.1.2014)

(top alignment block)

Sequence Name	
- ■ ■ ■ ■ +	
☒ Consensus	
9 Sequences	

Consensus sequence region 350–410:

`RILITPEGDDKPGAVGKVVPFFEAKVVDLDTGKTLGVNQRGELCVRGPMIMSGVVNNPEATNAL`

```
350      360      370      380      390      400      410
```

Sequence Name	Sequence (350–410)
5_1_hydroxymethyl_4-MP049_B10.ab1	RILITPEGDDKPGAVGKVVPFFEAKVVDLDTGKTLGVNQRGELCVRGPMIMSGVVNNPEATNAL
5_1_hydroxymethyl_11-MP049_C10.ab1	RILITPEGDDKPGAVGKVVPFFEAKVVDLDTGKTLGVNQRGELCVRGPMIMSGVVNNPEATNAL
5_1_morpholino_1-MP049_D10.ab1	RILITPEGDDKPGAVGKVVPFFEAKVVDLDTGKTLGVNQRGELCVRGPMIMSGVVNNPEATNAL
5_1_morpholino_3-MP049_E10.ab1	RILITPEGDDKPGAVGKVVPFFEAKVVDLDTGKTLGVNQRGELCVRGPMIMSGVVNNPEATNAL
5_1_morpholino_6-MP049_F10.ab1	RILITPEGDDKPGAVGKVVPFFEAKVVDLDTGKTLGVNQRGELCVRGPMIMSGVVNNPEATNAL
5_1_morpholino_7-MP049_G10.ab1	RILITPEGDDKPGAVGKVVPFFEAKVVDLDTGKTLGVNQRGELCVRGPMIMSGVVNNPEATNAL
5_1_morpholino_12-MP049_H10.ab1	RILITPEGDDKPGAVGKVVPFFEAKVVDLDTGKTLGVNQRGELCVRGPMIMSGVVNNPEATNAL
5_1_hydroxymethyl_2-MP049_A10.ab1	RILITPEGDDKPGAVGKVVPFFEAKVVDLDTGKTLGVNQRGELCVRGPMIMSGVVNNPEATNAL
_uc2WT	RILITPEGDDKPGAVGKVVPFFEAKVVDLDTGKTLGVNQRGELCVRGPMIMSGVVNNPEATNAL

(second alignment block)

Sequence Name	
- ■ ■ ■ ■ +	
☒ Consensus	
9 Sequences	

Consensus sequence region 410–460:

`NALIDKDGWLHSGDIAVWDEDEHFFIVDRLKSLIKYKGVQVAPAELEGILLQH`

```
410      420      430      440      450      460
```

Sequence Name	Sequence (410–460)
5_1_hydroxymethyl_4-MP049_B10.ab1	NALIDKDGWLHSGDIAVWDEDEHFFIVDRLKSLIKYKGVQVAPAELEGILLQH
5_1_hydroxymethyl_11-MP049_C10.ab1	NALIDKDGWLHSGDIAVXDEDEHFFIVDRLKSLIKYKGVQVAPAELEGILLQH
5_1_morpholino_1-MP049_D10.ab1	NALIDKDGWLHSGDIAVWDEDEHFFIVDRLKSLIKYKGVQVAPAELEGILLQH
5_1_morpholino_3-MP049_E10.ab1	NALIDKDGWLHSGDIAVWDEDEHFFIVDRLKSLIKYKGVQVAPAELEGILLQH
5_1_morpholino_6-MP049_F10.ab1	NALIDKDGWLHSGDIAVWDEDEHFFIVDRLKSLIKYKGVQVAPAELEGILLQH
5_1_morpholino_7-MP049_G10.ab1	NALIDKDGWLHSGDIAVWDEDEHFFIVDRLKSLIKYKGVQVAPAELEGILLQH
5_1_morpholino_12-MP049_H10.ab1	NALIDKDGWLHSGDIAVWDEDEHFFIVDRLKSLIKYKGVQVAPAELEGILLQH
5_1_hydroxymethyl_2-MP049_A10.ab1	NALIDKDGWLHSGDIAVWDEDEHFFIVDRLKSLIKYKGVQVAPAELEGILLQH
_uc2WT	NALIDKDGWLHSGDIAVWDEDEHFFIVDRLKSLIKYKGVQVAPAELEGILLQH

Selection of generation 1 screening alignments

T235A

Sequence Name	< Pos = 179
- ■ ■ ■ ■ +	
☒ Consensus	
12 Sequences	

Consensus sequence region 180–240:

`VDFVPESFDRDKTIALIMNSSGSTGLPKGVALPHRTACVRFSHARDPIFGNQIIPDTAILSVVPFHHGP`

```
180   190   200   210   220   230   240
```

Sequence Name	Sequence (180–240)
1_30_CF3_3-MP049_E06.ab1	VDFVPESFDRDKTIALIMNSSGSTGLPKGVALPHRTACVRFSHARDPIFGNQIIPDTAILSVVPFHHGP
1_30_CF3_17-MP049_C07.ab1	VDFVPESFDRDKTIALIMNSSGSTGLPKGVALPHRTACVRFSHARDPIFGNQIIPDTAILSVVPFHHGP
1_30_CF3_18-MP049_D07.ab1	VDFVPESFDRDKTIALXMNSSGSTGLPKGVALPHRTACVRFSHARDPIFGNQIIPDTAILSVVPFHHGP
1_30_CF3_19-MP049_E07.ab1	VDFVPESFDRDKTIALIMNSSGSTGLPKGVALPHRTACVRFSHARDPIFGNQIIPDTAILSVVPFHHGP
1_30_Dluc_20-MP049_F07.ab1	VDFVPESFDRDKTIALIMNSSGSTGLPKGVALPHRTACVRFSHARDPIFGNQIIPDTAILSVVPFHHGP
1_30_Dluc_21-MP049_G07.ab1	VDFVPESFDRDKTIALIMNSSGSTGLPKGVALPHRTACVRFSHARDPIFGNQIIPDTAILSVVPFHHGP
1_30_Dluc_22-MP049_H07.ab1	XXXXXXSFDRDKTIALIMNSSGSTGLPKGVALPHRTACVRFSHARDPIFGNQIIPDTAILSVVPFHHGP
1_30_Tbutylthio_5-MP049_F06.ab1	VDFVPESFDRDKTIALIMNSSGSTGLPKGVALPHRTACVRFSHARDPIFGNQIIPDTAILSVVPFHHGP
1_30_Tbutylthio_6-MP049_G06.ab1	VDFVPESFDRDKTIALIMNSSGSTGLPKGVALPHRTACVRFSHARDPIFGNQIIPDTAILSVVPFHHGP
1_30_Tbutylthio_13-MP049_B07.ab1	VDFVPESFDRDKTIALIMNSSGSTGLPKGVALPHRTACVRFSHARDPIFGNQIIPDTAILSVVPFHHGP
1_30_Benzimidluc_8-MP049_A07.ab1	VDFVPESFDRDKTIALIMNSSGSTGLPKGVALPHRTACVRFSHARDPIFGNQIIPDAAILSVVPFHHGP
Luc2WT	VDFVPESFDRDKTIALIMNSSGSTGLPKGVALPHRTACVRFSHARDPIFGNQIIPDTAILSVVPFHHGP

L287V:

Sequence Name	< Pos = 183
- ■ ■ ■ ■ +	
☒ Consensus	
4 Sequences	

Consensus sequence region 190–300:

`PESFDRDKTIALIMNSSGSTGLPKGVALPHRTACVRFSHARDPIFGNQIIPDTAILSVVPFHHGFGMFTTLGYLICGFRVVLMVRFEEELFLRSLQDVKIQSALLVPTLFSFFAKSTLIDKVI`

```
190   200   210   220   230   240   250   260   270   280   290
```

Sequence Name	Sequence (190–300)
Dluc-2-MP049_	PESFDRDKTIALIMNSSGSTGLPKGVALPHRTACVRFSHARDPIFGNQIIPDTAILSVVPFHHGFGMFTTLGYLICGFRVVLMVRFEEELFLRSLQDVKIQSALLVPTLFSFFAKSTLIDKVI
Dluc-3-MP049_	PESFDRDKTIALIMNSSGSTGLPKGVALPHRTACVRFSHARDPIFGNQIIPDTAILSVVPFHHGFGMFTTLGYLICGFRVVLMVRFEEELFLRSLQDVKIQSALVVPTLFSFFAKSTLIDKVI
Dluc-1-MP049_	PESFDRDKTIALIMNSSGSTGLPKGVALPHRTACVRFSHARDPIFGNQIIPDTAILSVVPFHHGFGMFTTLGYLICGFRVVLMVRFEEELFLRSLQDVKIQSALLVPTLFSFFAKSTLIDKVI
Luc2WT	PESFDRDKTIALIMNSSGSTGLPKGVALPHRTACVRFSHARDPIFGNQIIPDTAILSVVPFHHGFGMFTTLGYLICGFRVVLMVRFEEELFLRSLQDVKIQSALLVPTLFSFFAKSTLIDKVI

F227S

Sequence Name	< Pos = 197
- ■ ■ ■ ■ +	
☒ Consensus	
5 Sequences	

Consensus sequence region 200–270:

`NSSGSTGLPKGVALPHRTACVRFSHARDPIFGNQIIPDTAILSVVPFHHGFGMFTTLGYLICGFRVVLMVRFEEELFLRSLC`

```
200   210   220   230   240   250   260   270
```

Sequence Name	Sequence (200–270)
2_3_rescreen_5-M	NSSGSTGLPKGVALPHRTACVRFSHARDPIFGNQIIPDTAILSVVPFHHGFGMFTTLGYLICGFRVVLMVRFEEELFLRSLC
2_3_rescreen_7-M	NSSGSTGLPKGVALPHRTACVRFSHARDPIFGNQIIPDTAILSVVPFHHGFGMFTTLGYLICGFRVVLMVRFEEELFLRSLC
2_3_rescreen_16-	NSSGSTGLPKGVALPHRTACVRFSHARDPIFGNQIIPDTAILSVVPFHHGFGMFTTLGYLICGFRVVLMVRFEEELFLRSLC
2_3_rescreen_18-	NSSGSTGLPKGVALPHRTACVRFSHARDPISGNQIIPDTAILSVVPFHHGFGMFTTLGYLICGFRVVLMVRFEEELFLRSLC
Luc2WT	NSSGSTGLPKGVALPHRTACVRFSHARDPIFGNQIIPDTAILSVVPFHHGFGMFTTLGYLICGFRVVLMVRFEEELFLRSLC

I226T

Sequence Name | < Pos = 191

- ■■■■■ +
☒ Consensus
11 Sequences

Consensus: TIALIMNSSGSTGLPKGVALPHRTACVRFSHARDPIFGNQIIPDTAILSVVF
200   210   220   230   240

MP_rescreen-02-MP049_B11.ab1   TIALIMNSSGSTGLPKGVALPHRTACVRFSHARDPIFGNQIIPDTAILSVVF
MP_rescreen-03-MP049_C11.ab1   TIALIMNSSGSTGLPKGVALPHRTACVRFSHARDPTFGNQIIPDTAILSVVF
MP_rescreen-04-MP049_D11.ab1   TIALIMNSSGSTGLPKGVALPHRTACVRFSHARDPIFGNQIIPDTAILSVVF
MP_rescreen-05-MP049_E11.ab1   TIALIMNSSGSTGLPKGVALPHRTACVRFSHARDPIFGNQIIPDTAILSVVF
MP_rescreen-06-MP049_F11.ab1   TIALIMNSSGSTGLPKGVALPHRTACVRFSHARDPTFGNQIIPDTAILSVVF
MP_rescreen-12-MP049_G11.ab1   TIALIMNSSGSTGLPKGVALPHRTACVRFSHARDPIFGNQIIPDTAILSVVF
MP_rescreen-16-MP049_A12.ab1   TIALIMNSSGSTGLPKGVALPHRTACVRFSHARDPIFGNQIIPDTAILSVVF
MP_rescreen-18-MP049_B12.ab1   TIALIMNSSGSTGLPKGVALPHRTACVRFSHARDPIFGNQIIPDTAILSVVF
MP_rescreen-23-MP049_H11.ab1   TIALIMNSSGSTGLPKGVALPHRTACVRFSHARDPIFGNQIIPDTAILSVVF
MP_rescreen-01-MP049_A11.ab1   TIALIMNSSGSTGLPKGVALPHRTACVRFSHARDPIFGNQIIPDTAILSVVF
Luc2WT   TIALIMNSSGSTGLPKGVALPHRTACVRFSHARDPIFGNQIIPDTAILSVVF

F294S S307G and K329R

Sequence Name | < Pos = 260

- ■■■■■ +
☒ Consensus
6 Sequences

Consensus: FRVVLMYRFEEELFLRSLQDYKIQSALLVPTLFSFFAKSTLIDKYDLSNLHEIASGGAPLSKEVGEAVAKRFHLPGIRQGYGLT
60   270   280   290   300   310   320   330   340

5_14_screen_4-MP0   FRVVLMYRFEEELFLRSLQDYKIQSALLVPTLFSFFAKSTLIDKYDLSNLHEIASGGAPLSKEVGEAVAKRFHLPGIRQGYGLT
5_14_screen_12-MP   FRVVLMYRFEEELFLRSLQDYKIQSALLVPTLFSFFAKSTLIDKYDLSNLHEIASGGAPLSKEVGEAVAKRRFHLPGIRQGYGLT
5_14_screen_15-MP   FRVVLMYRFEEELFLRSLQDYKIQSALLVPTLFSSFAKSTLIDKYDLGNLHEIASGGAPLSKEVGEAVAKRFHLPGIRQGYGLT
5_14_screen_16-MP   FRVVLMYRFEEELFLRSLQDYKIQSALLVPTLFSSFAKSTLIDKYDLSNLHEIASGGAPLSKEVGEAVAKRFHLPGIRQGYGLT
5_14_screen_1-MP0   FRVVLMYRFEEELFLRSLQDYKIQSALLVPTLFSFFAKSTLIDKYDLSNLHEIASGGAPLSKEVGEAVAKRFHLPGIRQGYGLT
Luc2WT   FRVVLMYRFEEELFLRSLQDYKIQSALLVPTLFSFFAKSTLIDKYDLSNLHEIASGGAPLSKEVGEAVAKRFHLPGIRQGYGLT